Electronic Supplementary Material (ESI) for ChemComm.

Supporting Information

Polyol recognition in catalysis: Toward selective modification of glycosylated polypeptides with boronic acid-rhodium(II) catalysts

Reyner D. Vargas, Yuxuan Ding, Hallie O. Trial, Rouyu Qian, and Zachary T. Ball

Table of Contents

General Information

Chemicals

All chemicals were purchased from commercial suppliers and used without further purification. Fmoc-amino acids purchased from NovaBiochem. Diazo compound **8**[1] and sugar **S1**[1,2] were prepared from known protocols.

Buffers

TBHA buffer: *N*-(tert-Butyl)hydroxylamine hydrochloride (31.4 mg, 0.250 mmol, 10 mM final concentration) was dissolved in 20 mL of Milli-Q water, the solution was then adjusted to the desired pH (6.2-8.2) using aq HCl (1 M) before bringing the final volume to 25 mL.

Phosphates buffer: Sodium phosphate dibasic heptahydrate (15.1 mg, 0.056 mmol) and sodium phosphate monobasic monohydrate (26.8 mg, 0.194 mmol) were dissolved in 20 mL of Milli-Q water, the solution was then adjusted to pH 6.2 using aq HCl (1 M) before bringing the final volume to 25 mL.

Instrumentation

HPLC

Reverse-phase HPLC was performed on a Shimadzu SCL-40 with Phenomenex Jupiter 4µ Proteo 90A (250 x 4.6 mm analytical) and Phenomenex Jupiter 4µ Proteo 90A (240 x 15 mm preparative) columns. The analytical column was eluted with an initial isocratic flow of MeCN in water (5%) with 0.1% v/v TFA followed by a gradient of the same solvent system (5-70%) using a flow rate of 1 ml/min. The preparative column was eluted with a gradient of MeCN in water with 0.1% v/v TFA using a flow rate of 6 ml/min. Peptide detection was monitored using absorbance at 254 nm and 280 nm.

General procedure for HPLC analysis: Sample aliquots (5 µL) of the crude reaction mixture or prepared standards were injected directly onto the HPLC.

ESI-MS and LC-MS

Analysis of glycopeptide starting materials and reactions were conducted on Agilent Single Quadrupole-TOF LC/MS spectrometer with an Ascentis® Express Peptide ES-C18 column (15 cm × 2.1 mm, 2.7 um). The flow rate was 0.4 mL/min. A gradient of acetonitrile/water with 0.1% formic acid was employed.

LC-MS/MS and HRMS

Were conducted on Agilent Quadrupole-TOF LC/MS spectrometer with an Ascentis® Express Peptide ES-C18 column (15 cm × 2.1 mm, 2.7 um). The flow rate was 0.8 mL/min. A gradient of acetonitrile/water with 0.1% formic acid was employed.

Peptide synthesizer

Peptides were synthesized using a CEM Liberty Blue automated microwave peptide synthesizer.

Experimental Procedures

Glycopeptide Synthesis:

Glycopeptides **gpep 1-3** peptides precursors were synthesized using standard solid phase peptide synthesis protocols[3] using rink amide resin (P3Biosystems, 52001) and Fmoc-amino acid used without further purification. The crude (0.05 mmol) was then reacted with the desired amino-sugar (0.25 mmol) in the presence of HBtU (0.1 mmol), HoBT (0.08 mmol) and *i*Pr2NEt (0.25 mmol) in dimethylformamide (5 ml) for 2 h before being purified by reverse-phase preparative HPLC and characterized by ESI-MS and analytical HPLC, purified yields on figures S29-35.

Glycopeptides **gpep 4-10** peptides precursors were synthesized using the automated peptide synthesizer using rink amide resin (CEM, ProTide™ high swelling) and Fmoc-amino acids used without further purification. The crude (0.05 mmol) was then reacted with the desired amino-sugar (0.25 mmol) in the presence of HBtU (0.1 mmol), HoBT (0.08 mmol) and *i*Pr2NEt (0.25 mmol) in dimethylformamide (5 ml) for 2h before being purified by reverse-phase preparative HPLC and characterized by ESI-MS and analytical HPLC, purified yields on figures S39-45.

Glycopeptides **gpep 11** peptide precursor was synthesized using the automated peptide synthesizer using rink amide resin (CEM, ProTide™ high swelling) and Fmoc-amino acids used without further purification. The crude (0.05 mmol) was then reacted with the desired amino-sugar (0.75 mmol) in the presence of DIC (0.75 mmol), oxyma (0.75 mmol) and *i*Pr2NEt (1.5 mmol) in dimethylformamide (5 ml) for 2h before being purified by reverse-phase preparative HPLC and characterized by ESI-MS and analytical HPLC, to afford 10.5 mg (0.012 mmol, **25%**) of the purified product.

Experimental procedure for peptide modification and control reactions.

The studied glycopeptide (500 µM) was incubated with diazo compound **8** (5 mM) and the Rh(II) catalyst (25 µM) in TBHA buffer (10 mM, pH 6.2) at 4 °C overnight. Specifically, the glycopeptide (25 nmol, 2.5 µL of a 10 mM aq soln), diazo compound **8** (250 nmol, 2.5 µL of a 10 mM aq soln),rhodium catalyst **7** or **$Rh_2(OAc)_4$** (control catalyst) (1.25 nmol, 0.25 µL of 5 mM aq soln) were added to a solution of TBHA buffer (10 mM pH 7.2, 44.75 µL) and let at 4 °C overnight covered in aluminum foil. The crude reaction mixture was analyzed according to the general procedure for HPLC quantification. Further characterization was performed using Q-TOF LC -MS and -MSMS analysis.

General procedure for HPLC quantification.

The crude reaction was analyzed using the general procedure for HPLC analysis, then the unmodified glycopeptide peak was used to determine its remaining concentration with the corresponding linear regression equation. The estimated product yield was then calculated with the area of the corresponding product peaks versus the sum of all peptidic peaks.

General procedure for the catalyst screen (Table S1)

gpep1 (25 nmol, 2.5 µL of 10 mM aq soln), diazo compound **8** (1250 nmol, 12.5 µL of 50 mM soln), the studied Rh(II) catalyst (50 nmol, 2 µL of 25 mM aq soln) were added to a soln of TBHA buffer (10 mM pH 6.2, 35 µL) and let without stirring at 4 °C overnight covered in aluminum foil. The crude reaction

mixture was analyzed via LC-MS and according to the starting material conversion procedure under HPLC quantification.

General procedure for the optimization of the reaction conditions (Table 1)

gpep1 (25 nmol, 2.5 µL of 10 mM aq soln), diazo compound **8** (250-1250 nmol, 5 µL of 50 mM soln, 12.5 µL of 100 mM soln), Rh(II) catalyst **7** (0.25-50 nmol, 0.5 µL of 0.5 mM aq soln, 0.25-2.5 µL of 5 mM aq soln, 2 µL of 25 mM aq soln) and D-sorbitol (250-2500 nmol 2.5 µL of 100 mM aq soln, 2.5 µL of 1000 mM aq soln) were added to a soln of TBHA buffer (10 mM pH 5.2-8.2, 33.0-42.2 µL) and let without stirring at 4 °C overnight covered in aluminum foil. The crude reaction mixture was analyzed according to the general procedure for HPLC quantification.

Entries e and f are described in the general procedure for the catalyst screen (Table S1).

General procedure for the gpep2-9 reaction analysis (Table 2)

Gpep2-9 (25 nmol, 2.5 µL of 10 mM aq soln), diazo compound **8** (250 nmol, 2.5 µL of 50 mM soln), Rh(II) catalyst **7** (1.25 nmol, 0.25 µL of 5 mM aq soln) were added to a soln of TBHA buffer (10 mM pH 6.2, 33-44.8 µL) and let without stirring at 4 °C overnight covered in aluminum foil. The crude reaction mixture was analyzed according to the general procedure for HPLC quantification.

General procedure for the boronic ester formation study

4-aminophenylboronic acid (12.5 nmol, 2.5 µL of 5 mM aq soln), and D-sorbitol **8** (2.5 µmol, 2.5 µL of 1M soln) were added to TBHA buffer (10 mM pH 6.2, 45 µL) or phosphates buffer (10 mM pH 6.2, 45 µL). For the negative control, 4-aminophenylboronic acid (12.5 nmol, 2.5 µL of 5 mM aq soln) was added to 47.5 µL of Milli-Q water. All the solutions were analyzed by LC-MS.

Supplementary data

HPLC quantification

Glycopeptide quantification by HPLC, standards preparation and measurement.

200 µL of the glycopeptide 0.5 mM was prepared (10 µL of 10 mM aq soln in 190 µL in TBHA buffer), then 0.4, 0.3, 0.2, 0.1 mM were prepared by taking aliquots of the 0.5 mM mother solution and before bringing the final volume to 50 µL with TBHA buffer. The standards were then analyzed according to the general procedure for HPLC analysis, the area under the curve for every standard was then fitted against the concentration to obtain a linear regression equation.

HPLC quantification for gpep1

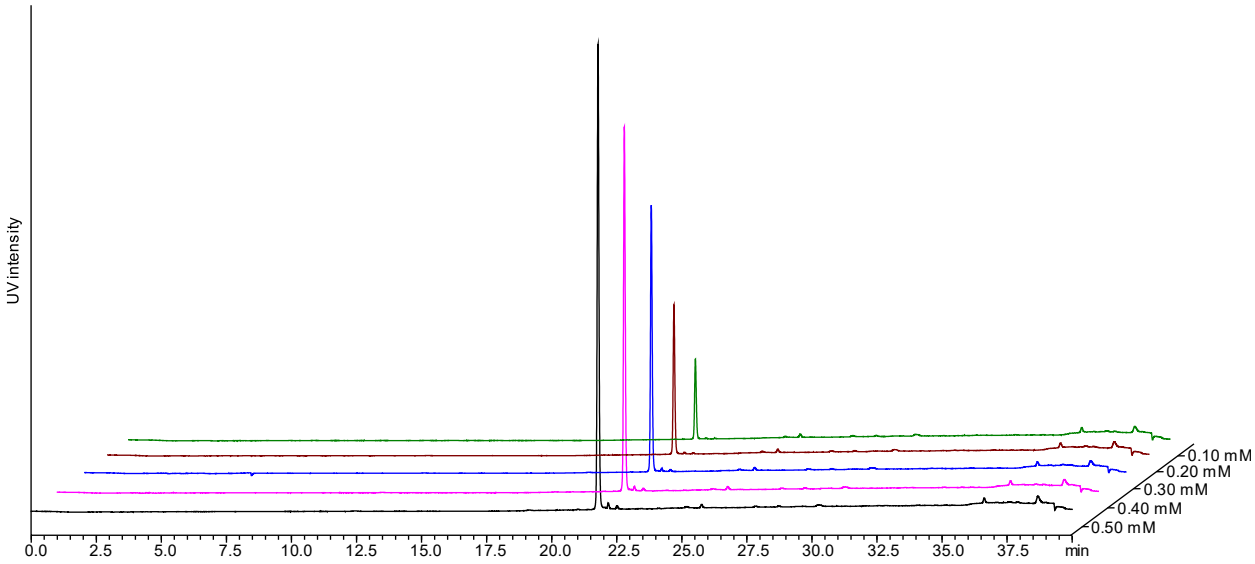

concentration (mM)	peak area	linear regression
0.50	1032477	$A = 2.098x10^6 \cdot c(mM)$ $R^2 = 0.9976$
0.40	889562	
0.30	631368	
0.20	369353	
0.10	188328	

Figure S1. HPLC traces (5-70% MeCN over 40 min at 280 nm) of starting material (**gpep1**) at five different concentrations along with its corresponding peak area and linear regression.

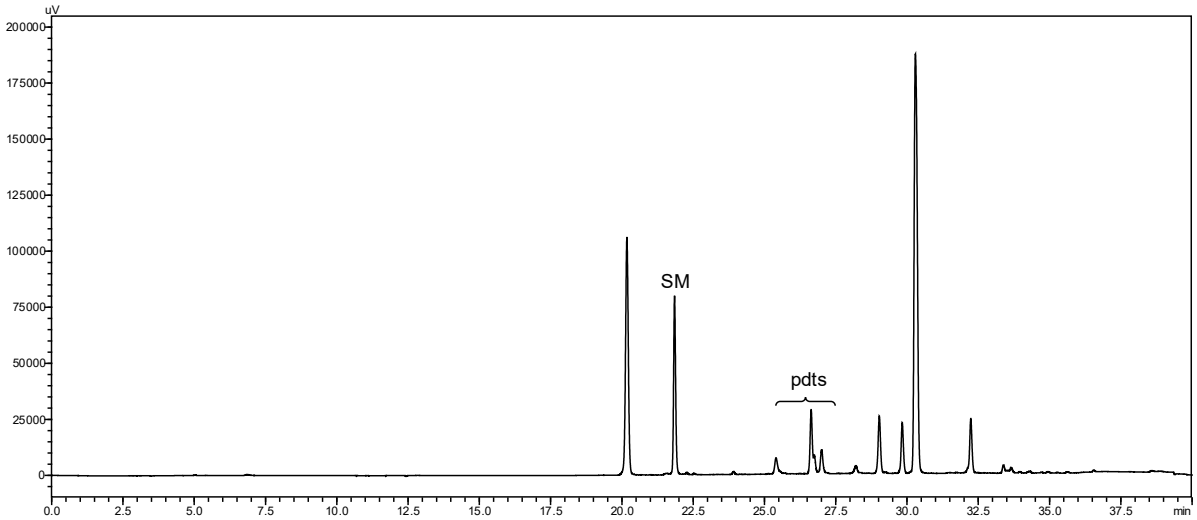

	peak area	SM conversion	yield
SM	668971	36%	-
products	249441	-	27%

$$SM_{conversion} = \frac{\left(0.50 - \frac{A_{sm}}{slope}\right)}{0.50} \cdot 100 = \frac{\left(0.50 - \frac{668971}{2.098x10^{6}}\right)}{0.50} \cdot 100 = \mathbf{36}\%$$

$$product_{yield} = \frac{A_{pdts}}{A_{pdts} + A_{sm}} \cdot 100 = \frac{249441}{249441 + 662540} \cdot 100 = \mathbf{27}\%$$

Figure S2. Sample of the SM conversion and estimated product yield for the modification reaction using **gpep1**.

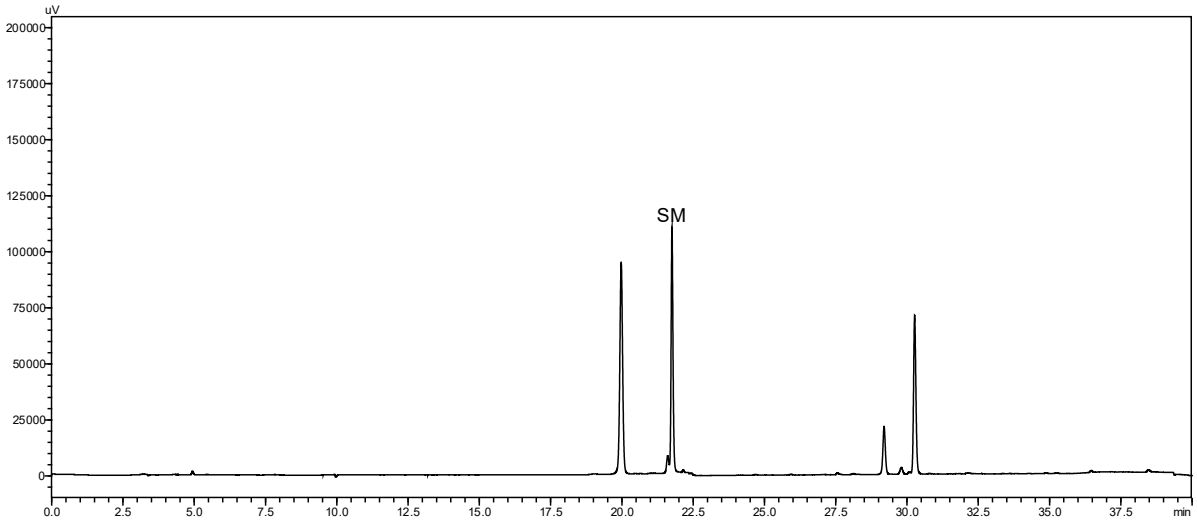

Figure S3. HPLC trace of the control reaction of **gpep1**.

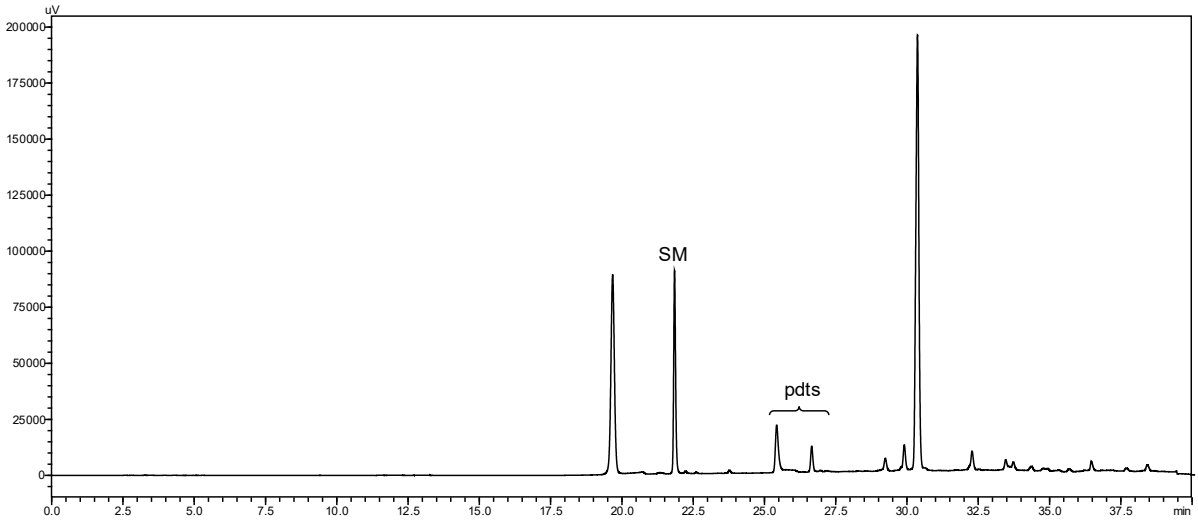

	peak area	SM conversion	yield
SM	836053	20%	-
products	112390	-	12%

Figure S4. Sample of the SM conversion and estimated product yield for the modification reaction using **gpep1** in phosphates buffer 10 mM pH 6.2.

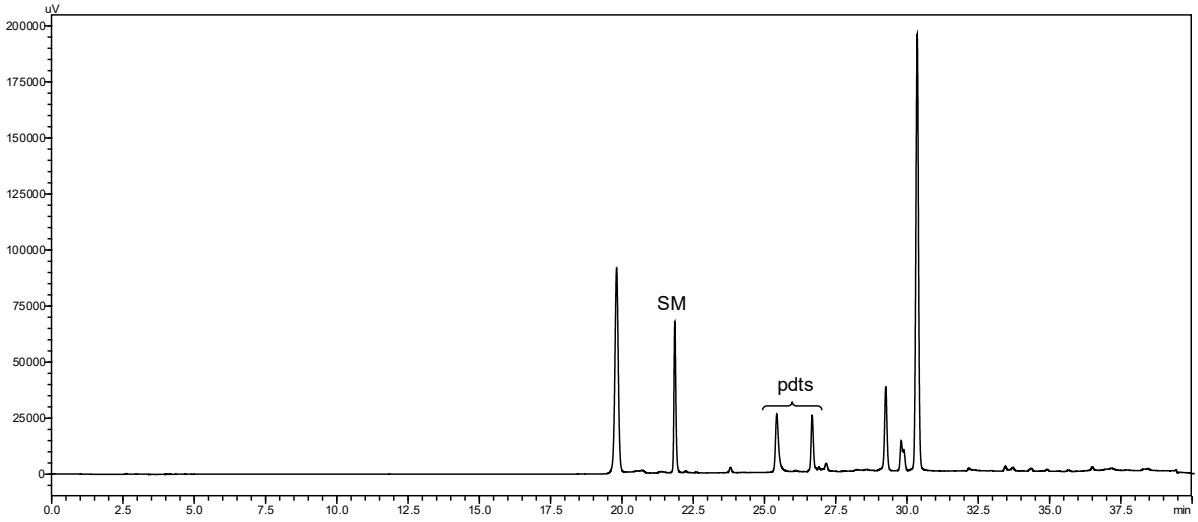

	peak area	SM conversion	yield
SM	724859	31%	-
products	197353	-	21%

Figure S5. Sample of the SM conversion and estimated product yield for the modification reaction using **gpep1** in PBS buffer 10 mM pH 6.2.

HPLC quantification for gpep2

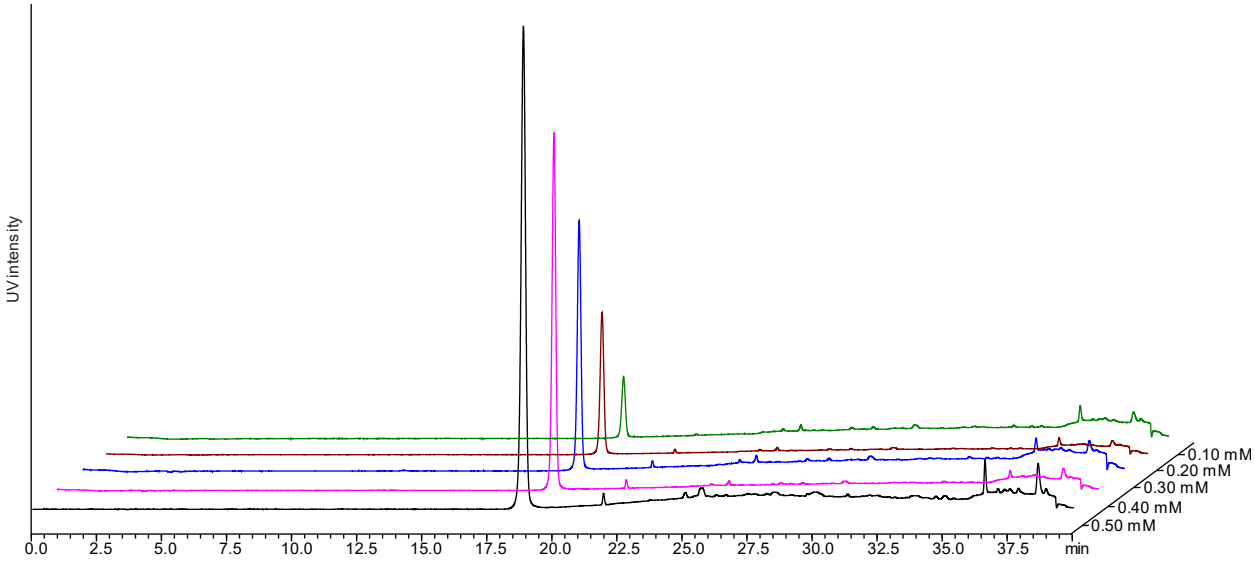

concentration (mM)	peak area	linear regression
0.50	668106	$A = 1.313x10^6 \cdot c(mM)$ $R^2 = 0.9989$
0.40	521123	
0.30	380820	
0.20	273923	
0.10	106897	

Figure S6. HPLC traces (5-70% MeCN over 40 min at 280 nm) of starting material (**gpep2**) at five different concentrations along with its corresponding peak area and linear regression.

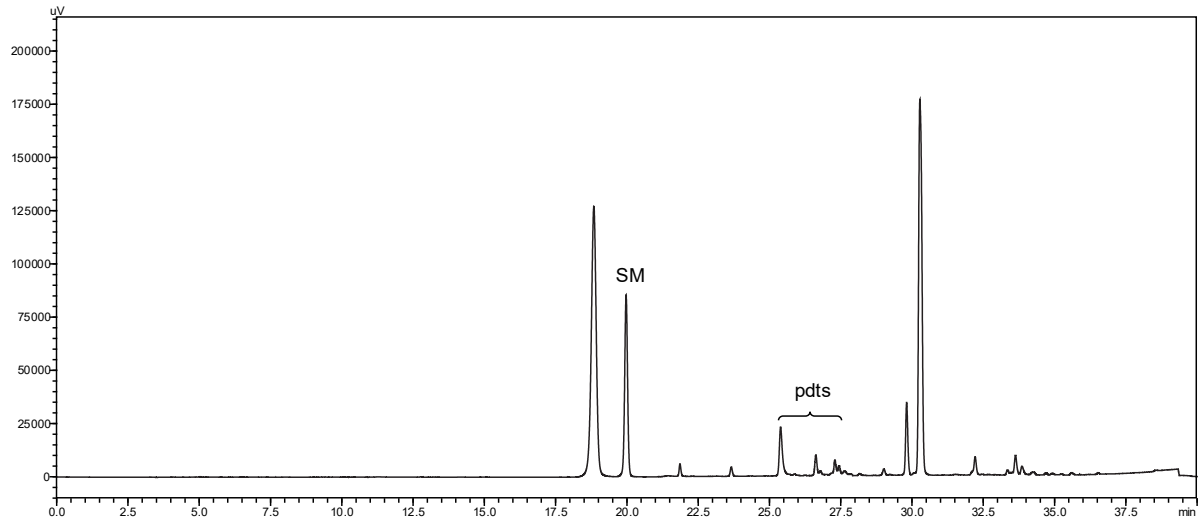

	peak area	SM conversion	yield
SM	486975	26%	-
products	94594	-	16%

$$SM_{conversion} = \frac{\left(0.50 - \frac{A_{sm}}{slope}\right)}{0.50} \cdot 100 = \frac{\left(0.50 - \frac{486975}{1.313x10^{6}}\right)}{0.50} \cdot 100 = \mathbf{26}\%$$

$$product_{yield} = \frac{A_{pdts}}{A_{pdts} + A_{sm}} \cdot 100 = \frac{94594}{94954 + 486975} \cdot 100 = \mathbf{16}\%$$

Figure S7. Sample of the SM conversion and estimated product yield for the modification reaction using **gpep2**.

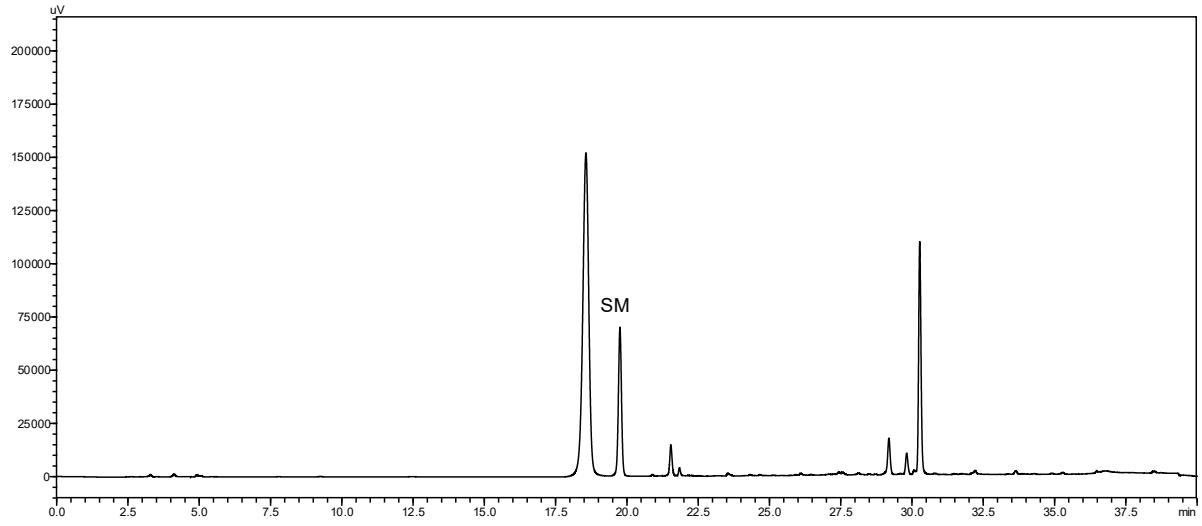

Figure S8. HPLC trace of the control reaction of **gpep2**.

HPLC quantification for gpep3

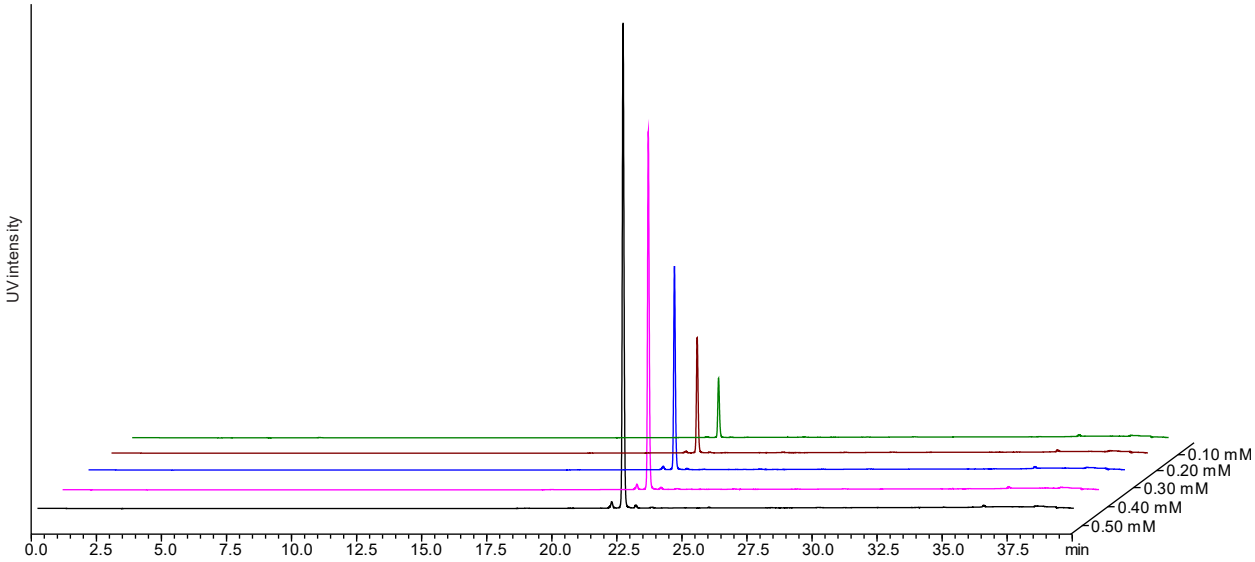

concentration (mM)	peak area	linear regression
0.50	1622245	$A = 3.291x10^6 \cdot c(mM)$ $R^2 = 0.9975$
0.40	1376463	
0.30	924680	
0.20	717788	
0.10	272004	

Figure S9. HPLC traces (5-70% MeCN over 40 min at 280 nm) of starting material (**gpep3**) at five different concentrations along with its corresponding peak area and linear regression.

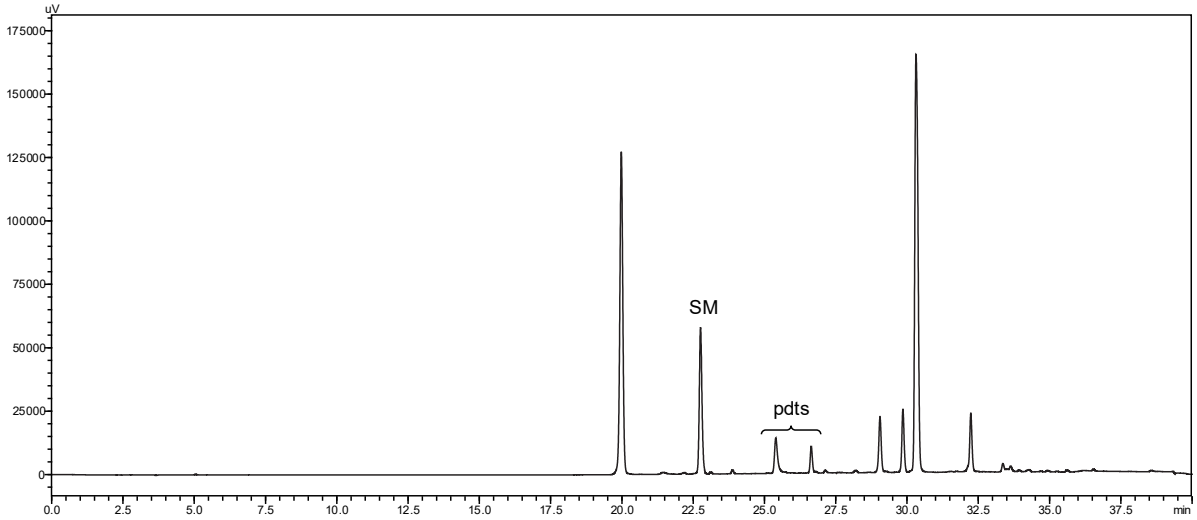

	peak area	SM conversion	yield
SM	1058938	36%	-
products	415063	-	28%

$$SM_{conversion} = \frac{\left(0.50 - \frac{A_{sm}}{slope}\right)}{0.50} \cdot 100 = \frac{\left(0.50 - \frac{1058938}{3.291x10^{6}}\right)}{0.50} \cdot 100 = \mathbf{36}\%$$

$$product_{yield} = \frac{A_{pdts}}{A_{pdts} + A_{sm}} \cdot 100 = \frac{415063}{415063 + 1058938} \cdot 100 = \mathbf{28}\%$$

Figure S10. Sample of the SM conversion and estimated product yield for the modification reaction using **gpep3**.

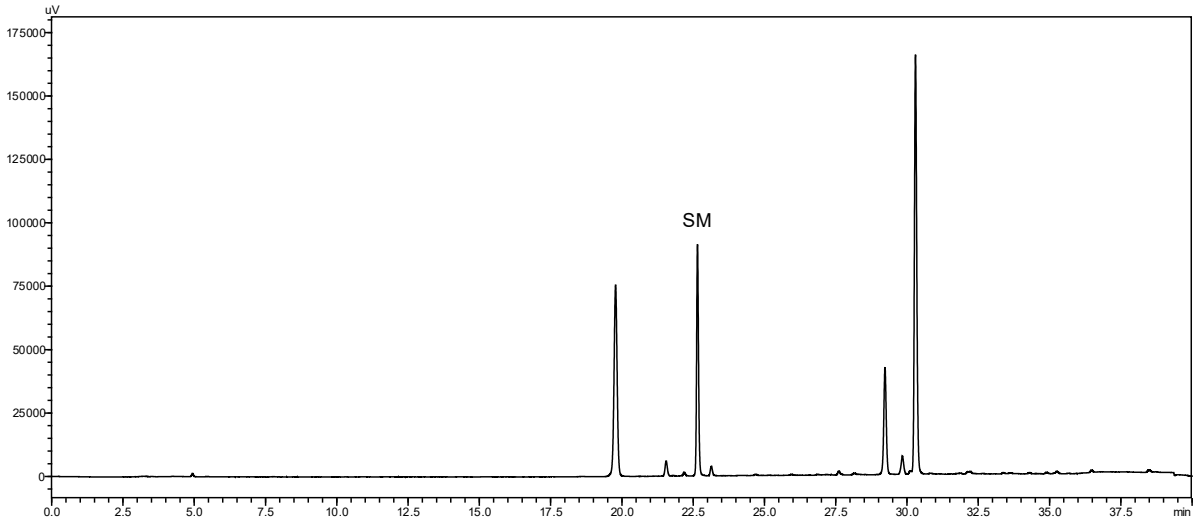

Figure S11. HPLC trace of the control reaction of **gpep3**.

HPLC quantification for gpep4

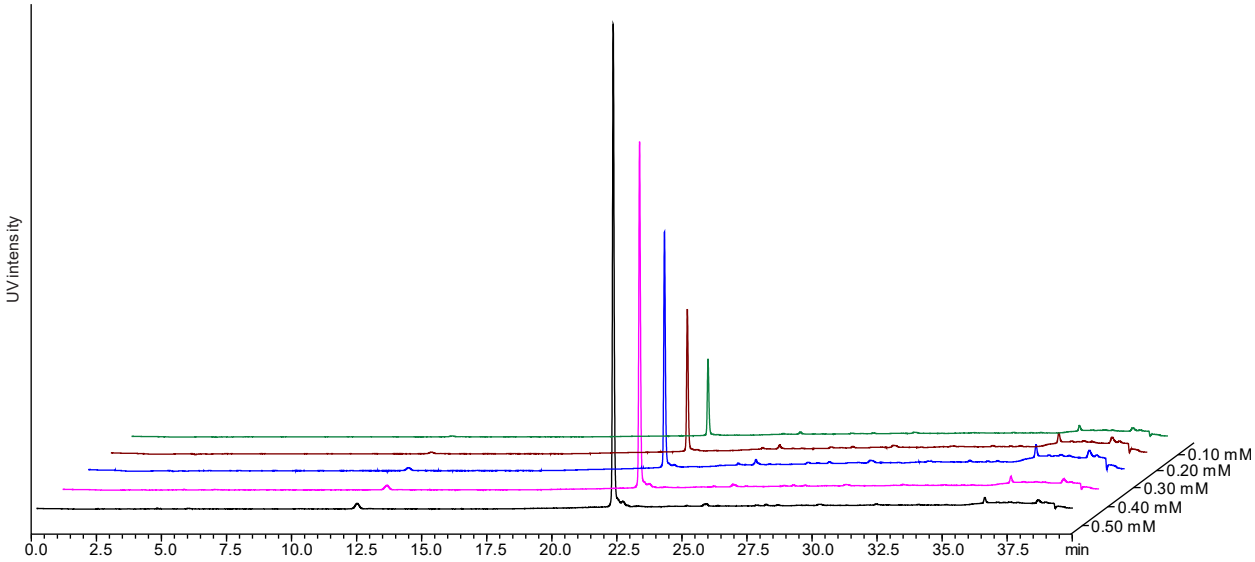

concentration (mM)	peak area	linear regression
0.50	484827	$A = 9.612x10^5 \cdot c(mM)$ $R^2 = 0.9957$
0.40	373317	
0.30	271503	
0.20	91510	
0.10	19877	

Figure S12. HPLC traces (5-70% MeCN over 40 min at 280 nm) of starting material (**gpep4**) at five different concentrations along with its corresponding peak area and linear regression.

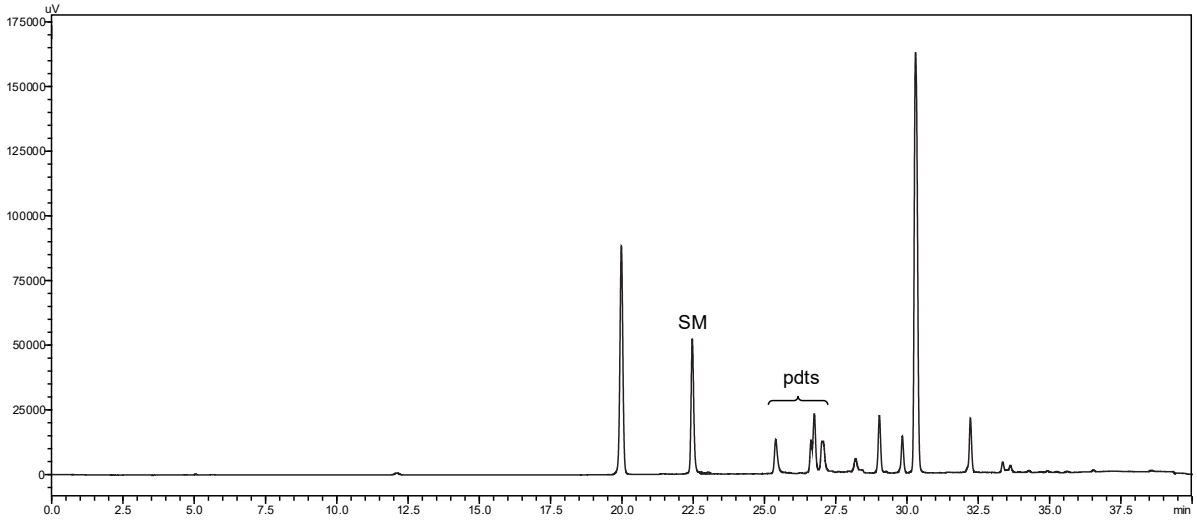

	peak area	SM conversion	yield
SM	172482	64%	-
products	177963	-	51%

$$SM_{conversion} = \frac{\left(0.50 - \frac{A_{sm}}{slope}\right)}{0.50} \cdot 100 = \frac{\left(0.50 - \frac{172482}{9.612x10^5}\right)}{0.50} \cdot 100 = \mathbf{64}\%$$

$$product_{yield} = \frac{A_{pdts}}{A_{pdts} + A_{sm}} \cdot 100 = \frac{177963}{177963 + 172482} \cdot 100 = \mathbf{51}\%$$

Figure S13. Sample of the SM conversion and estimated product yield for the modification reaction using **gpep4**.

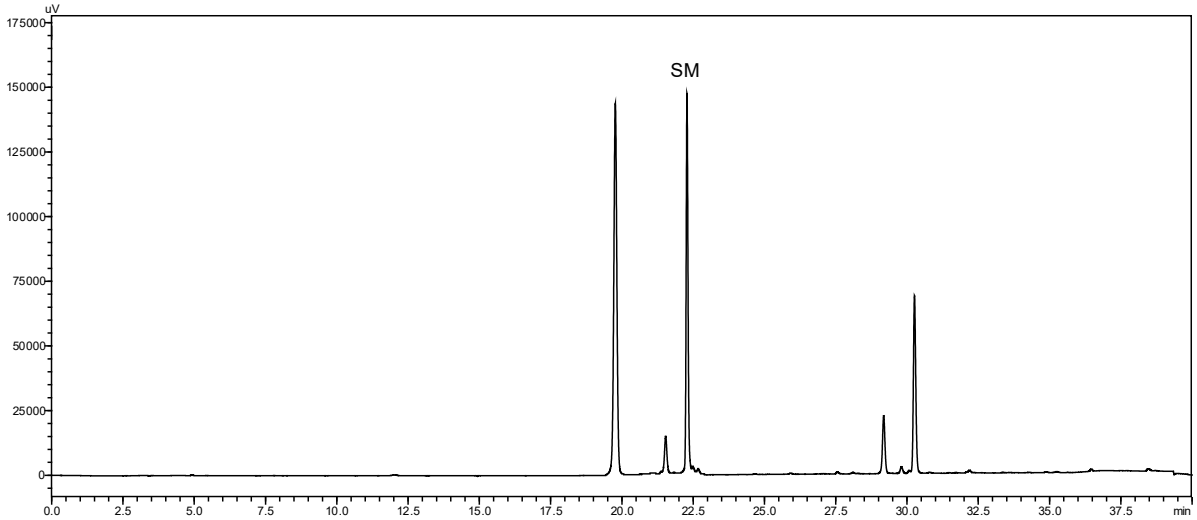

Figure S14. HPLC trace of the control reaction of **gpep4**.

HPLC quantification for gpep5

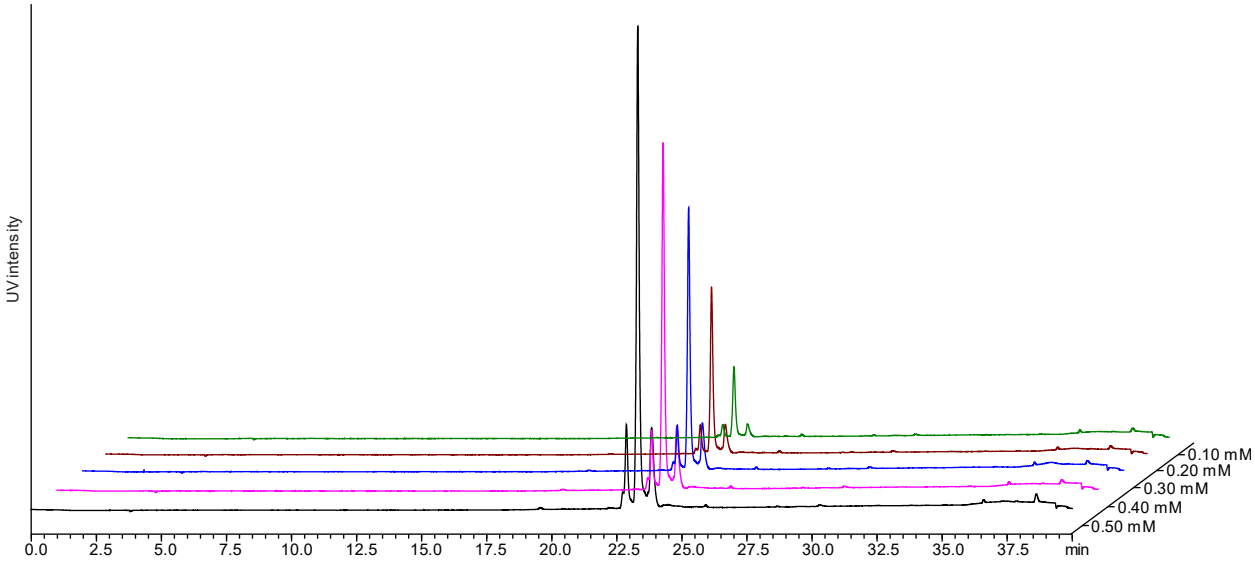

concentration (mM)	peak area	linear regression
0.50	860308	$A = 1.699x10^6 \cdot c(mM)$ $R^2 = 0.9960$
0.40	642437	
0.30	533391	
0.20	296917	
0.10	117649	

Figure S15. HPLC traces (5-70% MeCN over 40 min at 280 nm) of starting material (**gpep5**) at five different concentrations along with its corresponding peak area and linear regression.

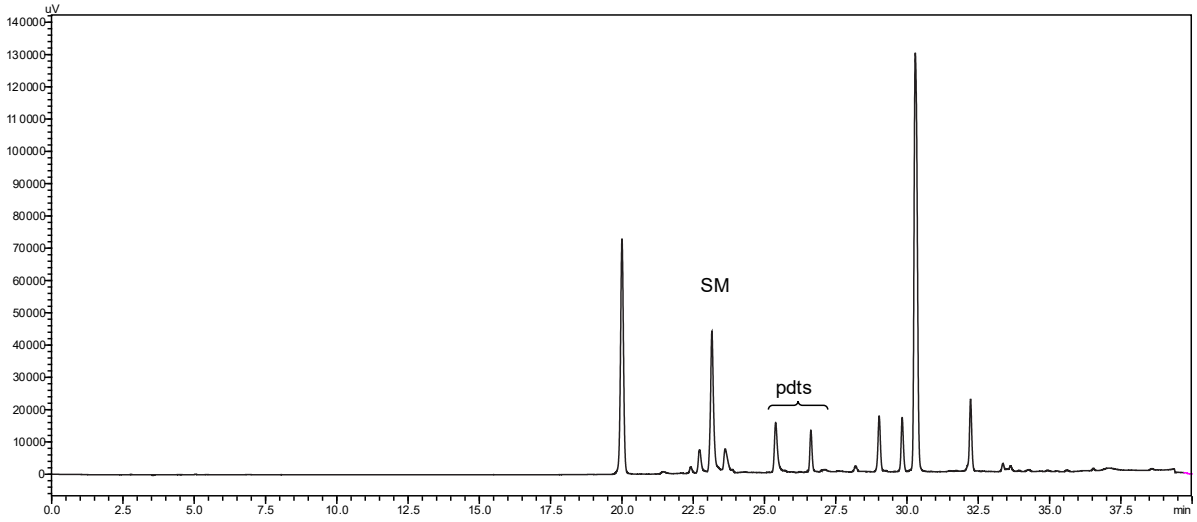

	peak area	SM conversion	yield
SM	619264	26%	-
products	130732	-	17%

$$SM_{conversion} = \frac{\left(0.50 - \frac{A_{sm}}{slope}\right)}{0.50} \cdot 100 = \frac{\left(0.50 - \frac{619264}{1.699x10^{6}}\right)}{0.50} \cdot 100 = \mathbf{26}\%$$

$$product_{yield} = \frac{A_{pdts}}{A_{pdts} + A_{sm}} \cdot 100 = \frac{130732}{130732 + 619264} \cdot 100 = \mathbf{17}\%$$

Figure S16. Sample of the SM conversion and estimated product yield for the modification reaction using **gpep5**.

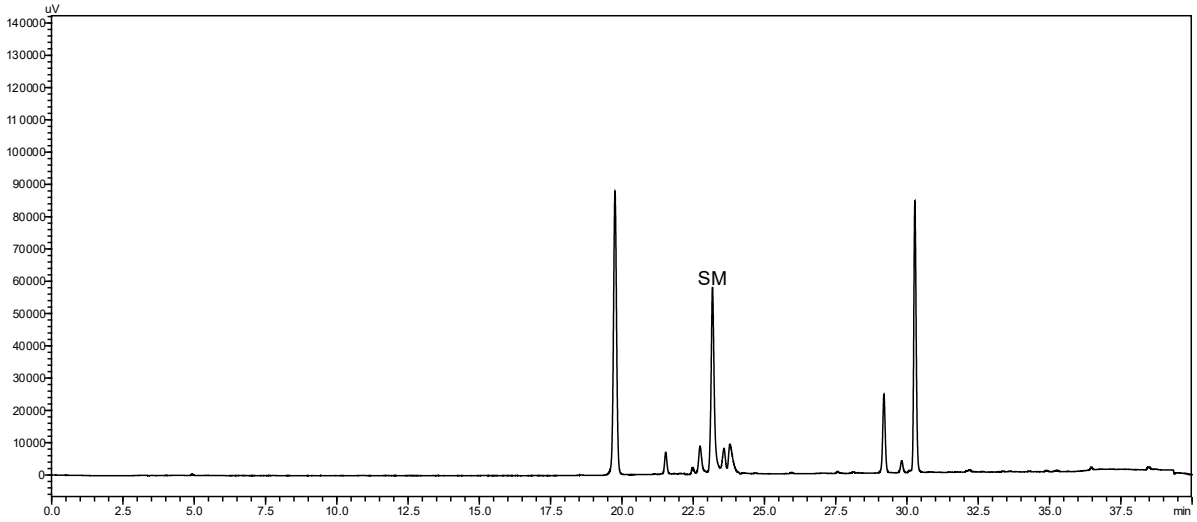

Figure S17. HPLC trace of the control reaction of **gpep5**.

HPLC quantification for gpep6

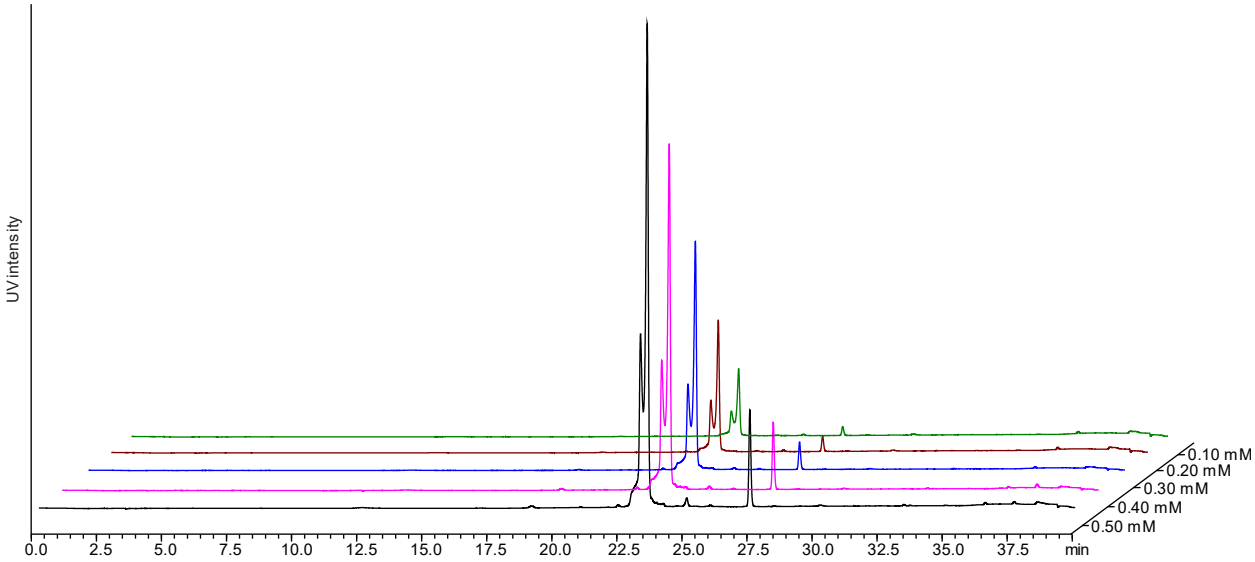

concentration (mM)	peak area	linear regression
0.50	1418713	$A = 2.711x10^6 \cdot c(mM)$ $R^2 = 0.9973$
0.40	1026596	
0.30	782853	
0.20	569111	
0.10	225368	

Figure S18. HPLC traces (5-70% MeCN over 40 min at 280 nm) of starting material (**gpep6**) at five different concentrations along with its corresponding peak area and linear regression.

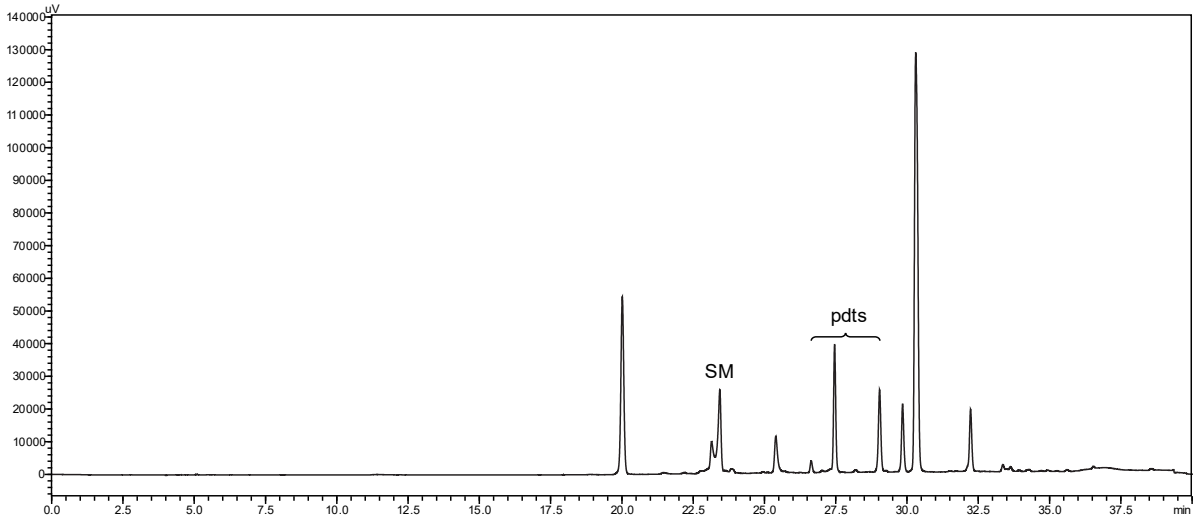

	peak area	SM conversion	yield
SM	411682	70%	-
products	401154	-	49%

$$SM_{conversion} = \frac{\left(0.50 - \frac{A_{sm}}{slope}\right)}{0.50} \cdot 100 = \frac{\left(0.50 - \frac{411682}{2.711x10^{6}}\right)}{0.50} \cdot 100 = \mathbf{36}\%$$

$$product_{yield} = \frac{A_{pdts}}{A_{pdts} + A_{sm}} \cdot 100 = \frac{401154}{401154 + 411682} \cdot 100 = \mathbf{27}\%$$

Figure S19. Sample of the SM conversion and estimated product yield for the modification reaction using **gpep6**.

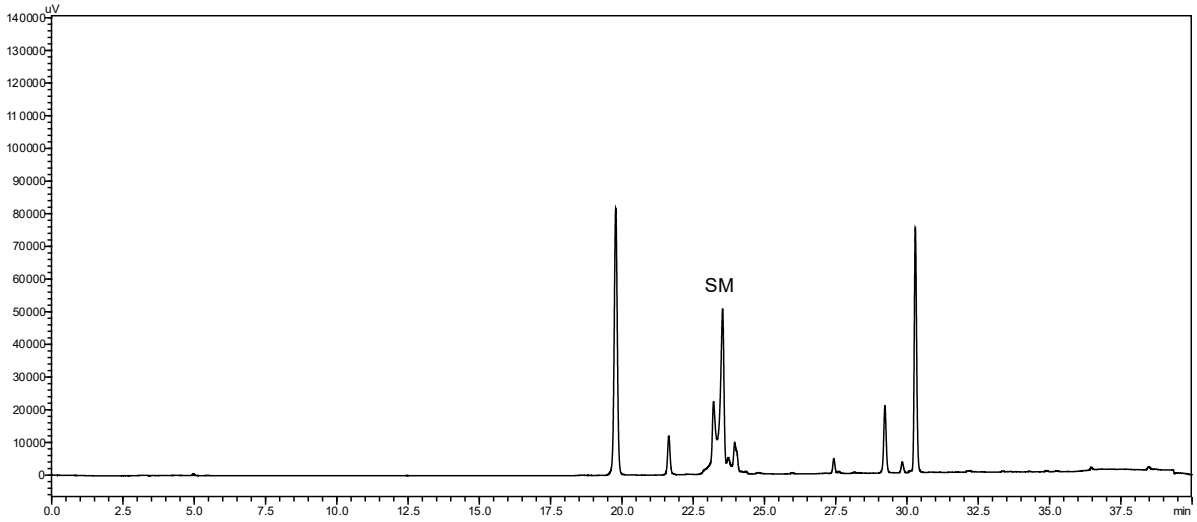

Figure S20. HPLC trace of the control reaction of **gpep6**.

HPLC quantification for gpep7

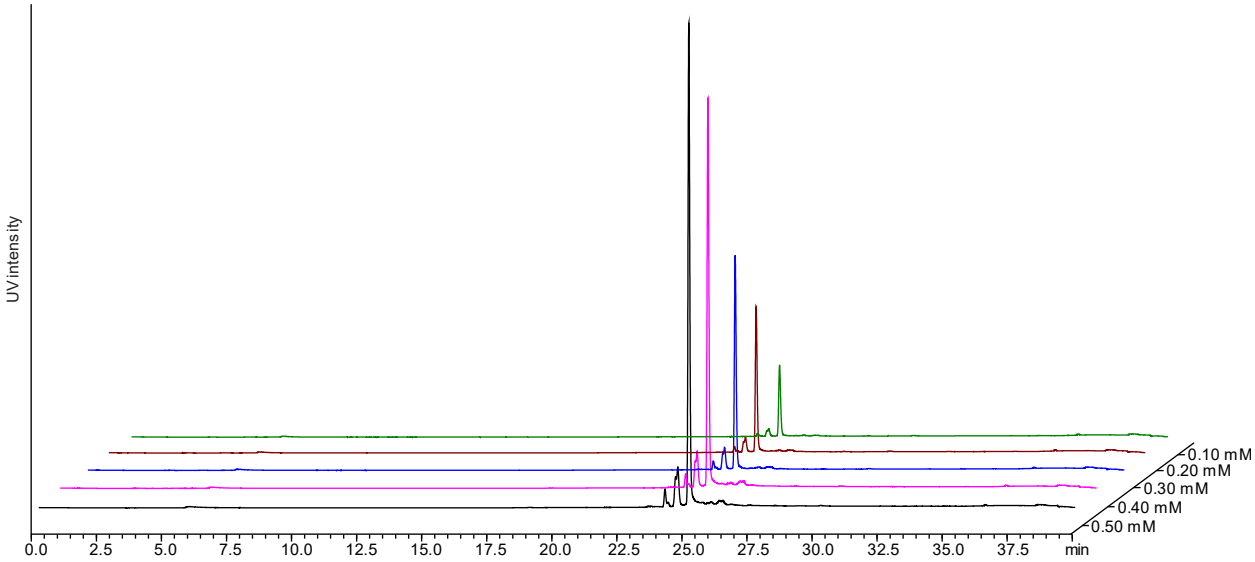

concentration (mM)	peak area	linear regression
0.50	1278243	$A = 2.595x10^6 \cdot c(mM)$ $R^2 = 0.9913$
0.40	1060942	
0.30	728598	
0.20	562427	
0.10	230084	

Figure S21. HPLC traces (5-70% MeCN over 40 min at 280 nm) of starting material (**gpep7**) at five different concentrations along with its corresponding peak area and linear regression.

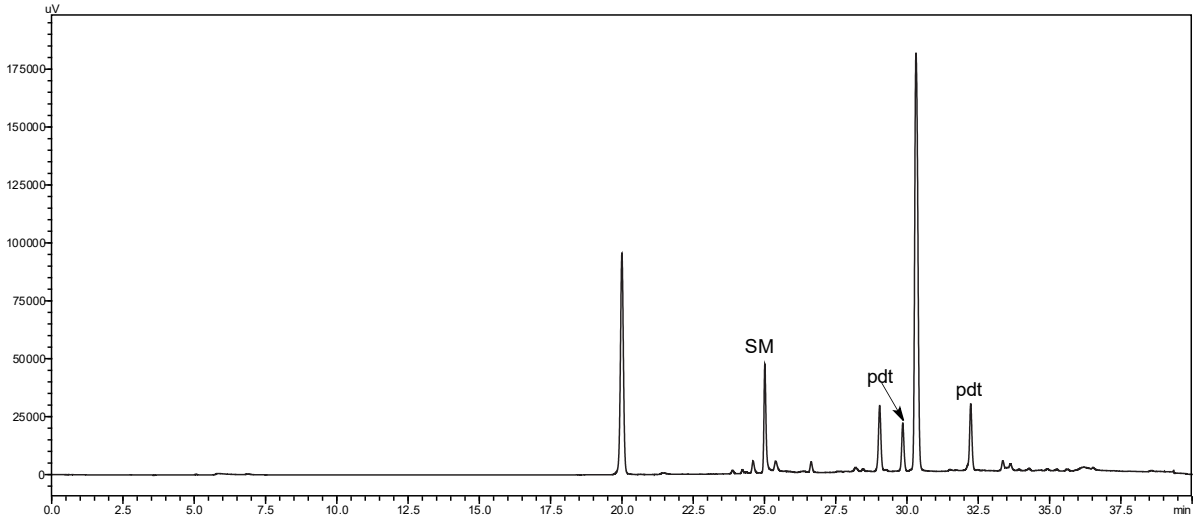

	peak area	SM conversion	yield
SM	516826	60%	-
products	424964	-	45%

$$SM_{conversion} = \frac{\left(0.50 - \frac{A_{sm}}{slope}\right)}{0.50} \cdot 100 = \frac{\left(0.50 - \frac{516826}{2.595x10^{6}}\right)}{0.50} \cdot 100 = \mathbf{60}\%$$

$$product_{yield} = \frac{A_{pdts}}{A_{pdts} + A_{sm}} \cdot 100 = \frac{424964}{424964 + 516826} \cdot 100 = \mathbf{45}\%$$

Figure S22. Sample of the SM conversion and estimated product yield for the modification reaction using **gpep7**.

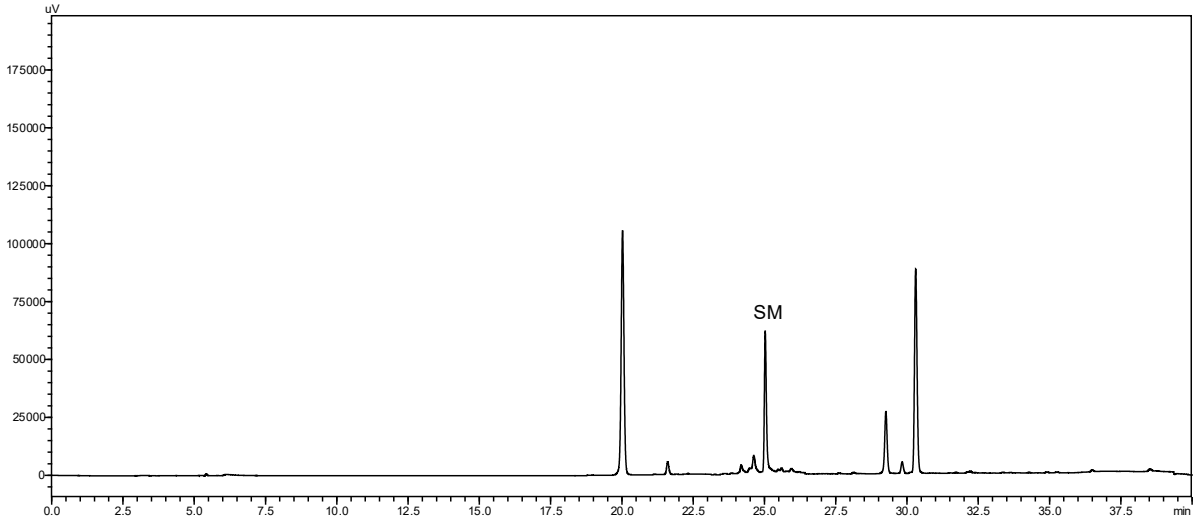

Figure S23. HPLC trace of the control reaction of **gpep7**.

HPLC quantification for gpep8

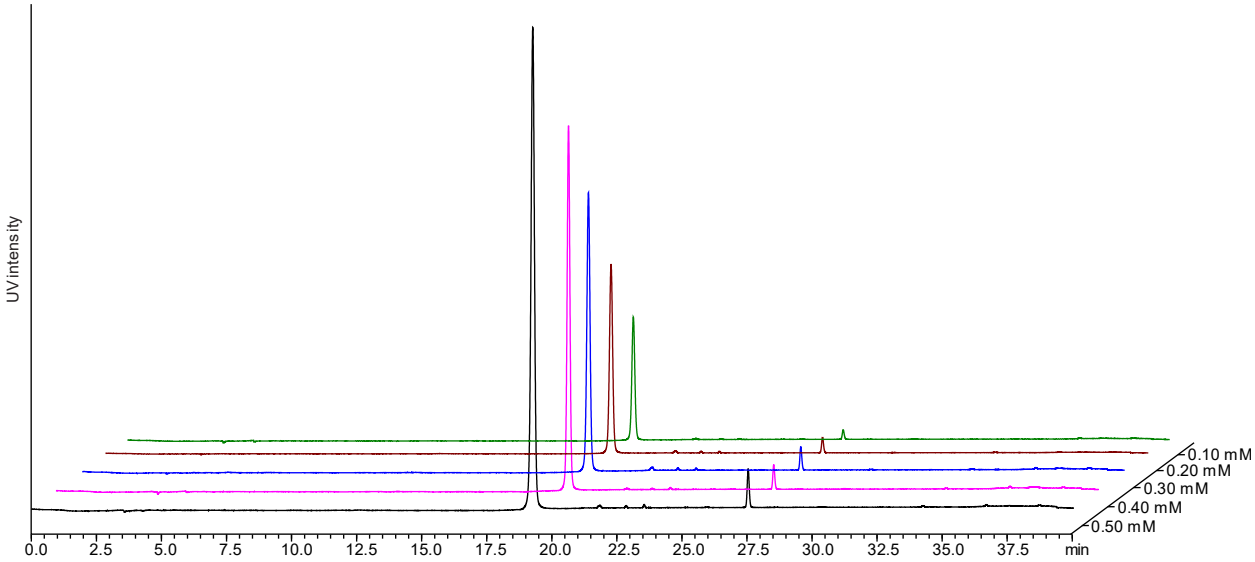

concentration (mM)	peak area	linear regression
0.50	1244351	$A = 2.446x10^6 \cdot c(mM)$ $R^2 = 0.9987$
0.40	958150	
0.30	696837	
0.20	510184	
0.10	286201	

Figure S24. HPLC traces (5-70% MeCN over 40 min at 280 nm) of starting material (**gpep8**) at five different concentrations along with its corresponding peak area and linear regression.

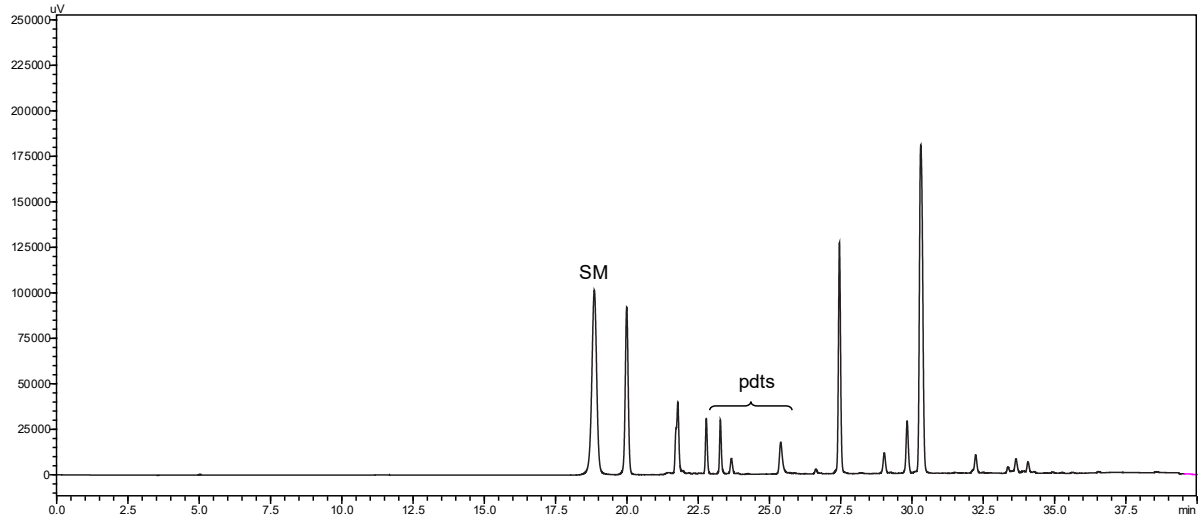

	peak area	SM conversion	yield
SM	698704	43%	-
products	379543	-	35%

$$SM_{conversion} = \frac{\left(0.50 - \frac{A_{sm}}{slope}\right)}{0.50} \cdot 100 = \frac{\left(0.50 - \frac{698704}{2.446x10^{6}}\right)}{0.50} \cdot 100 = \mathbf{43}\%$$

$$product_{yield} = \frac{A_{pdts}}{A_{pdts} + A_{sm}} \cdot 100 = \frac{379543}{379543 + 698704} \cdot 100 = \mathbf{35}\%$$

Figure S25. Sample of the SM conversion and estimated product yield for the modification reaction using **gpep8**.

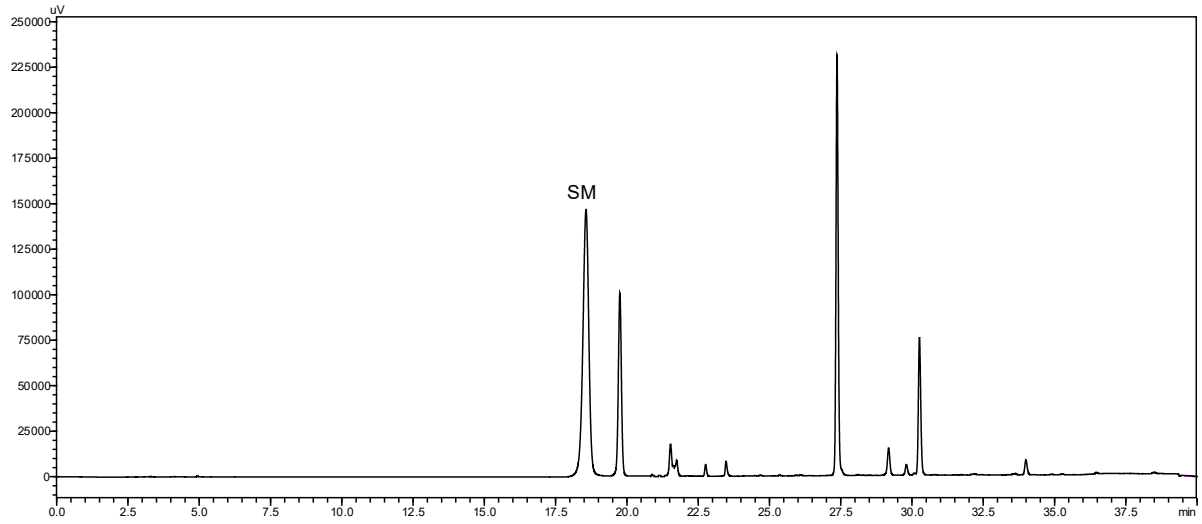

Figure S26. HPLC trace of the control reaction of **gpep8**.

HPLC quantification for gpep9

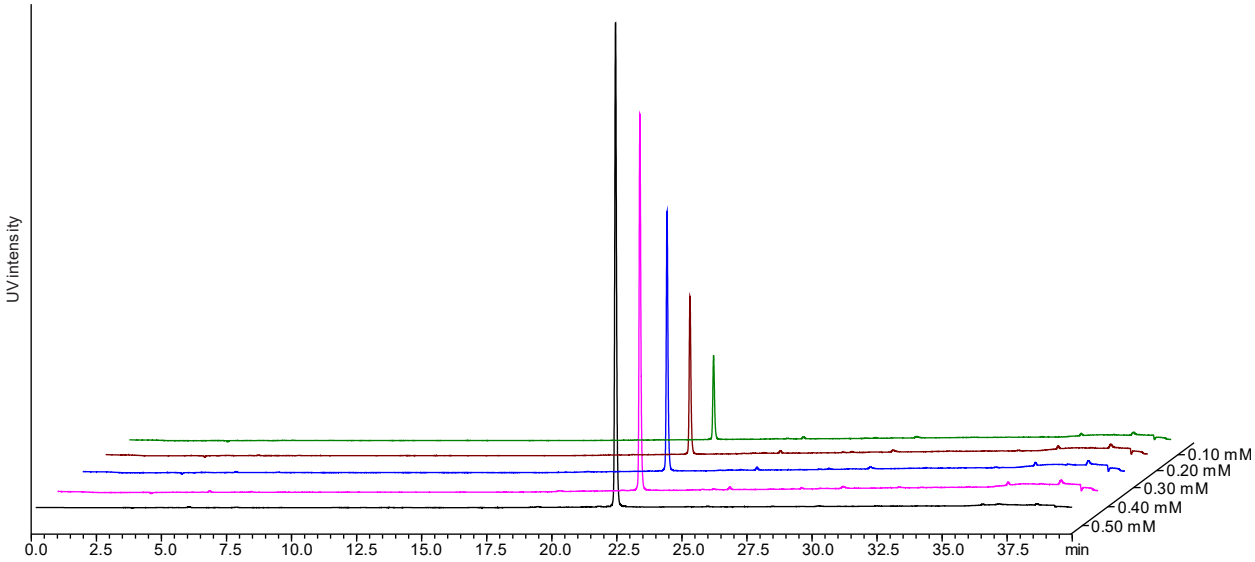

concentration (mM)	peak area	linear regression
0.50	1434913	$A = 2.812x10^6 \cdot c(mM)$ $R^2 = 0.9981$
0.40	1076185	
0.30	889646	
0.20	545267	
0.10	229586	

Figure S27. HPLC traces (5-70% MeCN over 40 min at 280 nm) of starting material (**gpep9**) at five different concentrations along with its corresponding peak area and linear regression.

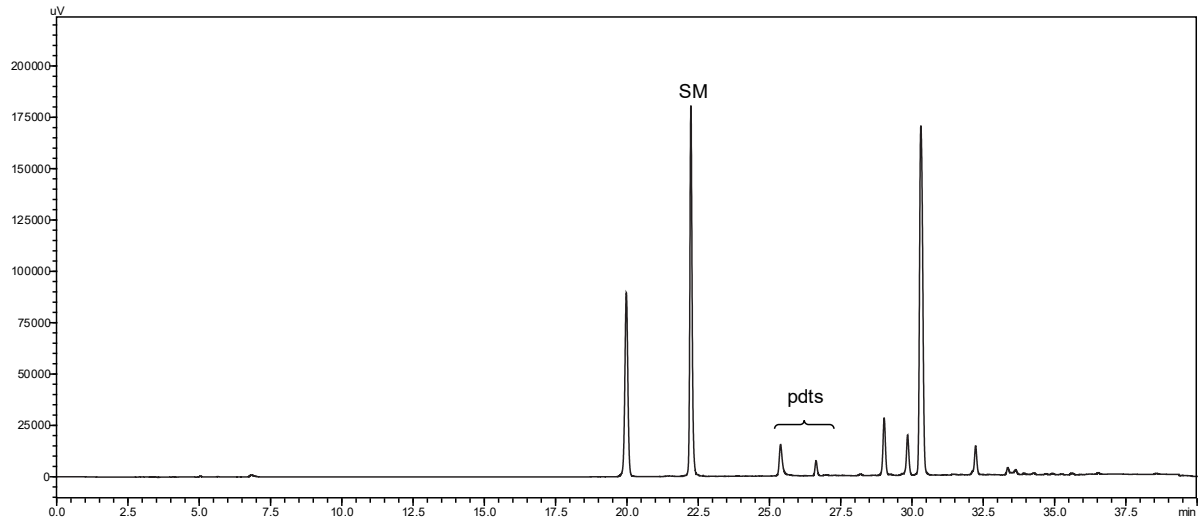

	peak area	SM conversion	yield
SM	1337812	5%	-
products	44939	-	3%

$$SM_{conversion} = \frac{\left(0.50 - \frac{A_{sm}}{slope}\right)}{0.50} \cdot 100 = \frac{\left(0.50 - \frac{1337812}{2.812x10^{6}}\right)}{0.50} \cdot 100 = \mathbf{5}\%$$

$$product_{yield} = \frac{A_{pdts}}{A_{pdts} + A_{sm}} \cdot 100 = \frac{44939}{44939 + 1337812} \cdot 100 = \mathbf{3}\%$$

Figure S28. Sample of the SM conversion and estimated product yield for the modification reaction using **gpep9**.

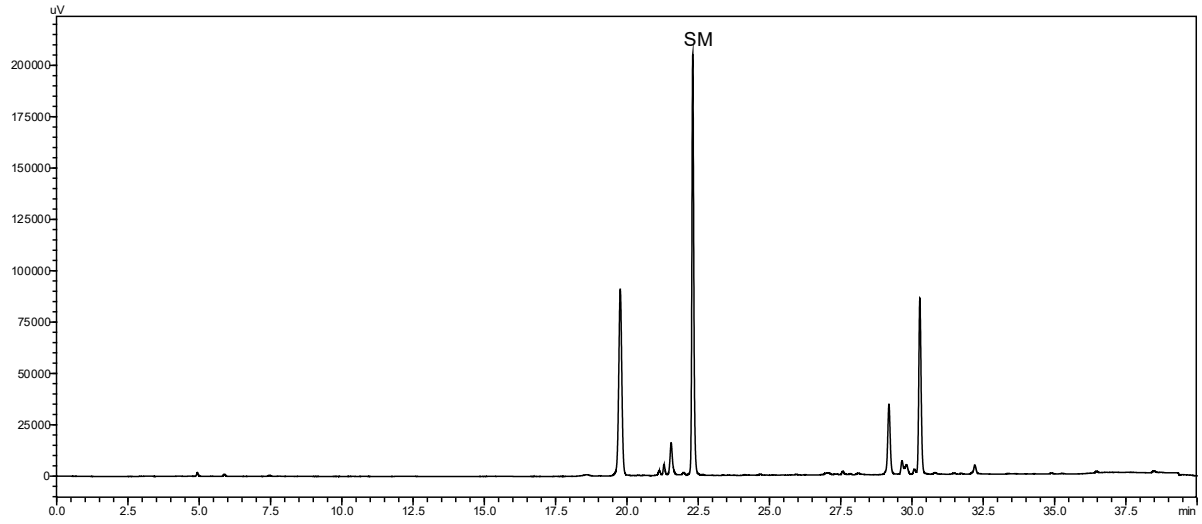

Figure S29. HPLC trace of the control reaction of **gpep9**.

Table S1 initial catalyst screening

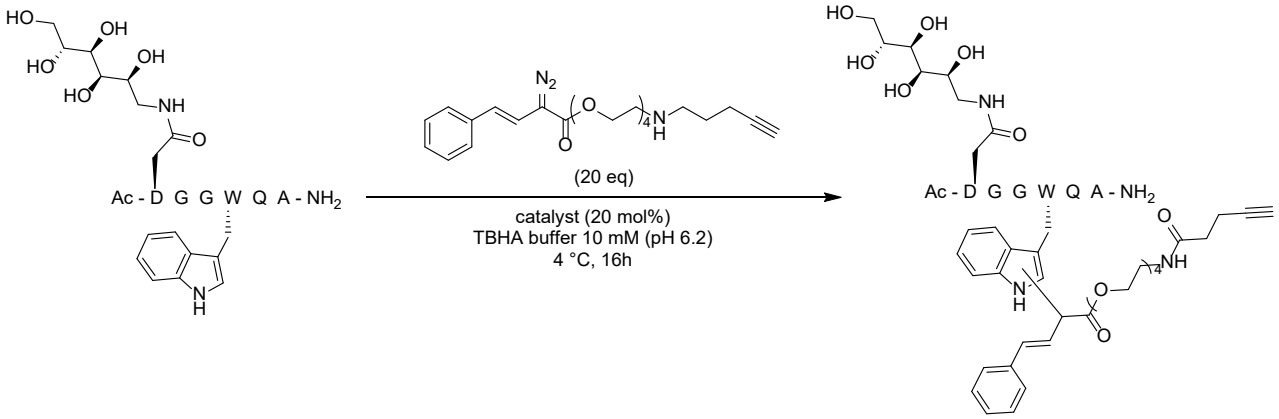

entry	catalyst	product observed by MS	SM conversion
a	Rh_2OAc_4	no	-
b	1	no	-
c	2	no	-
d	3	no	-
e	4	no	-
f	5	no	-
g	6	yes	**15%**
h	7	yes	**40%**

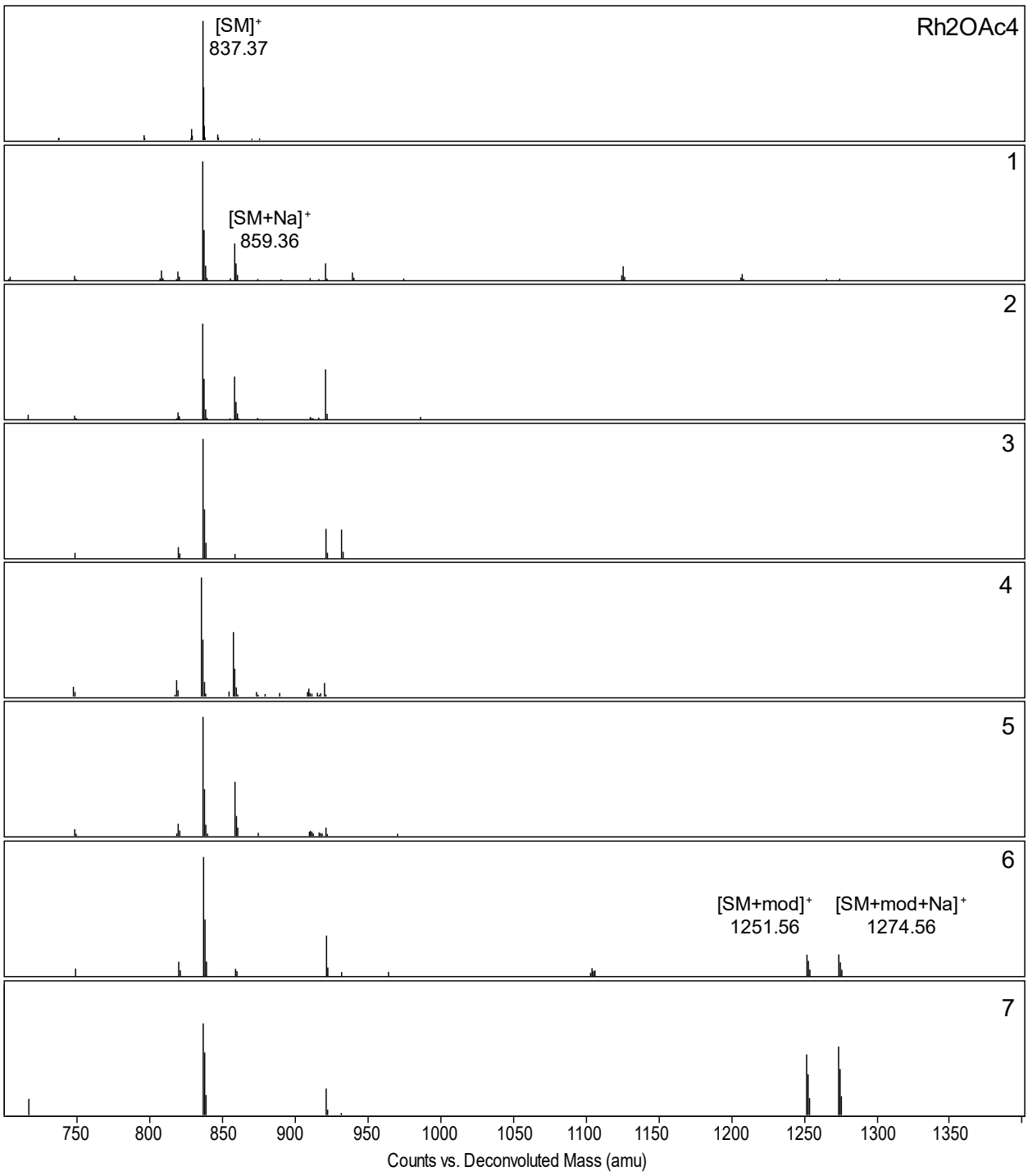

Figure S30. Deconvoluted MS spectra of the EIC (500 – 1500 m/z) for the crude reaction mixture of **gpep1** with the catalyst scope and diazo compound **8**. Unmodified **gpep1** [M]+ and [M+Na]+ was observed at 837.37 and 859.36 respectively. Modified **gpep1+mod** was observed at 1251.56 and 1274.56 respectively.

Table S2 attempted conditions for modification of gpep10 and gpep11.

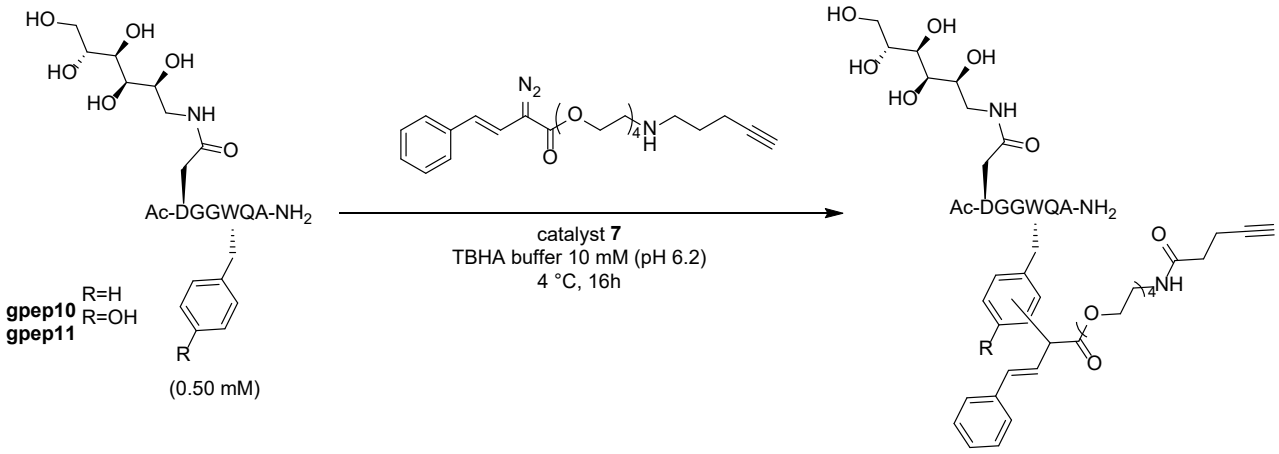

entry	diazo compound (eq)	datalyst	pH	LC-MS analysis
a	10	5 mol%	6.2	No modification observed
b	50	0.5 eq	↓	↓
c	↓	2	↓	↓
d	100	↓	↓	↓
e	↓	↓	7.2	↓
f	200	5	6.2	↓

LC-MS reactions characterization analysis

gpep1

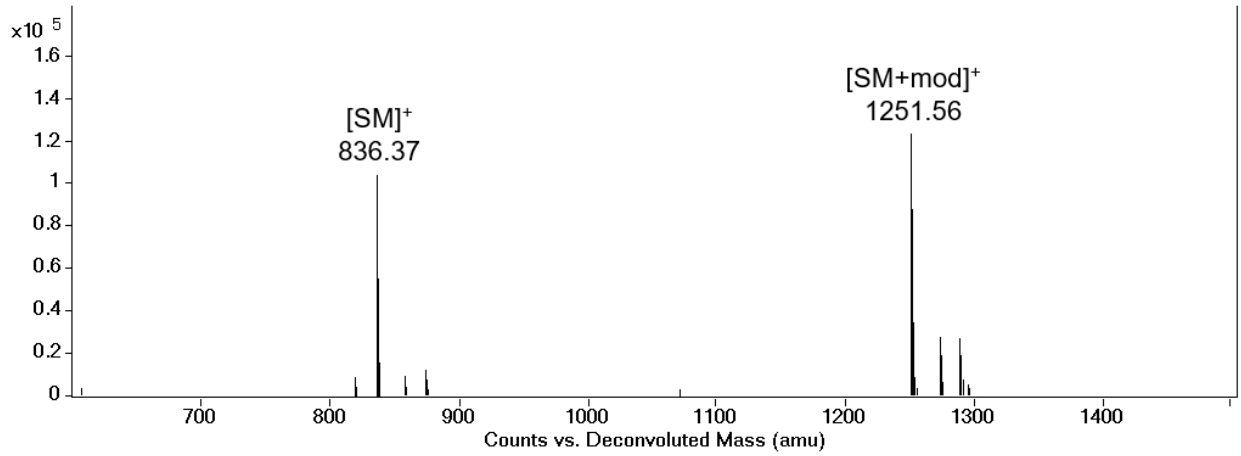

Figure S31. Deconvoluted EIC (500-1500 m/z) MS spectrum of the crude reaction of **gpep1** with diazo compound **8** using catalyst **7**. 836.37 and 1251.56 correspond to $[SM]^+$ and $[SM+mod]^+$ respectively.

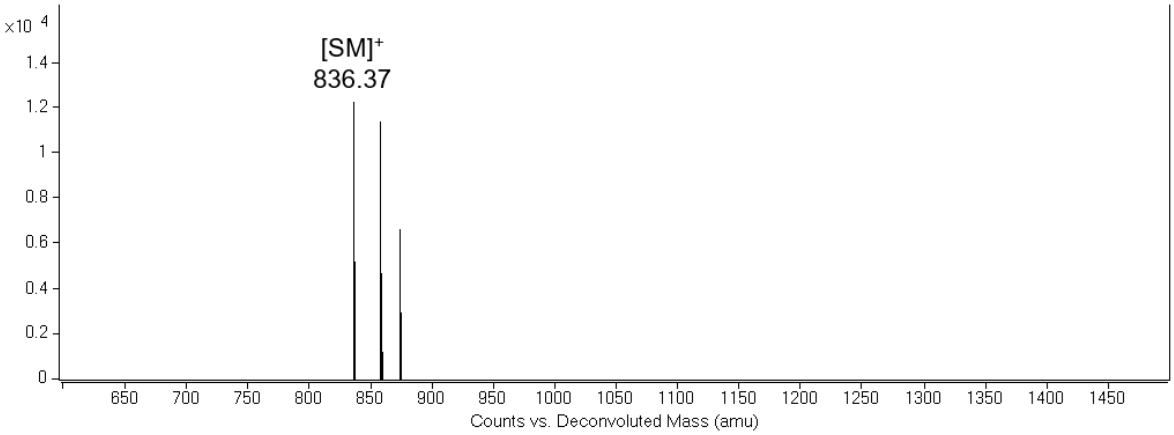

Figure S32. Deconvoluted EIC (500-1500 m/z) MS spectrum of the crude reaction of **gpep1** with diazo compound **8** using control catalyst $\mathbf{Rh_2OAc_4}$. 836.37 correspond to $[SM]^+$.

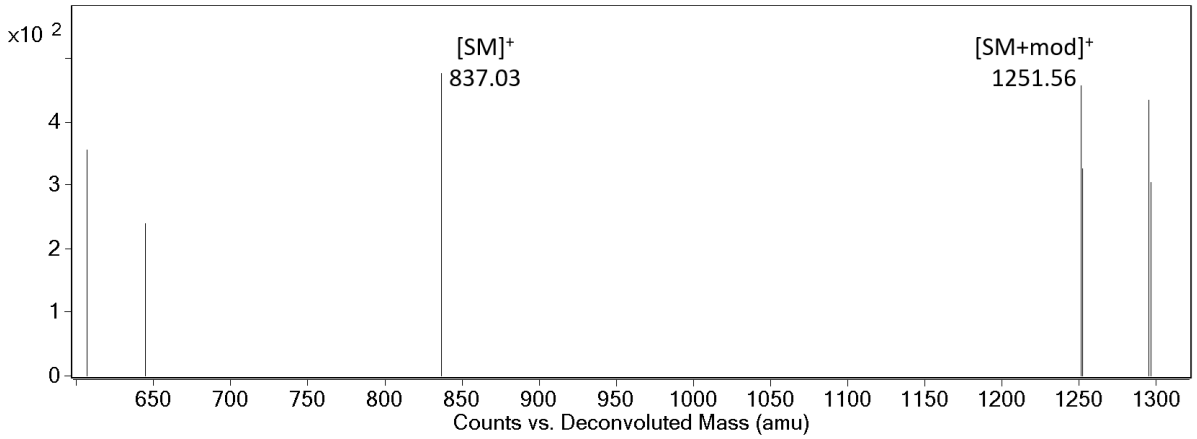

Figure S33. Deconvoluted EIC (500-1500 m/z) MS spectrum of the crude reaction of **gpep1** with diazo compound **8** using catalyst **7** in phosphates buffer. 837.03 and 1251.56 correspond to $[SM]^+$ and $[SM+mod]^+$ respectively.

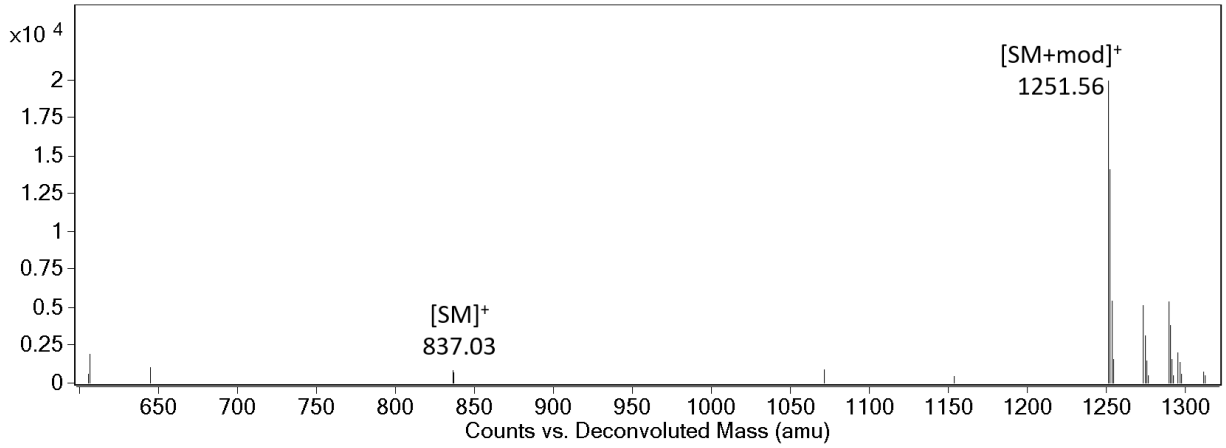

Figure S34. Deconvoluted EIC (500-1500 m/z) MS spectrum of the crude reaction of **gpep1** with diazo compound **8** using catalyst **7** in PBS buffer. 837.03 and 1251.56 correspond to $[SM]^+$ and $[SM+mod]^+$ respectively.

gpep2

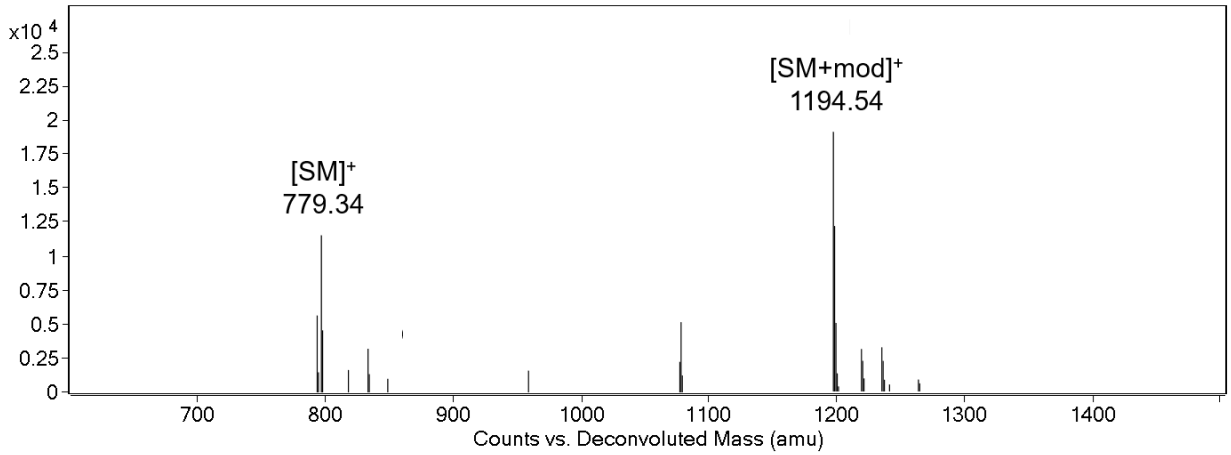

Figure S35. Deconvoluted EIC (500-1500 m/z) MS spectrum of the crude reaction of **gpep2** with diazo compound **8** using catalyst **7**. 779.34 and 1194.54 correspond to $[SM]^+$ and $[SM+mod]^+$ respectively.

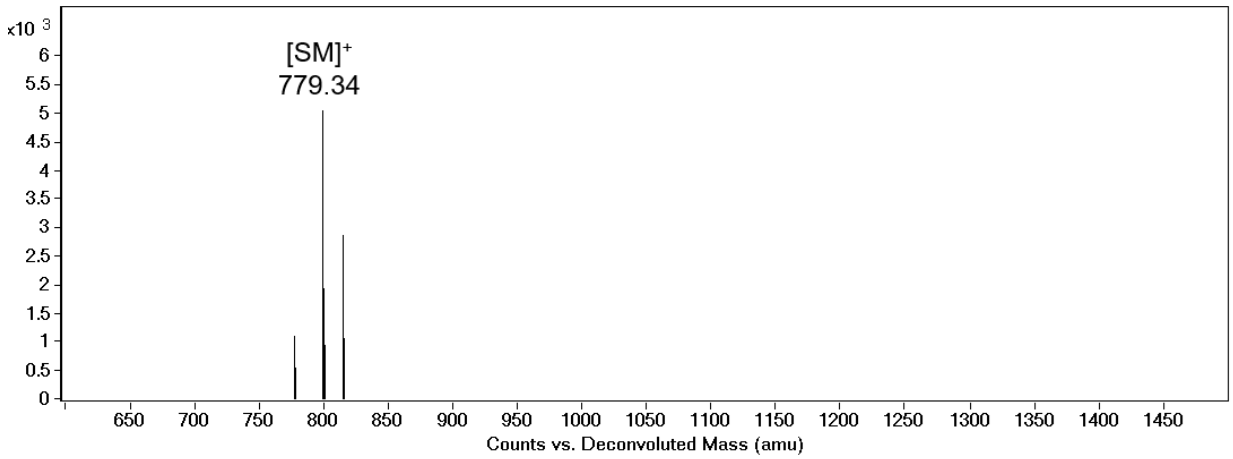

Figure S36. Deconvoluted EIC (500-1500 m/z) MS spectrum of the crude reaction of **gpep2** with diazo compound **8** using control catalyst $\mathbf{Rh_2OAc_4}$. 779.34 corresponds to $[SM]^+$.

gpep3

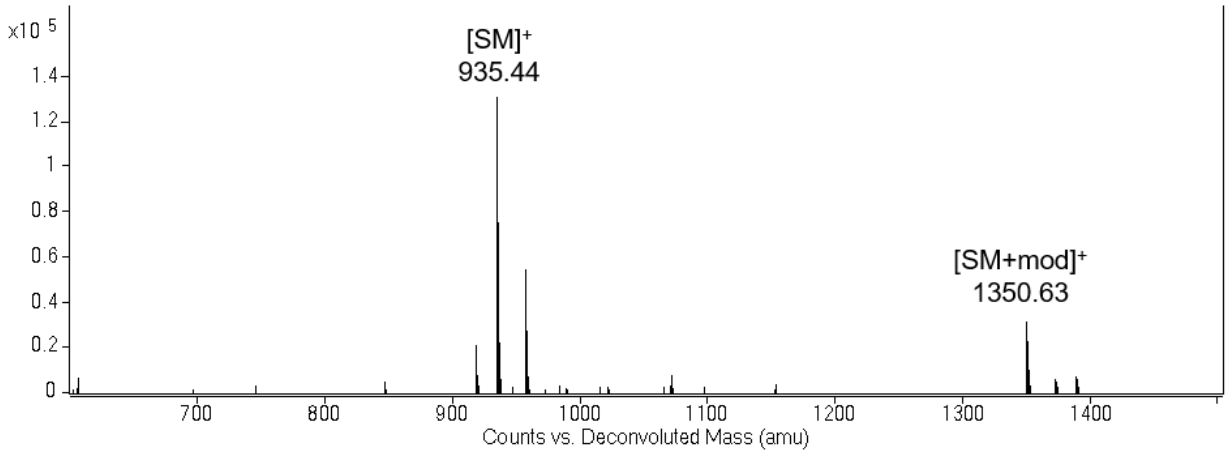

Figure S37. Deconvoluted EIC (500-1500 m/z) MS spectrum of the crude reaction of **gpep3** with diazo compound **8** using catalyst **7**. 935.44 and 1350.63 correspond to $[SM]^+$ and $[SM+mod]^+$ respectively.

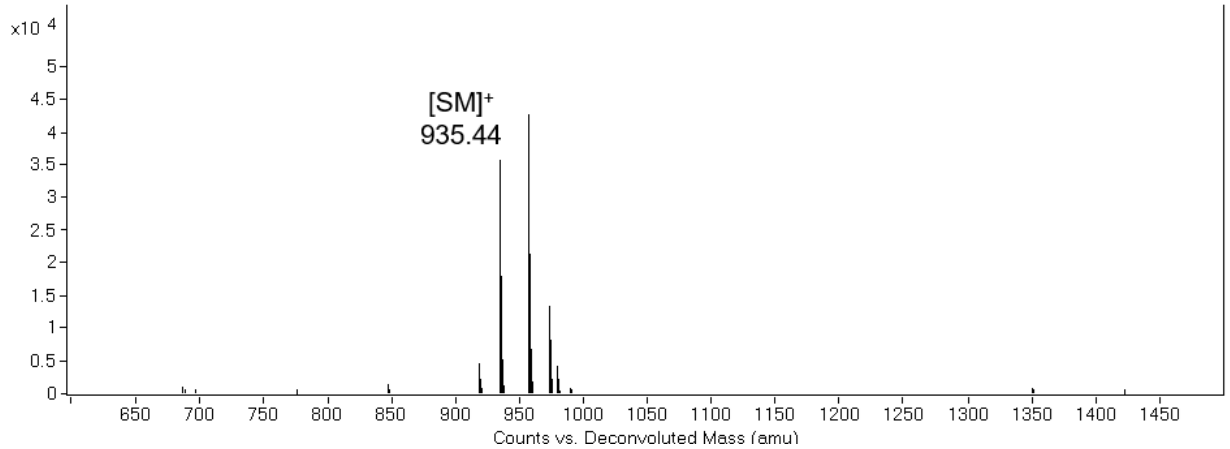

Figure S38. Deconvoluted EIC (500-1500 m/z) MS spectrum of the crude reaction of **gpep3** with diazo compound **8** using control catalyst $\mathbf{Rh_2OAc_4}$. 935.44 correspond to $[SM]^+$.

gpep4

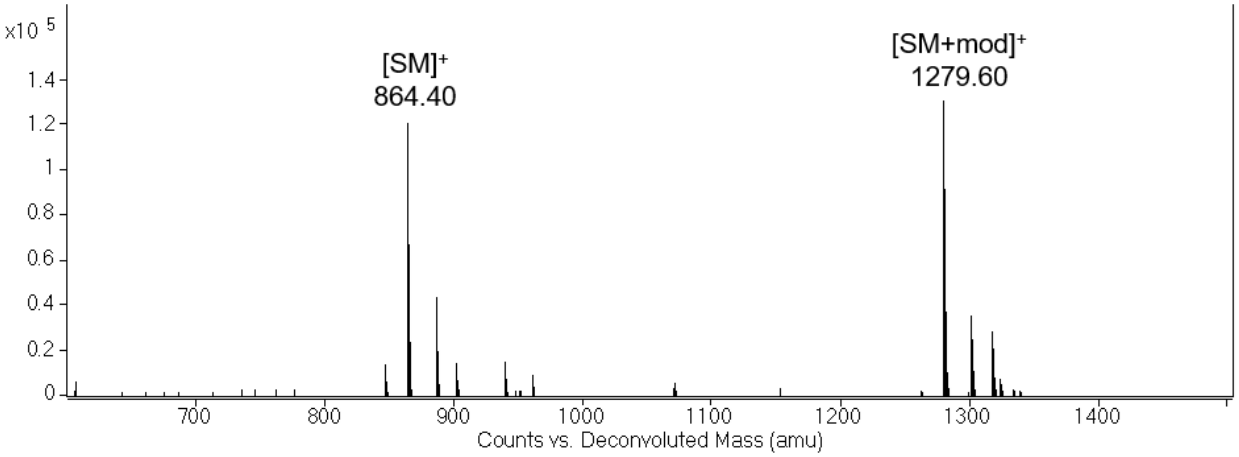

Figure S39. Deconvoluted EIC (500-1500 m/z) MS spectrum of the crude reaction of **gpep4** with diazo compound **8** using catalyst **7**. 864.40 and 1279.60 correspond to $[SM]^+$ and $[SM+mod]^+$ respectively.

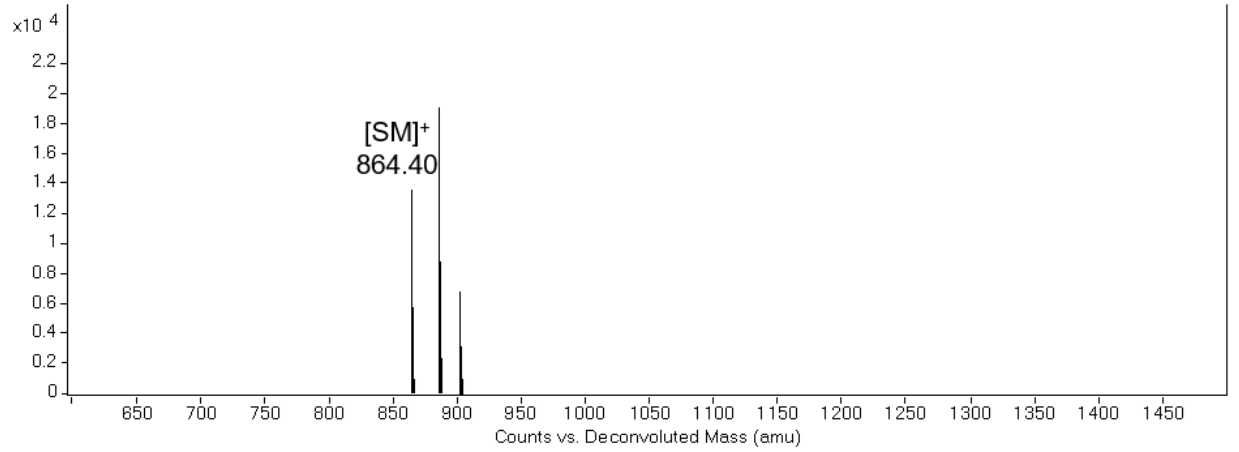

Figure S40. Deconvoluted EIC (500-1500 m/z) MS spectrum of the crude reaction of **gpep4** with diazo compound **8** using control catalyst $\mathbf{Rh_2OAc_4}$. 864.40 correspond to $[SM]^+$.

gpep5

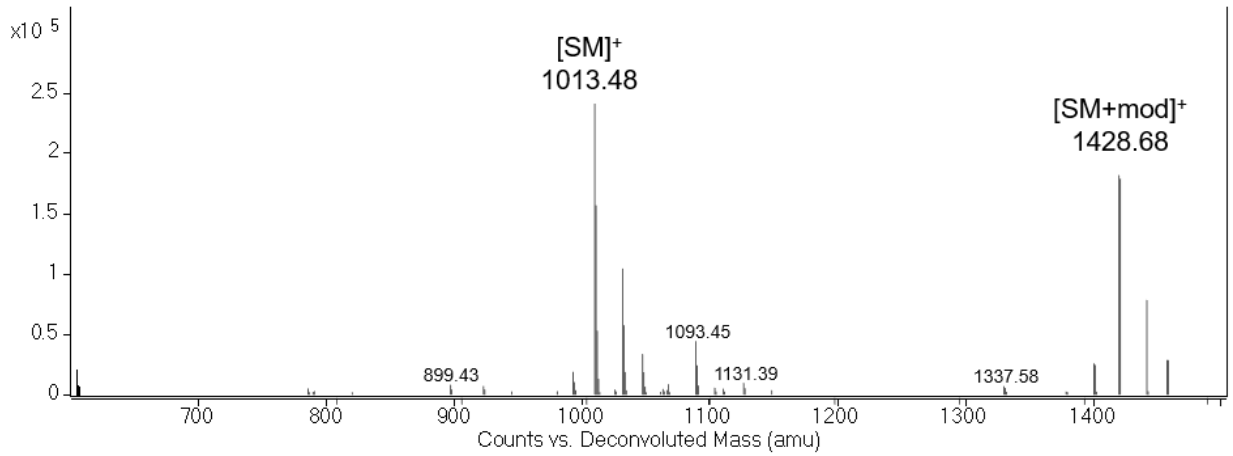

Figure S41. Deconvoluted EIC (500-1500 m/z) MS spectrum of the crude reaction of **gpep5** with diazo compound **8** using catalyst **7**. 1013.48 and 1428.68 correspond to $[SM]^+$ and $[SM+mod]^+$ respectively.

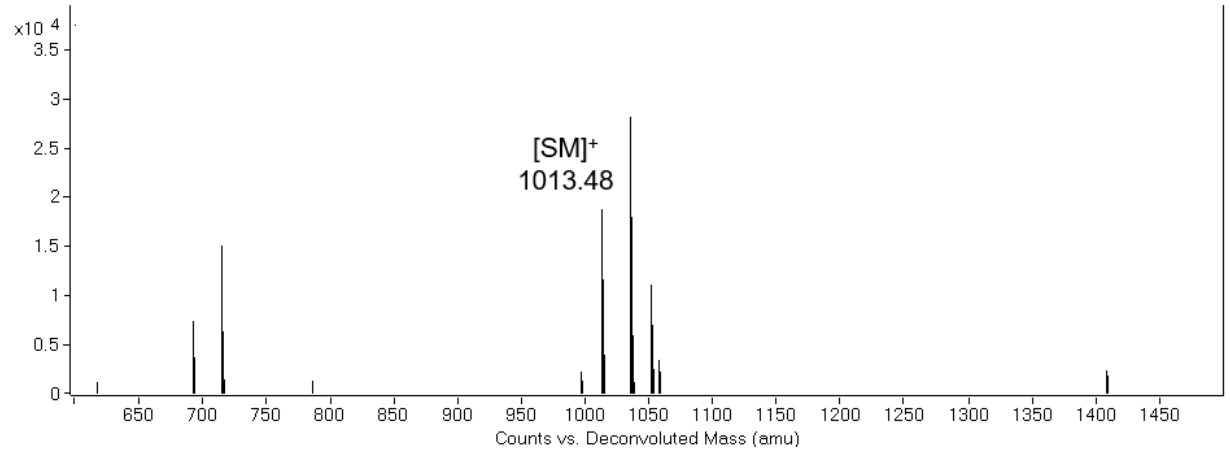

Figure S42. Deconvoluted EIC (500-1500 m/z) MS spectrum of the crude reaction of **gpep5** with diazo compound **8** using control catalyst $\mathbf{Rh_2OAc_4}$. 1013.48 corresponds to $[SM]^+$.

gpep6

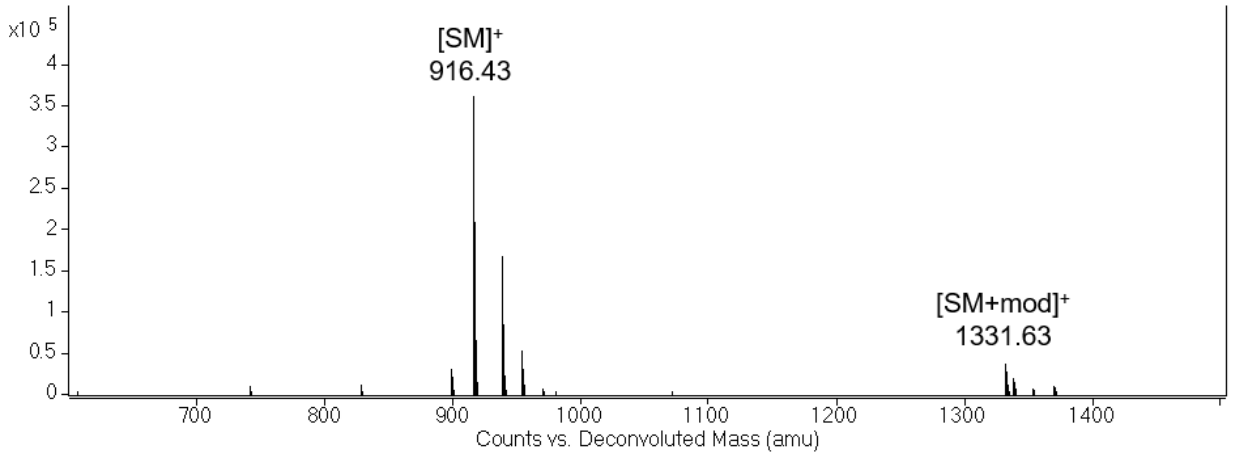

Figure S43. Deconvoluted EIC (500-1500 m/z) MS spectrum of the crude reaction of **gpept6** with diazo compound **8** using catalyst **7**. 916.43 and 1331.63 correspond to $[SM]^+$ and $[SM+mod]^+$ respectively.

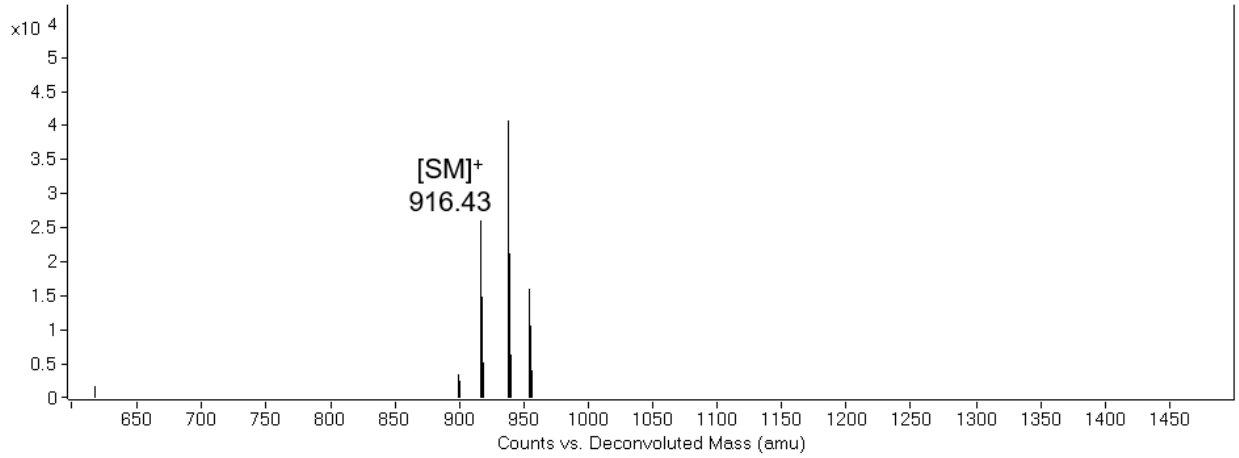

Figure S44. Deconvoluted EIC (500-1500 m/z) MS spectrum of the crude reaction of **gpep6** with diazo compound **8** using control catalyst $\mathbf{Rh_2OAc_4}$. 916.43 correspond to $[SM]^+$.

gpep7

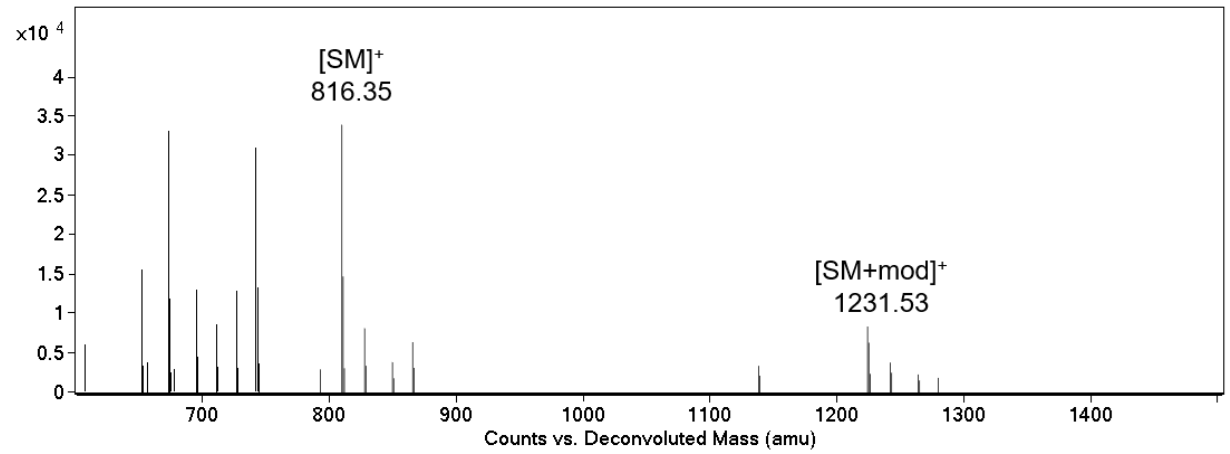

Figure S45. Deconvoluted EIC (500-1500 m/z) MS spectrum of the crude reaction of **gpep7** with diazo compound **8** using catalyst **7**. 1065.53 and 1480.73 correspond to $[SM]^+$ and $[SM+mod]^+$ respectively.

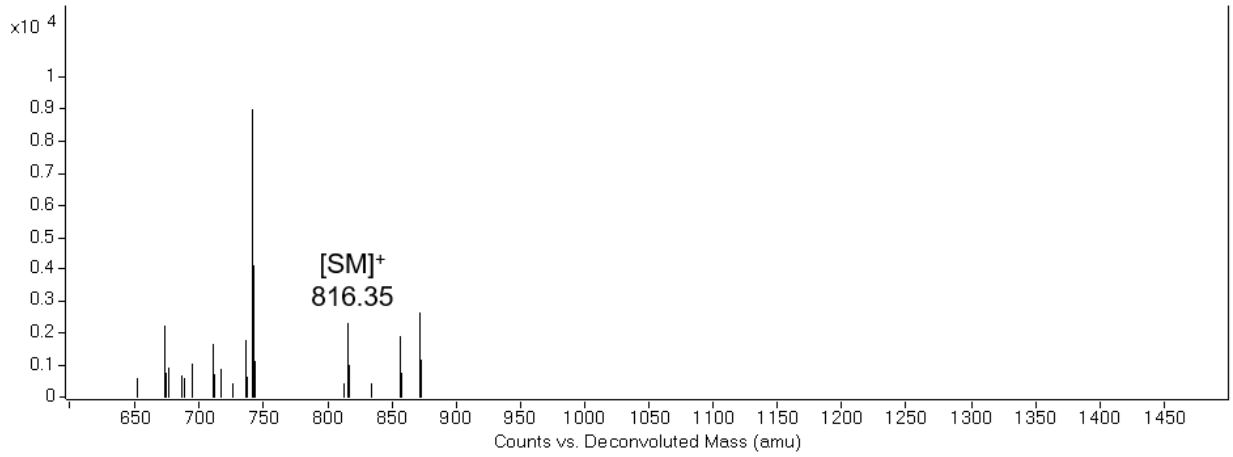

Figure S46. Deconvoluted EIC (500-1500 m/z) MS spectrum of the crude reaction of **gpep7** with diazo compound **8** using control catalyst $\mathbf{Rh_2OAc_4}$. 1065.53 correspond to $[SM]^+$.

gpep8

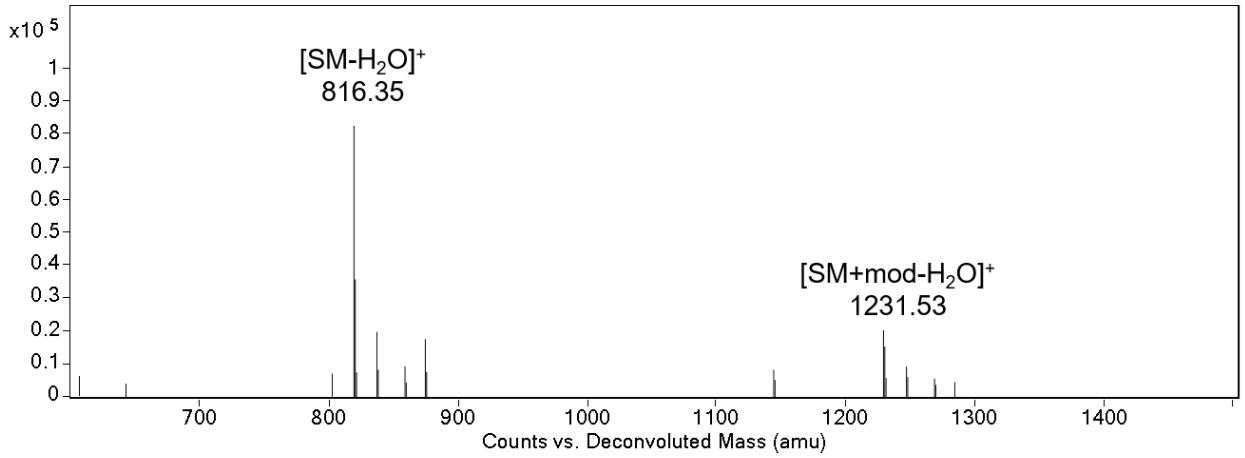

Figure S47. Deconvoluted EIC (500-1500 m/z) MS spectrum of the crude reaction of **gpep1** with diazo compound **8** using catalyst **7**. 816.35 and 1231.53 correspond to $[SM]^+$ and $[SM+mod\text{-}H_2O]^+$ respectively.

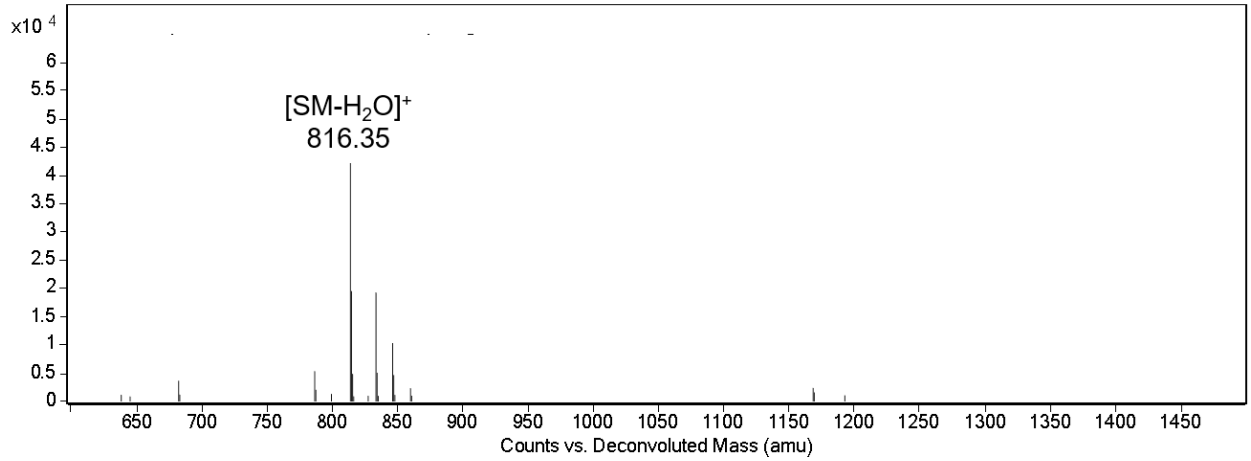

Figure S48. Deconvoluted EIC (500-1500 m/z) MS spectrum of the crude reaction of **gpep8** with diazo compound **8** using control catalyst $\mathbf{Rh_2OAc_4}$. 816.34 correspond to $[SM\text{-}H_2O]^+$.

gpep9

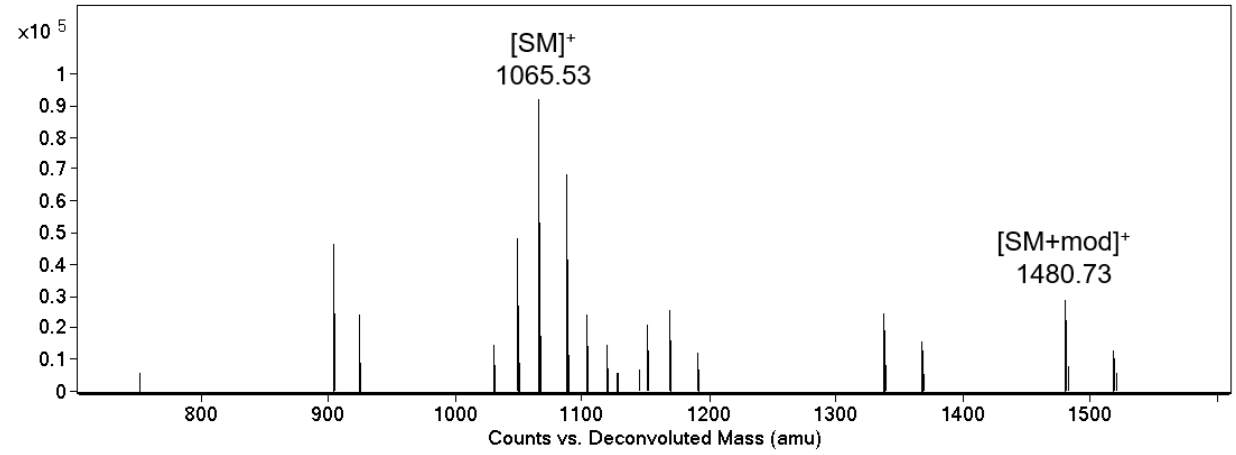

Figure S49. Deconvoluted EIC (500-1500 m/z) MS spectrum of the crude reaction of **gpep9** with diazo compound **8** using catalyst **7**. 848.37 and 1263.57 correspond to $[SM]^+$ and $[SM+mod]^+$ respectively.

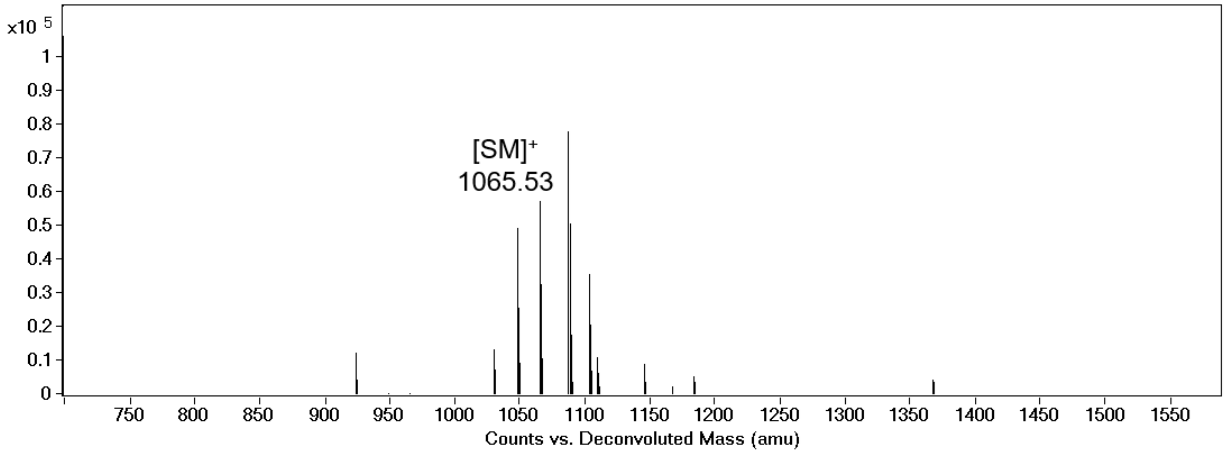

Figure S50. Deconvoluted EIC (500-1500 m/z) MS spectrum of the crude reaction of **gpep8** with diazo compound **8** using control catalyst $\mathbf{Rh_2OAc_4}$. 1065.53 correspond to $[SM]^+$.

gpep10

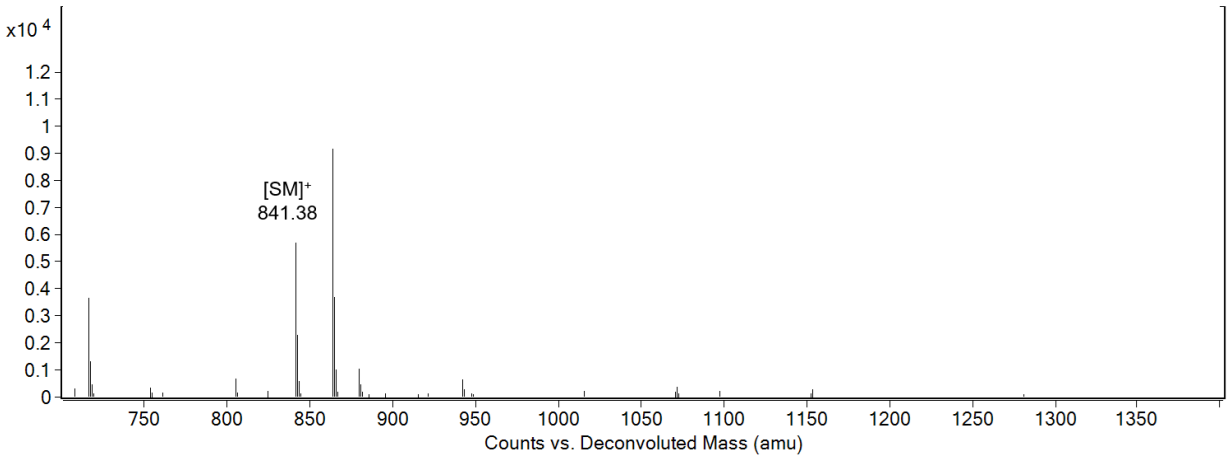

Figure S51. Deconvoluted EIC (500-1500 m/z) MS spectrum of the crude reaction of **gpep10** with diazo compound **8** using catalyst **7**. 825.39 correspond to $[SM]^+$.

gpep11

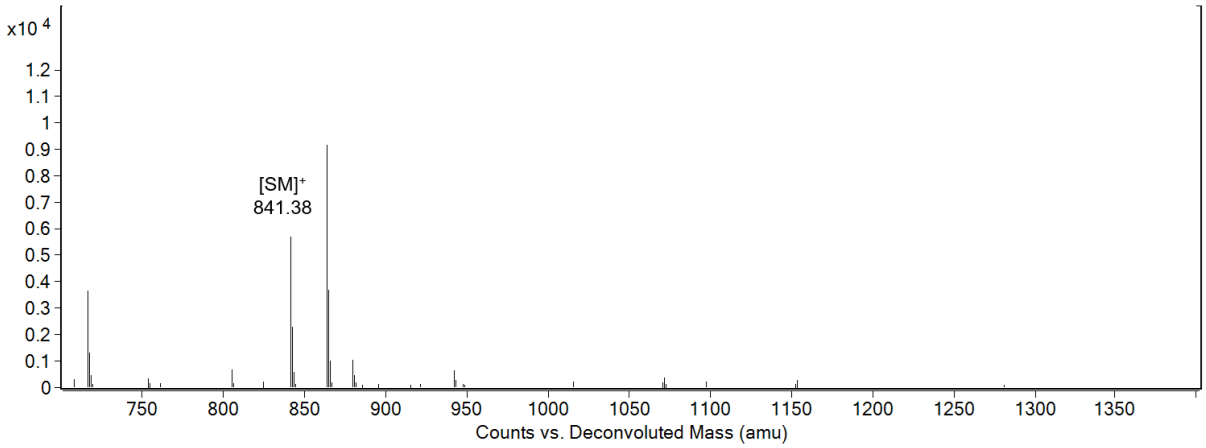

Figure S52. Deconvoluted EIC (500-1500 m/z) MS spectrum of the crude reaction of **gpep11** with diazo compound **8** using catalyst **7**. 841.38 correspond to $[SM]^+$.

MS/MS analysis of selected modified peptide products

MS/MS spectrum of modified gpep1

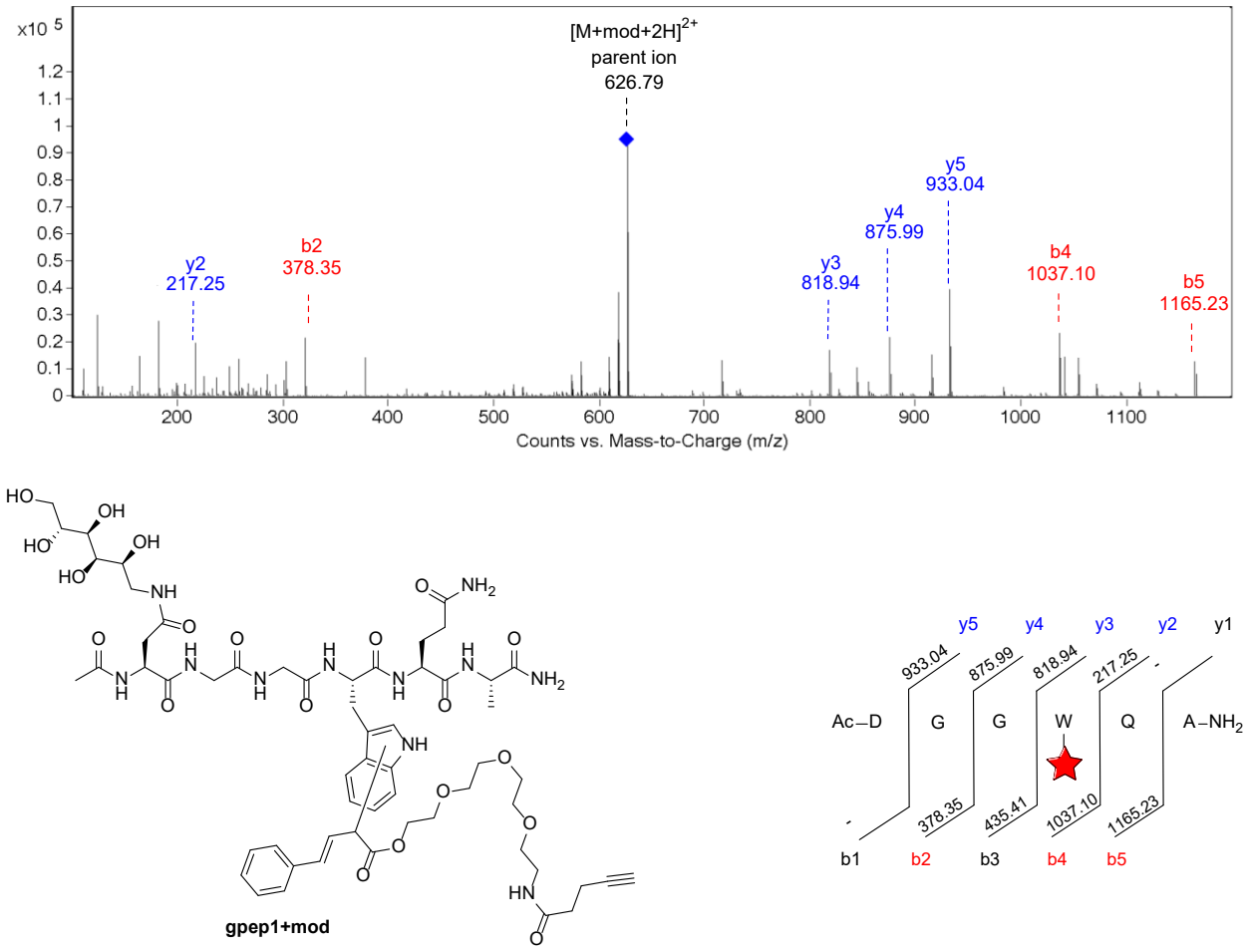

Figure S53. ESI-MS/MS fragmentation spectrum and fragmentation ladder of **gpep1** modified with diazo compound **8**.

MS/MS spectrum of modified gpep2

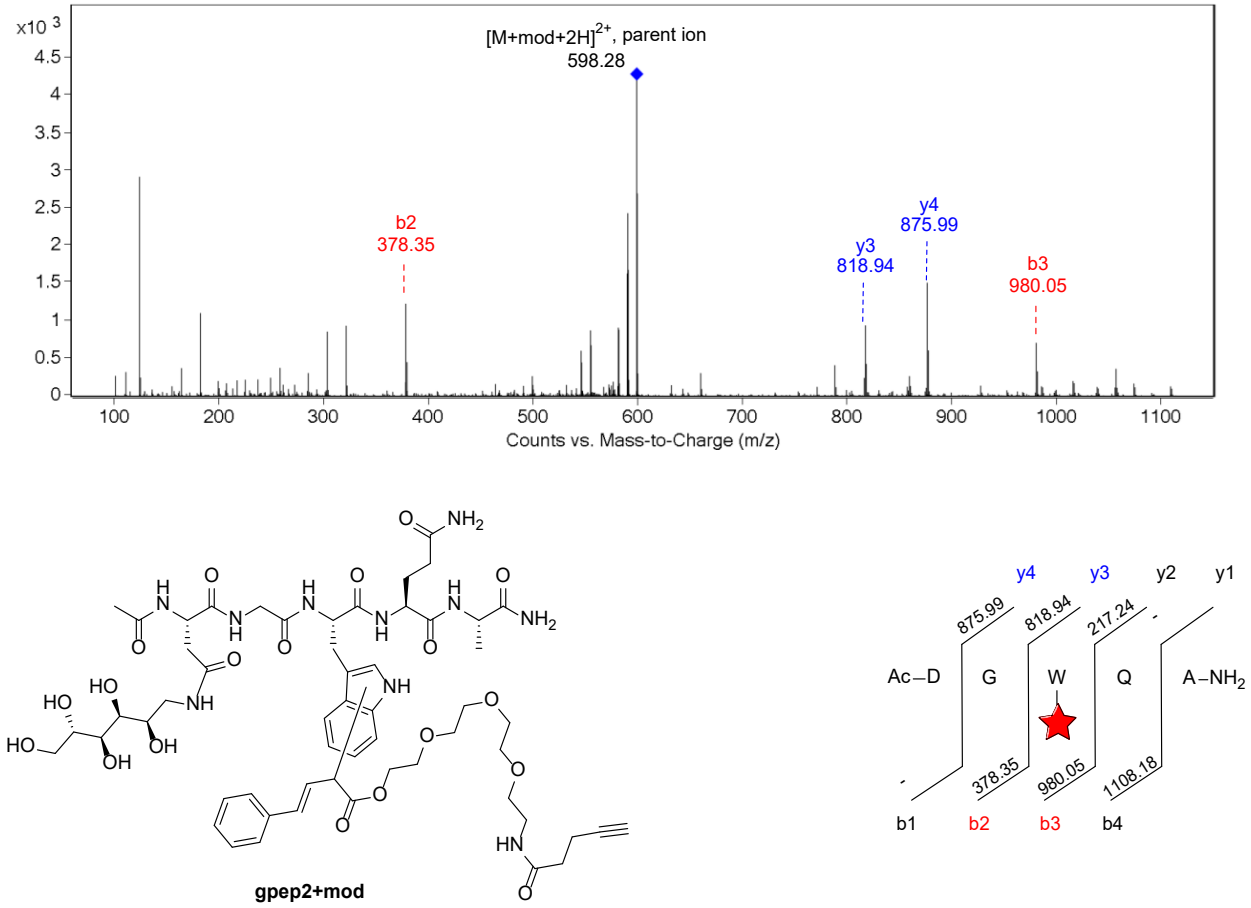

Figure S54. ESI-MS/MS fragmentation spectrum and fragmentation ladder of **gpep2** modified with diazo compound **8**.

MS/MS spectrum of modified gpep3

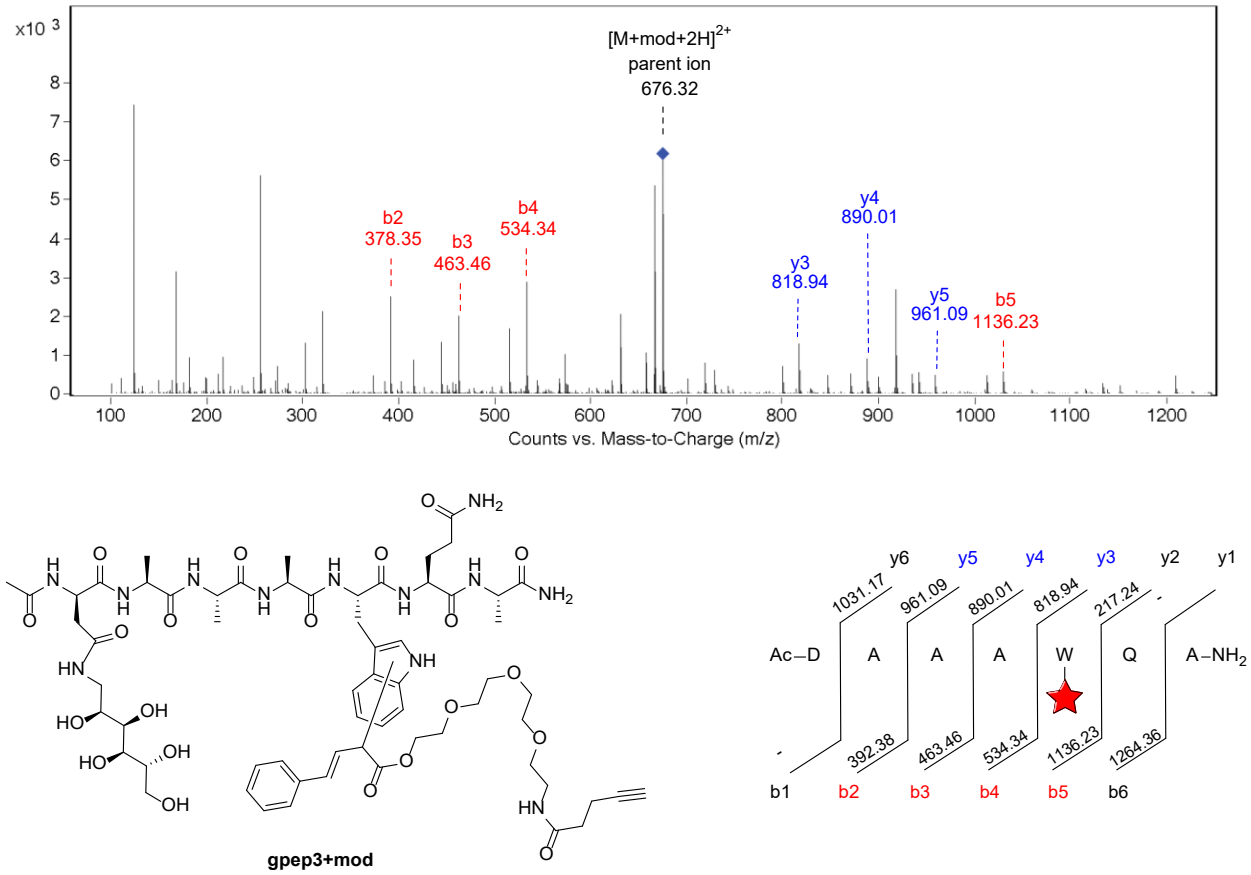

Figure S55. ESI-MS/MS fragmentation spectrum and fragmentation ladder of **gpep3** modified with diazo compound **8**.

MS/MS spectrum of modified gpep4

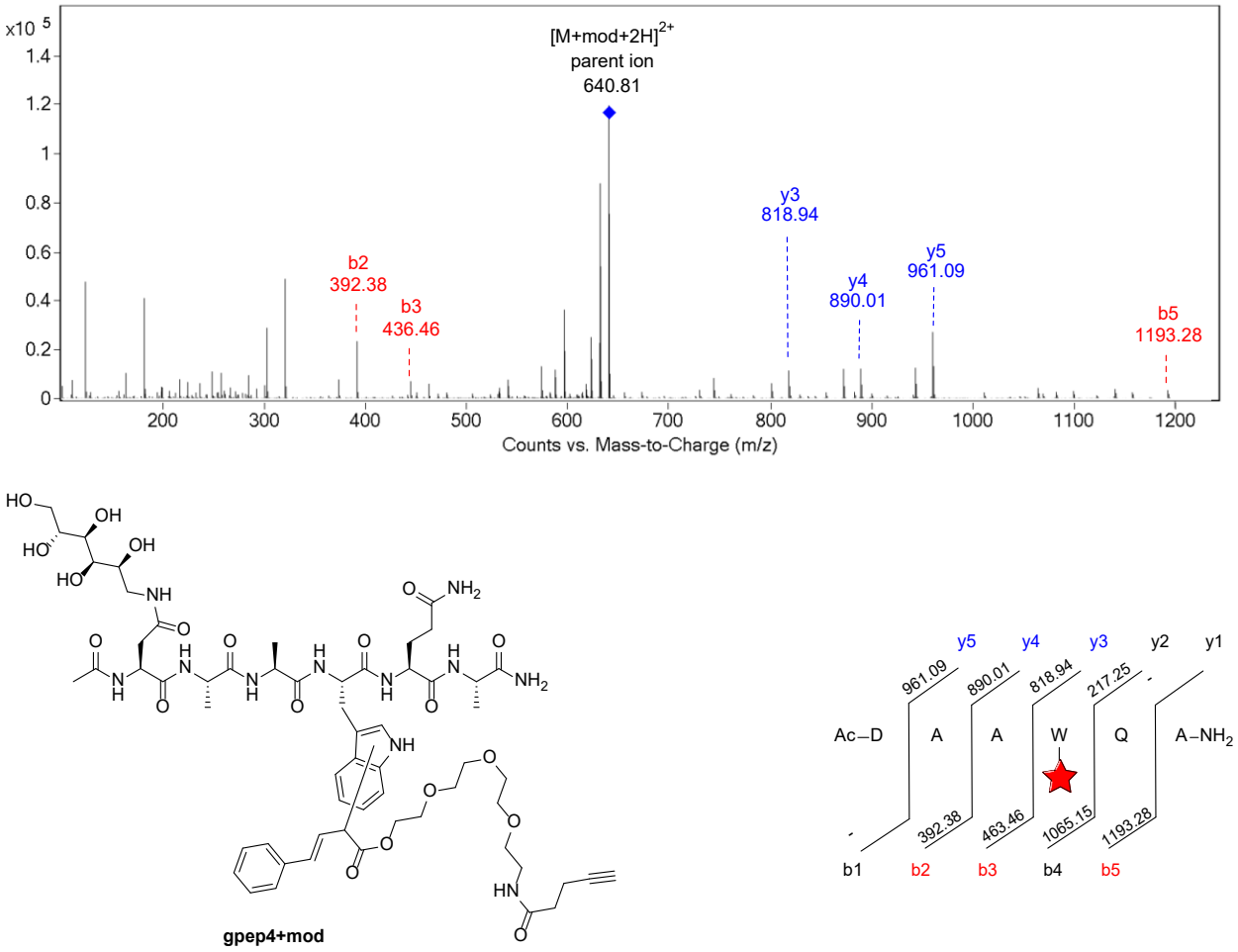

Figure S56. ESI-MS/MS fragmentation spectrum and fragmentation ladder of **gpep4** modified with diazo compound **8**.

MS/MS spectrum of modified gpep5

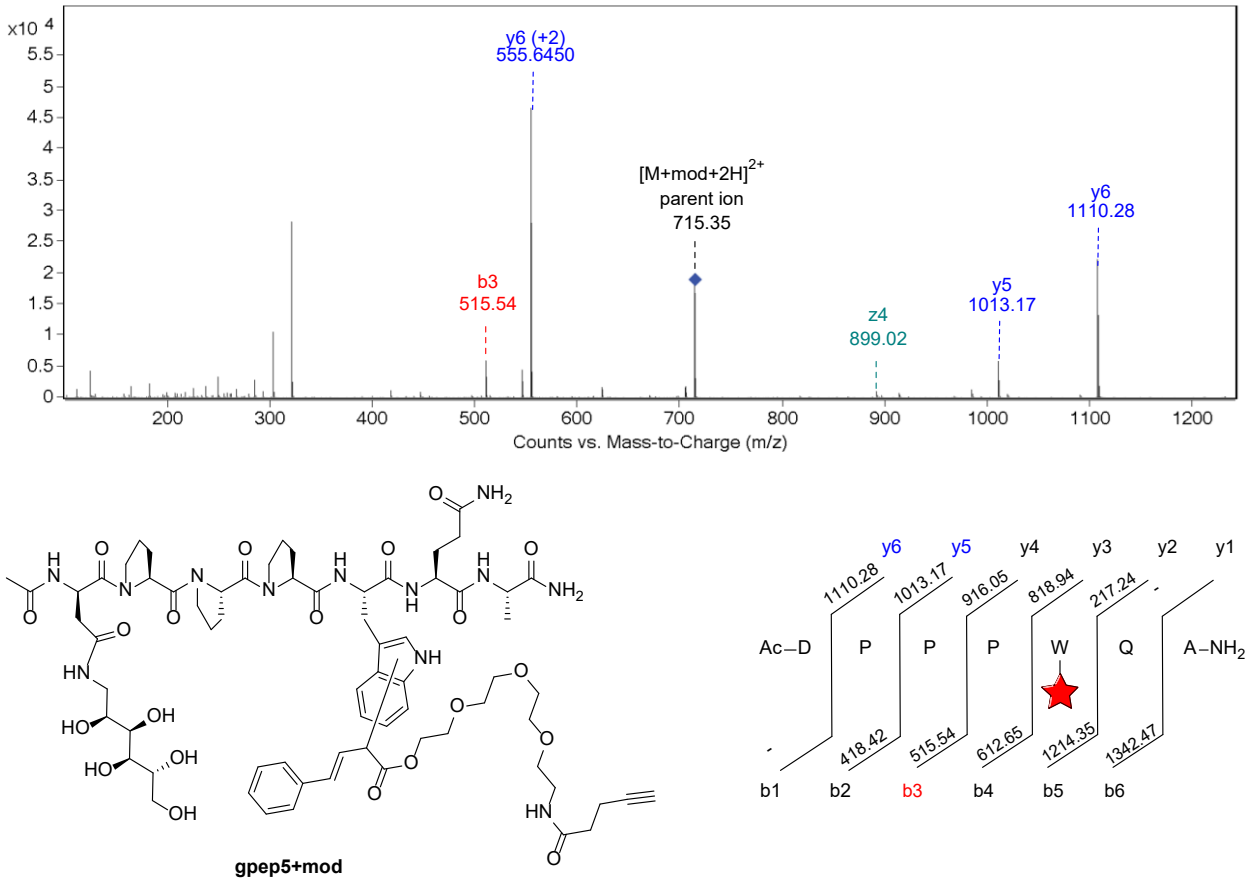

Figure S57. ESI-MS/MS fragmentation spectrum and fragmentation ladder of **gpep5** modified with diazo compound **8**.

MS/MS spectrum of modified gpep6

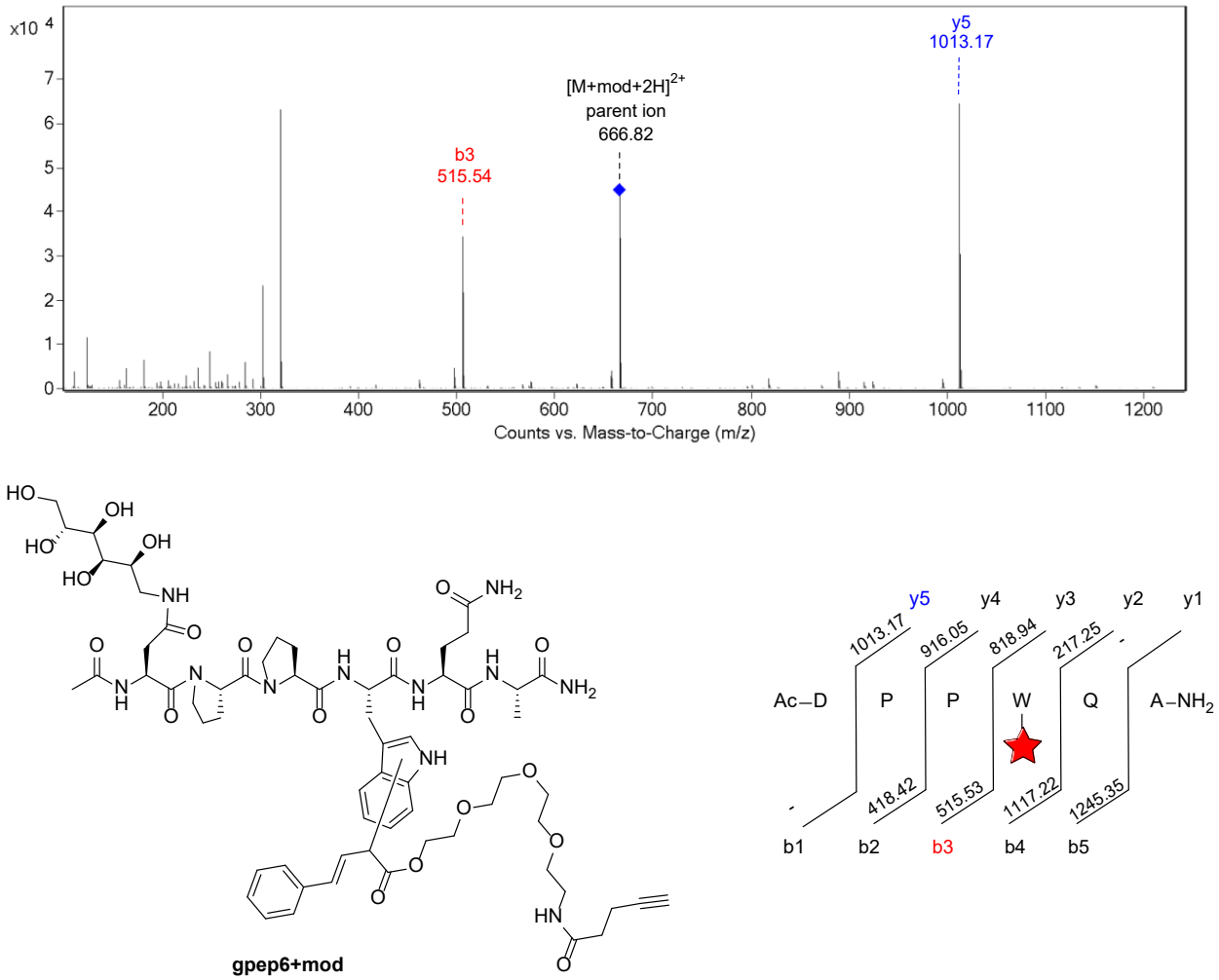

Figure S58. ESI-MS/MS fragmentation spectrum and fragmentation ladder of **gpep6** modified with diazo compound **8**.

MS/MS spectrum of modified gpep7

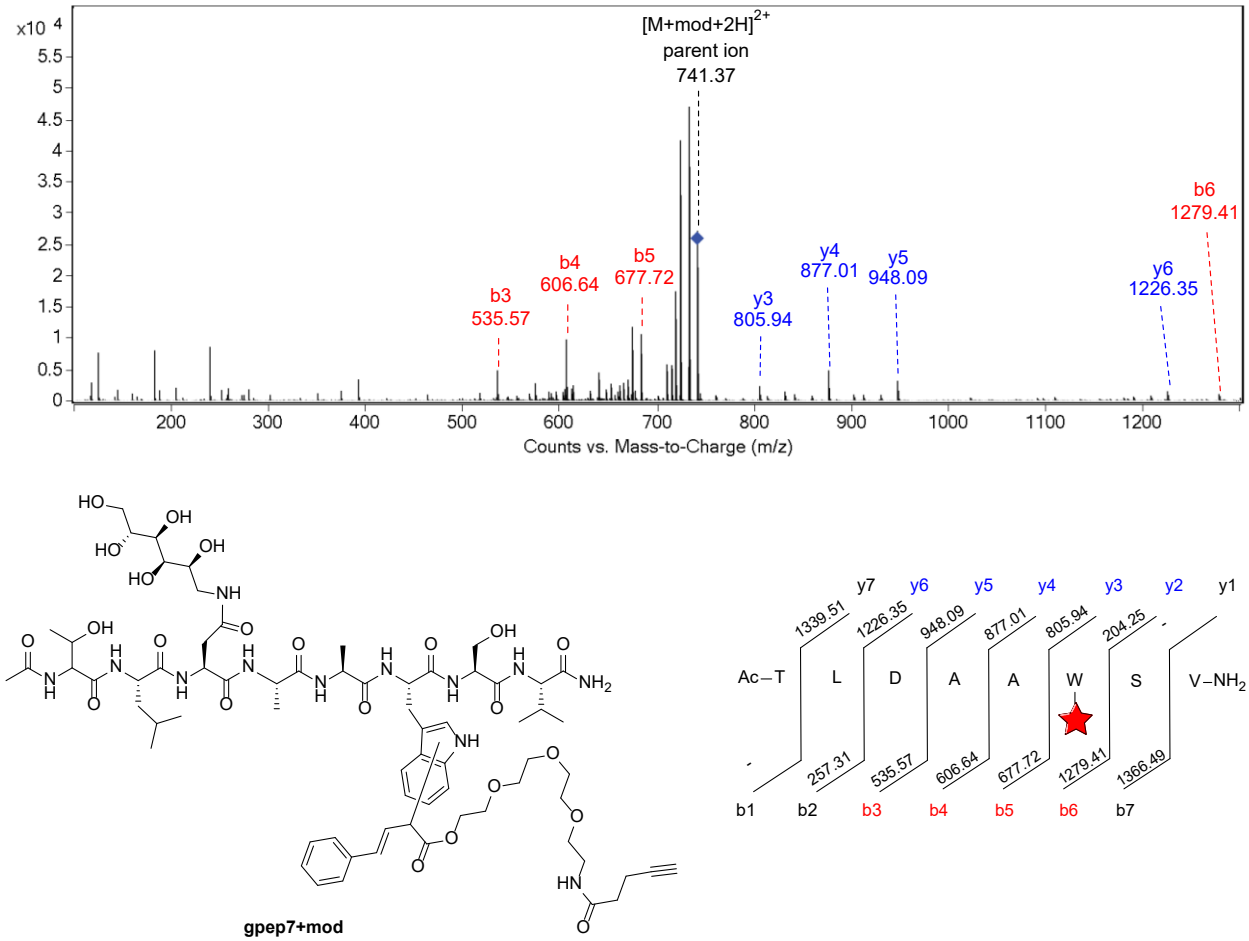

Figure S59. ESI-MS/MS fragmentation spectrum and fragmentation ladder of **gpep7** modified with diazo compound **8**.

MS/MS spectrum of modified gpep8

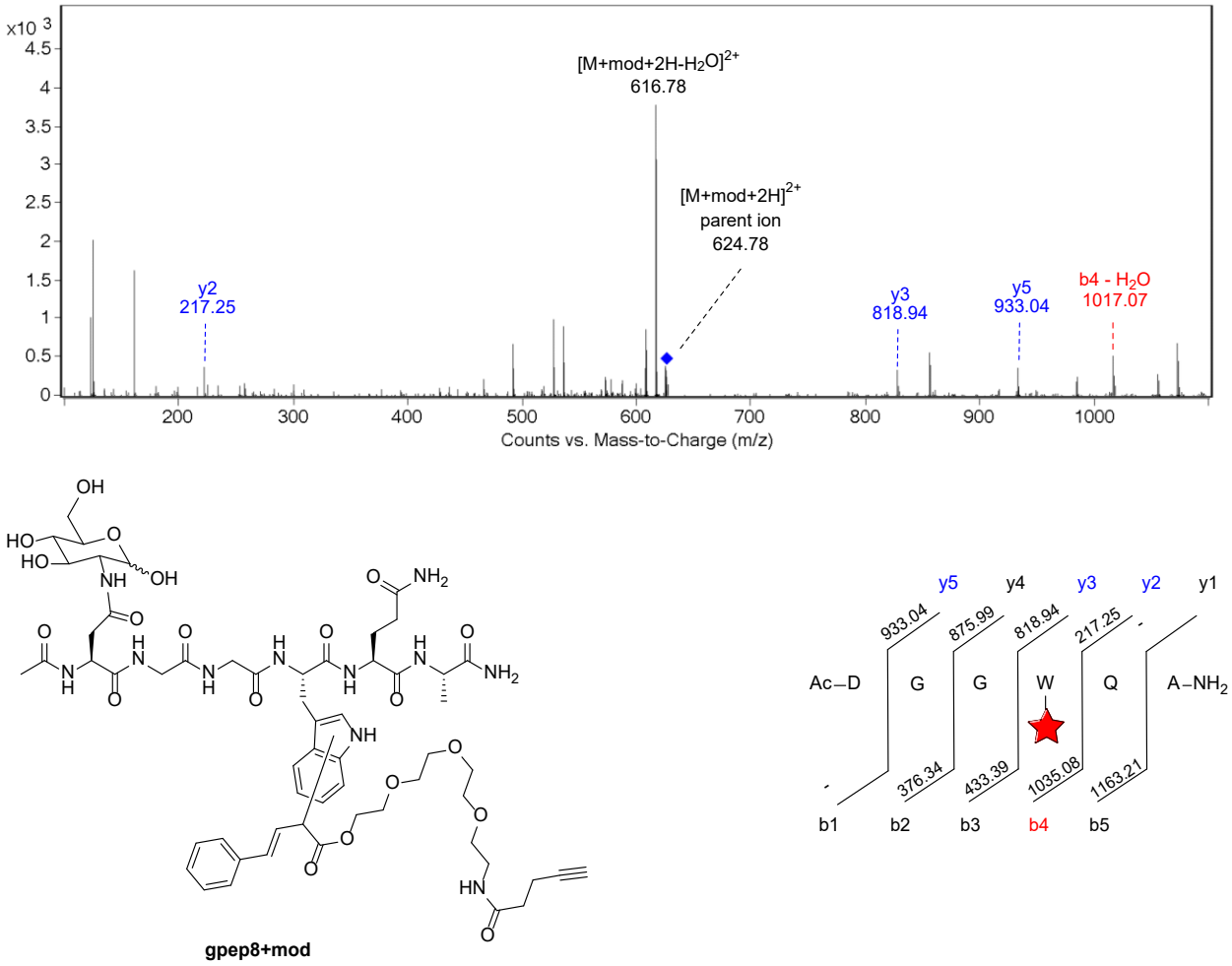

Figure S60. ESI-MS/MS fragmentation spectrum and fragmentation ladder of **gpep8** modified with diazo compound **8**.

MS/MS spectrum of modified gpep9

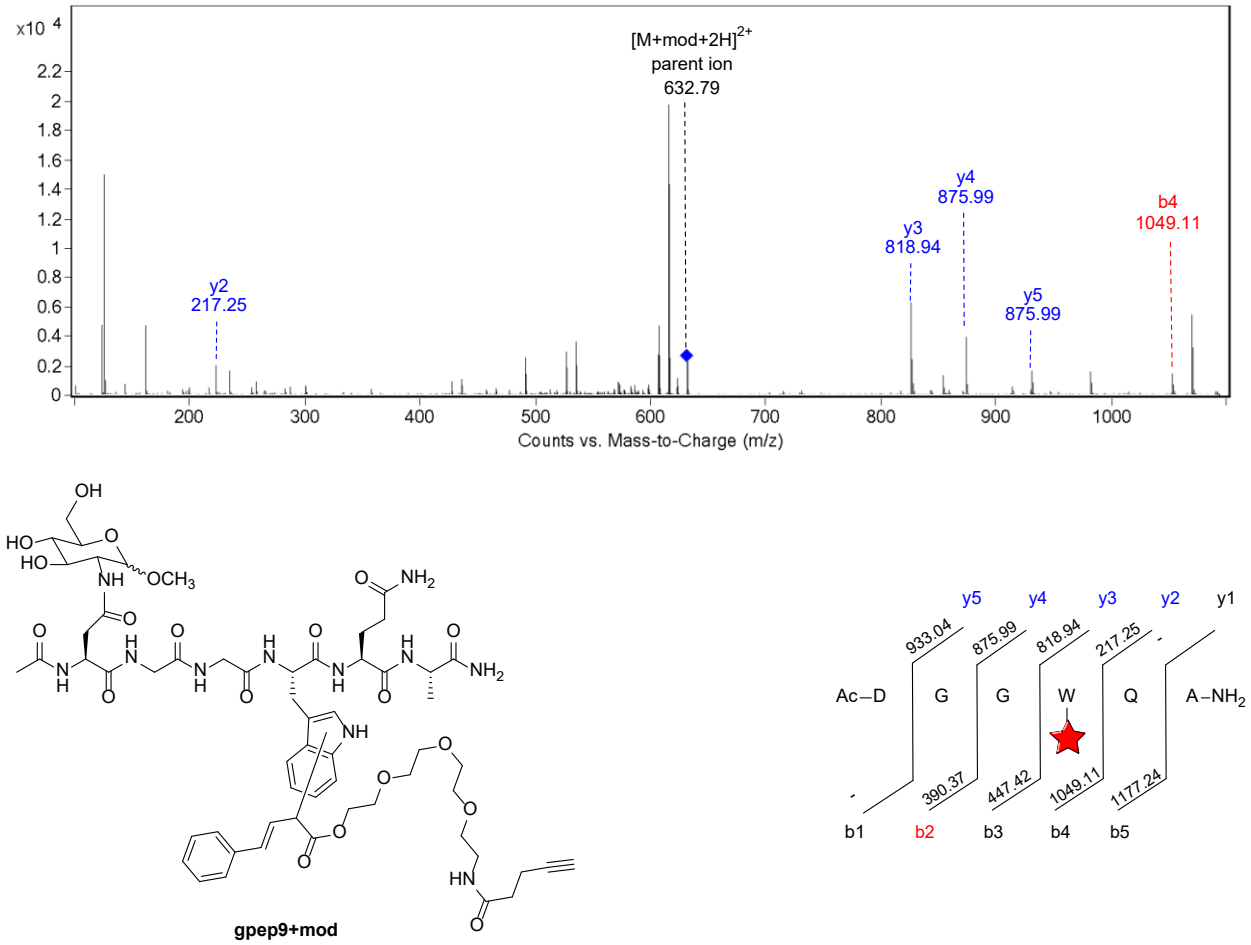

Figure S61. ESI-MS/MS fragmentation spectrum and fragmentation ladder of **gpep9** modified with diazo compound **8**.

Boronic ester formation study

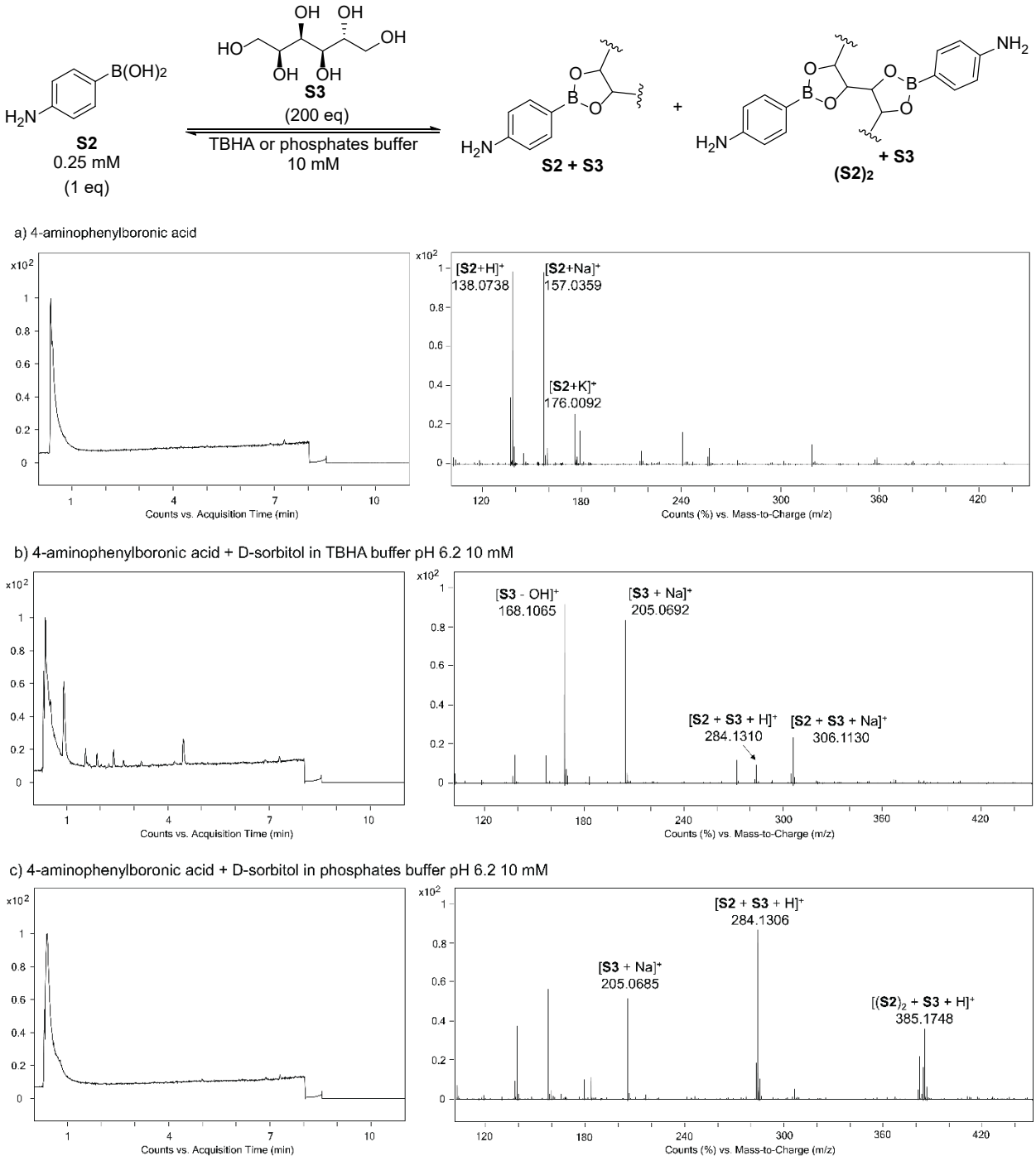

Figure S62. LC-MS chromatogram and EIC-MS spectrum (0.37 – 0.47 min) of 4-aminophenylboronic acid in a) water, b) TBHA buffer pH 6.2 10 mM with 200 eq of D-sorbitol, c) phosphates buffer pH 6.2 10 mM with 200 eq of D-sorbitol. Formation of the corresponding boronic esters is observed in both b) and c).

Characterization-HPLC, ESI-MS, LC-MS, LC-MS/MS, HRMS

HPLC and ESI-MS of synthesized boronic acid-Rh(II) catalysts from Figure 1 and 2

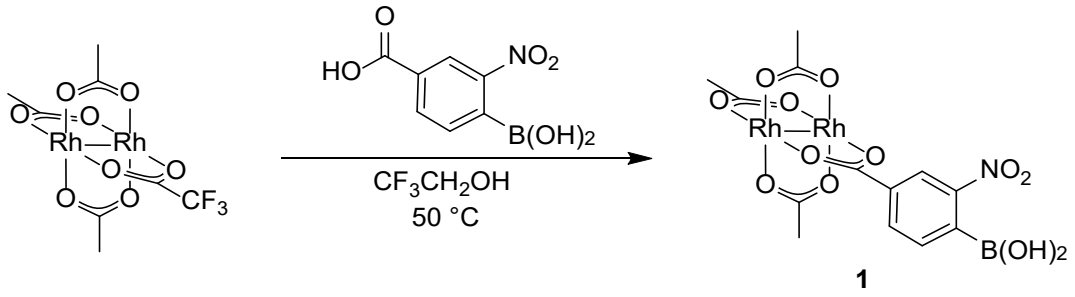

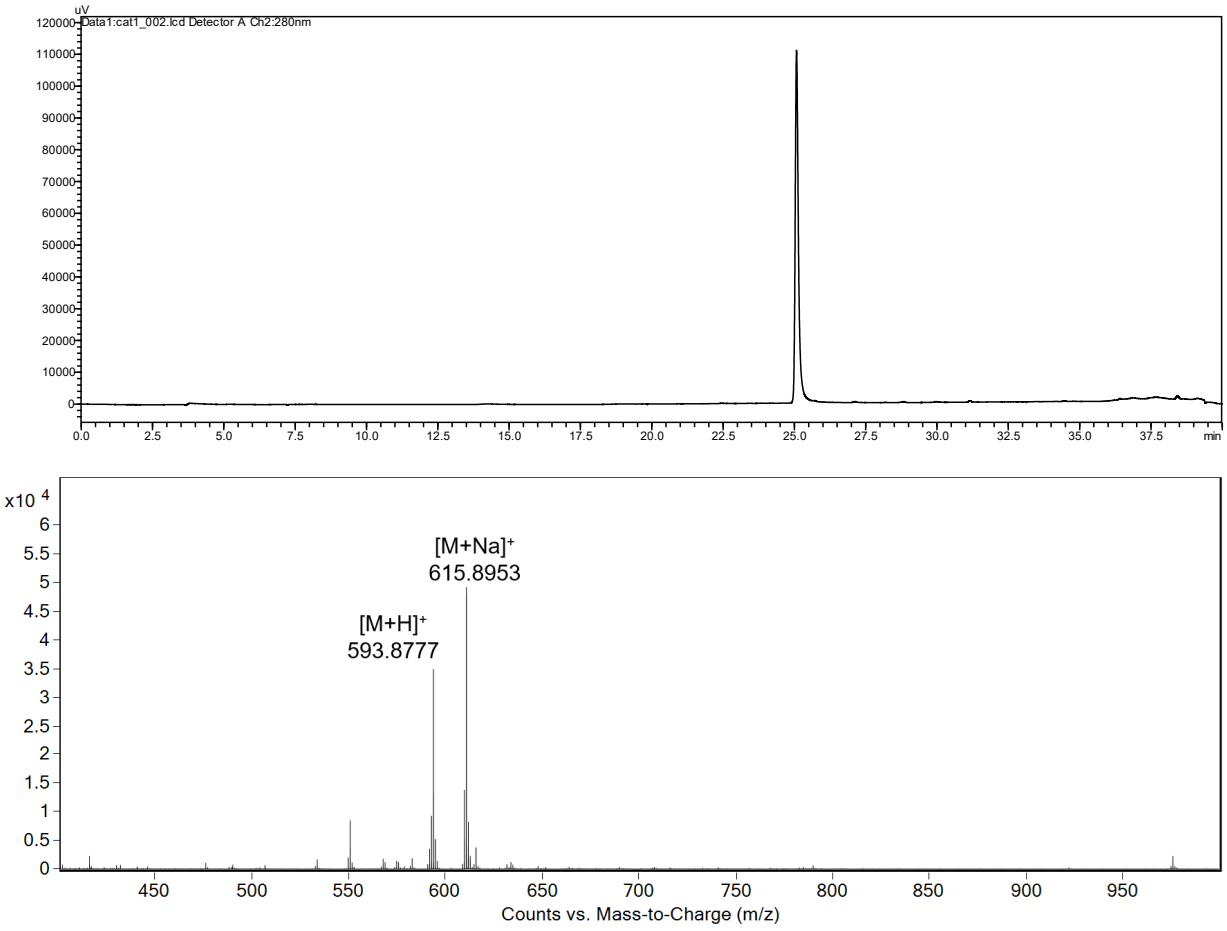

Figure S63. RP-HPLC trace at 280 nm (5-70% MeCN over 40 min) and ESI-MS spectrum of purified boronic acid-Rh(II) conjugate catalyst **1**. m/z 593.8777 and 615.8953 correspond to $[M+H]^+$ and $[M+Na]^+$ respectively.

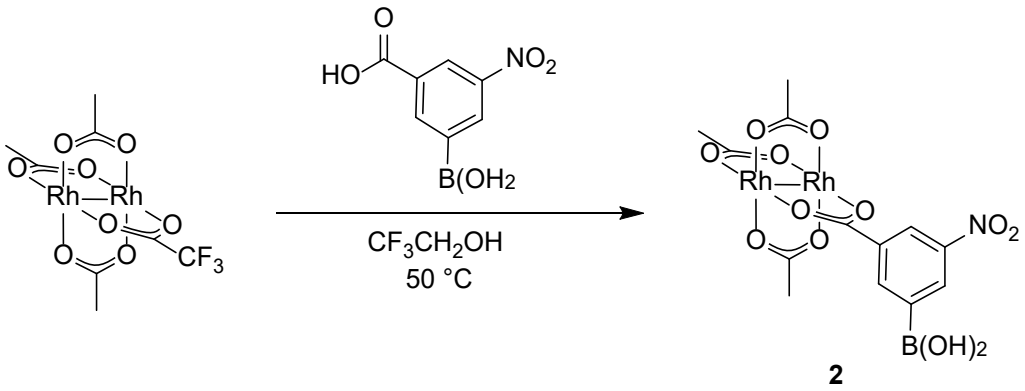

2

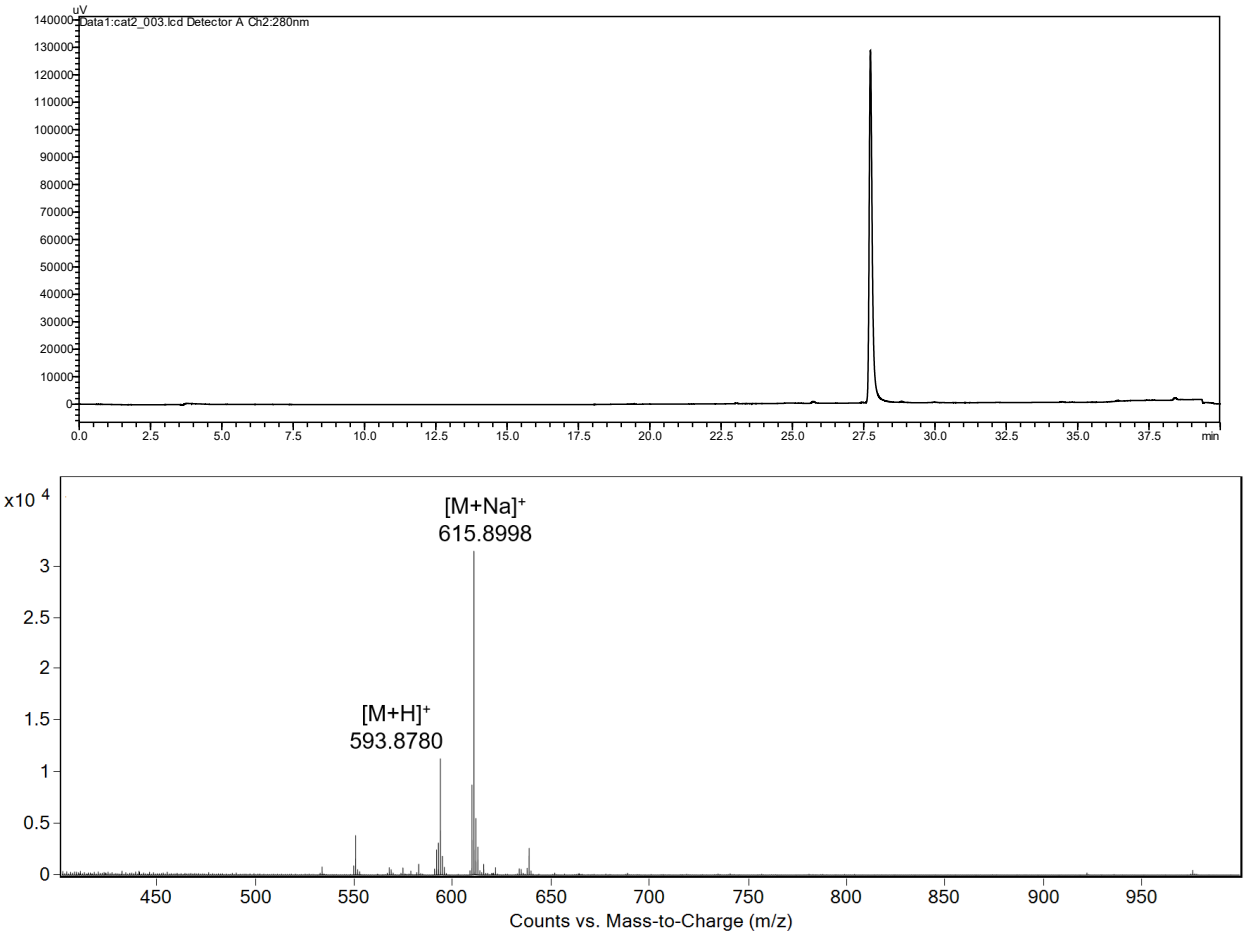

Figure S64. RP-HPLC trace at 280 nm (5-70% MeCN over 40 min) and ESI-MS spectrum of purified boronic acid-Rh(II) conjugate catalyst **2**. m/z 593.8780 and 615.8998 correspond to $[M+H]^+$ and $[M+Na]^+$ respectively.

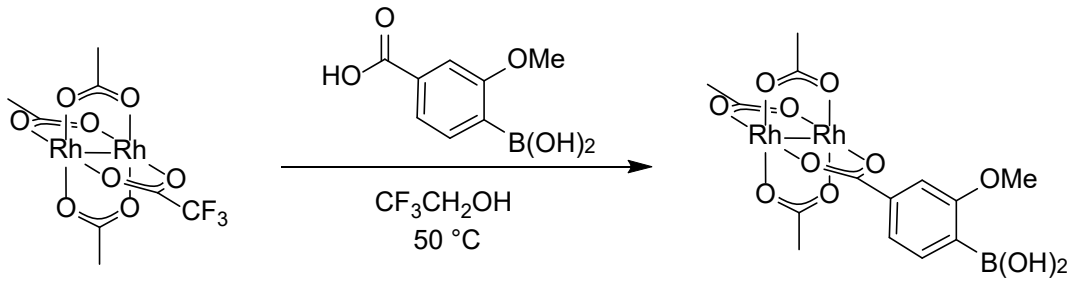

3

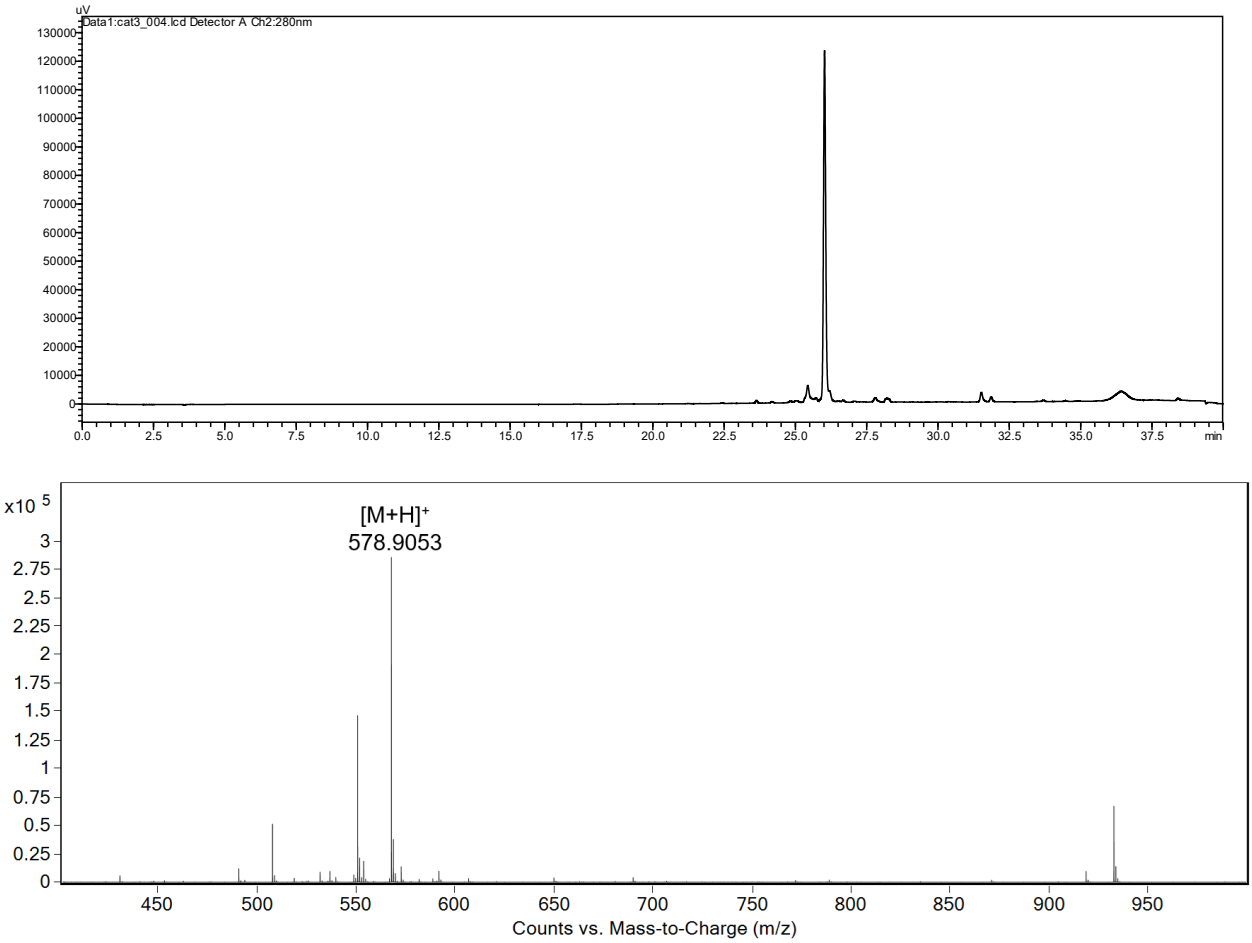

Figure S65. RP-HPLC trace at 280 nm (5-70% MeCN over 40 min) and ESI-MS spectrum of purified boronic acid-Rh(II) conjugate catalyst **3**. m/z 578.9053 corresponds to $[M+H]^+$.

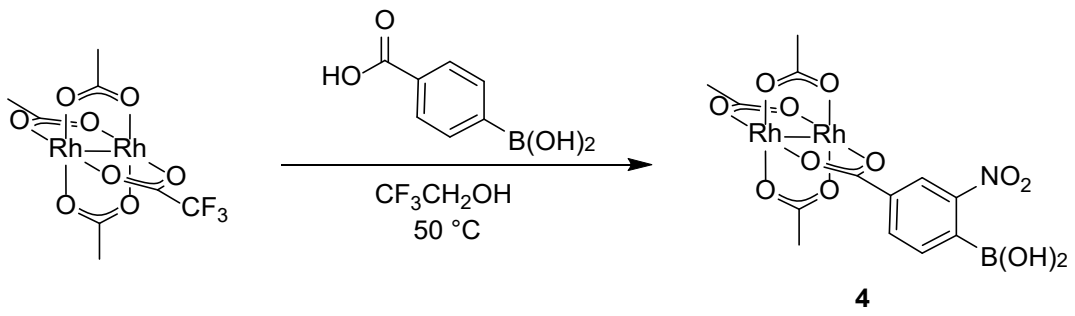

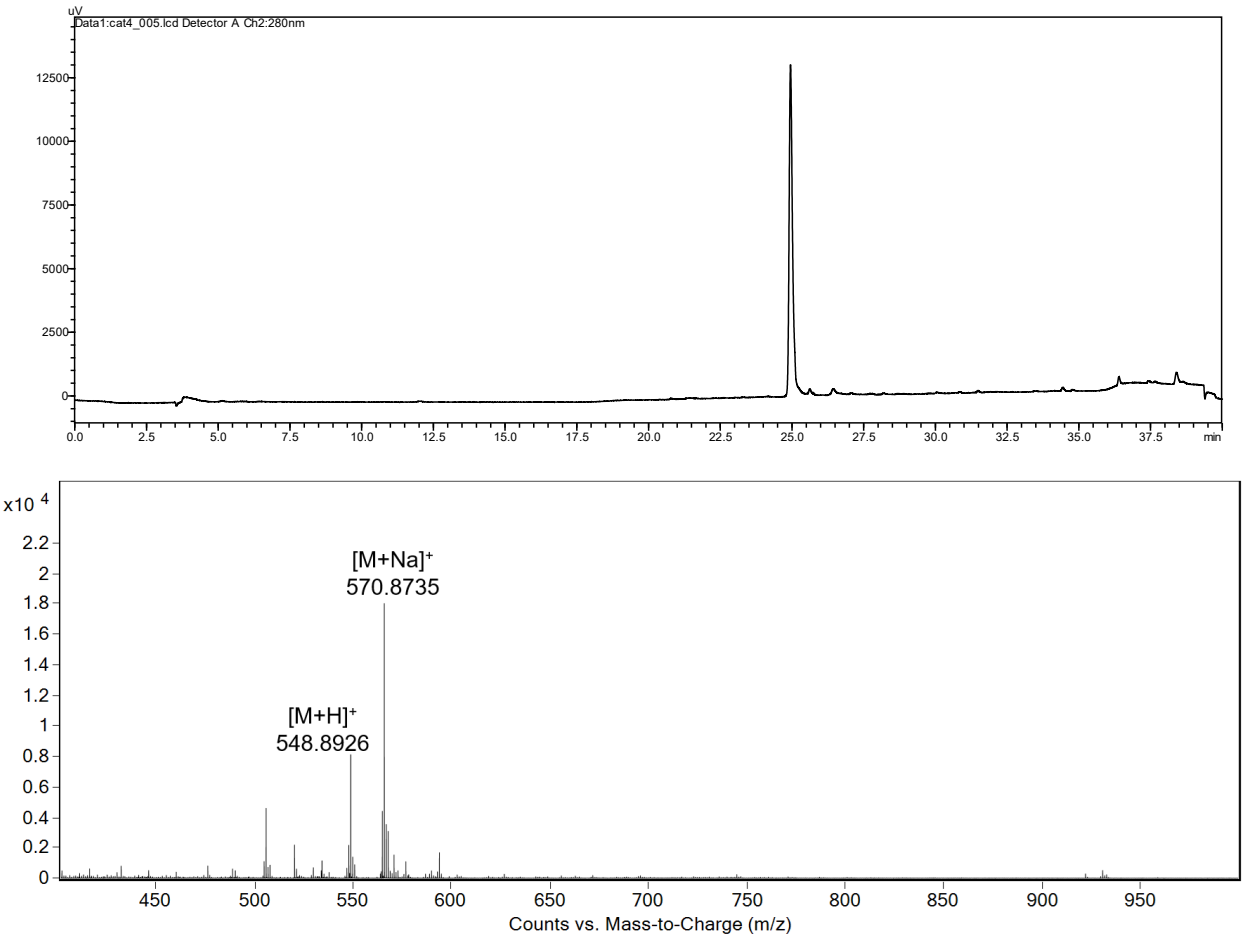

Figure S66. RP-HPLC trace at 280 nm (5-70% MeCN over 40 min) and ESI-MS spectrum of purified boronic acid-Rh(II) conjugate catalyst **4**. m/z 548.8926 and 570.8735 correspond to $[M+H]^+$ and $[M+Na]^+$ respectively.

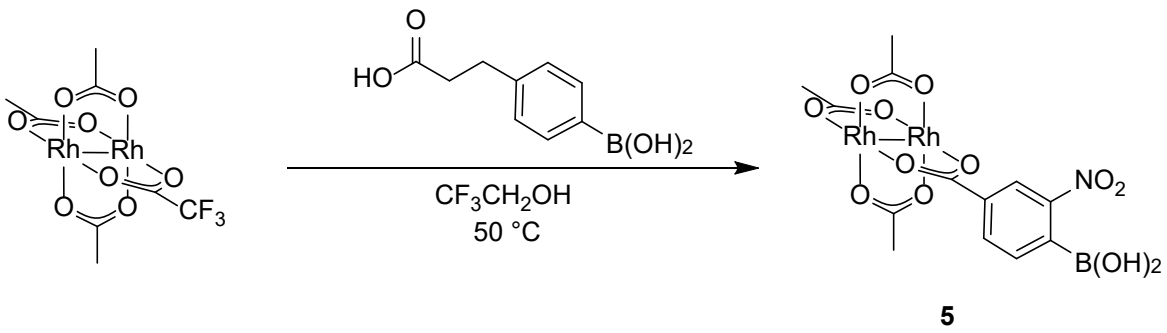

5

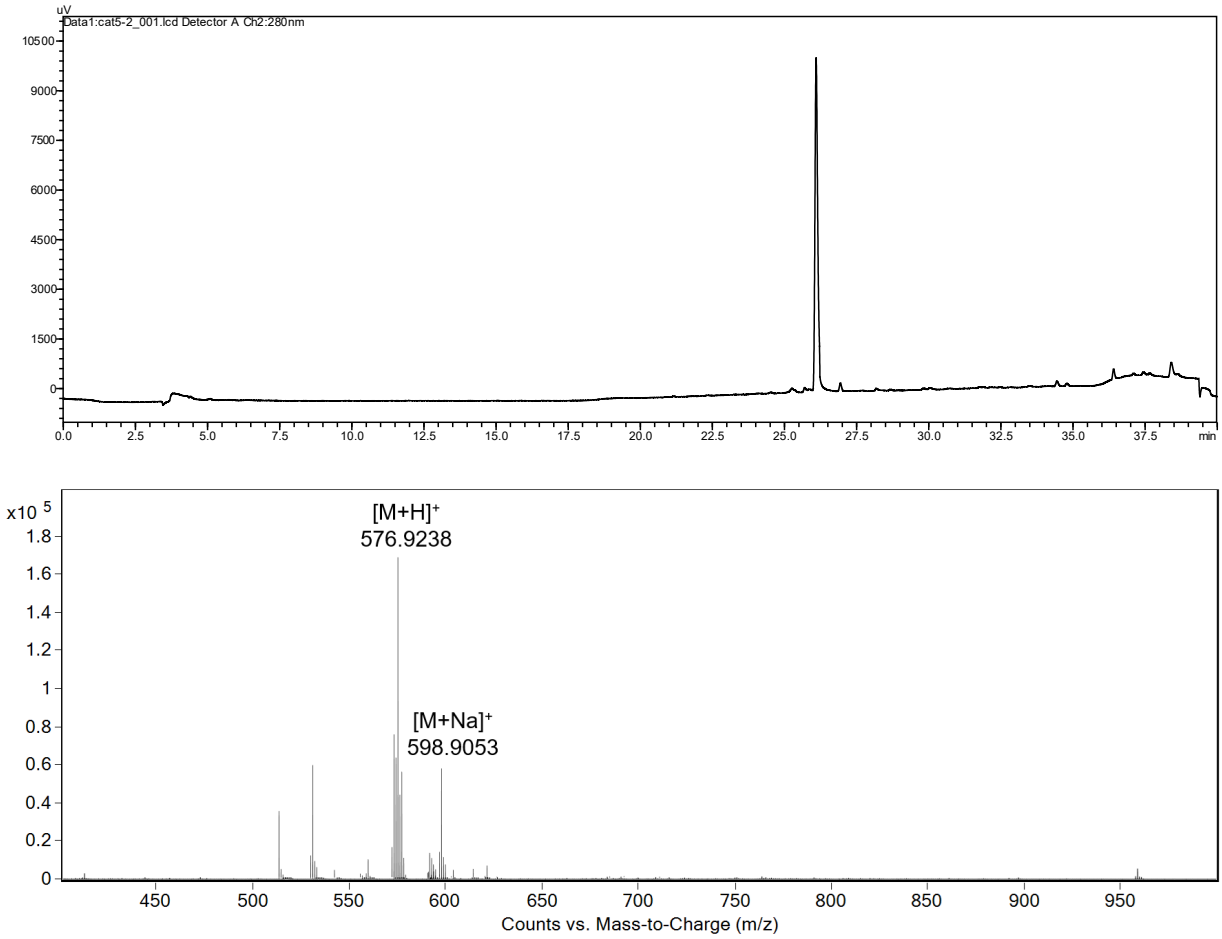

Figure S67. RP-HPLC trace at 280 nm (5-70% MeCN over 40 min) and ESI-MS spectrum of purified boronic acid-Rh(II) conjugate catalyst **5**. m/z 576.9238 and 598.9053 correspond to $[M+H]^+$ and $[M+Na]^+$ respectively.

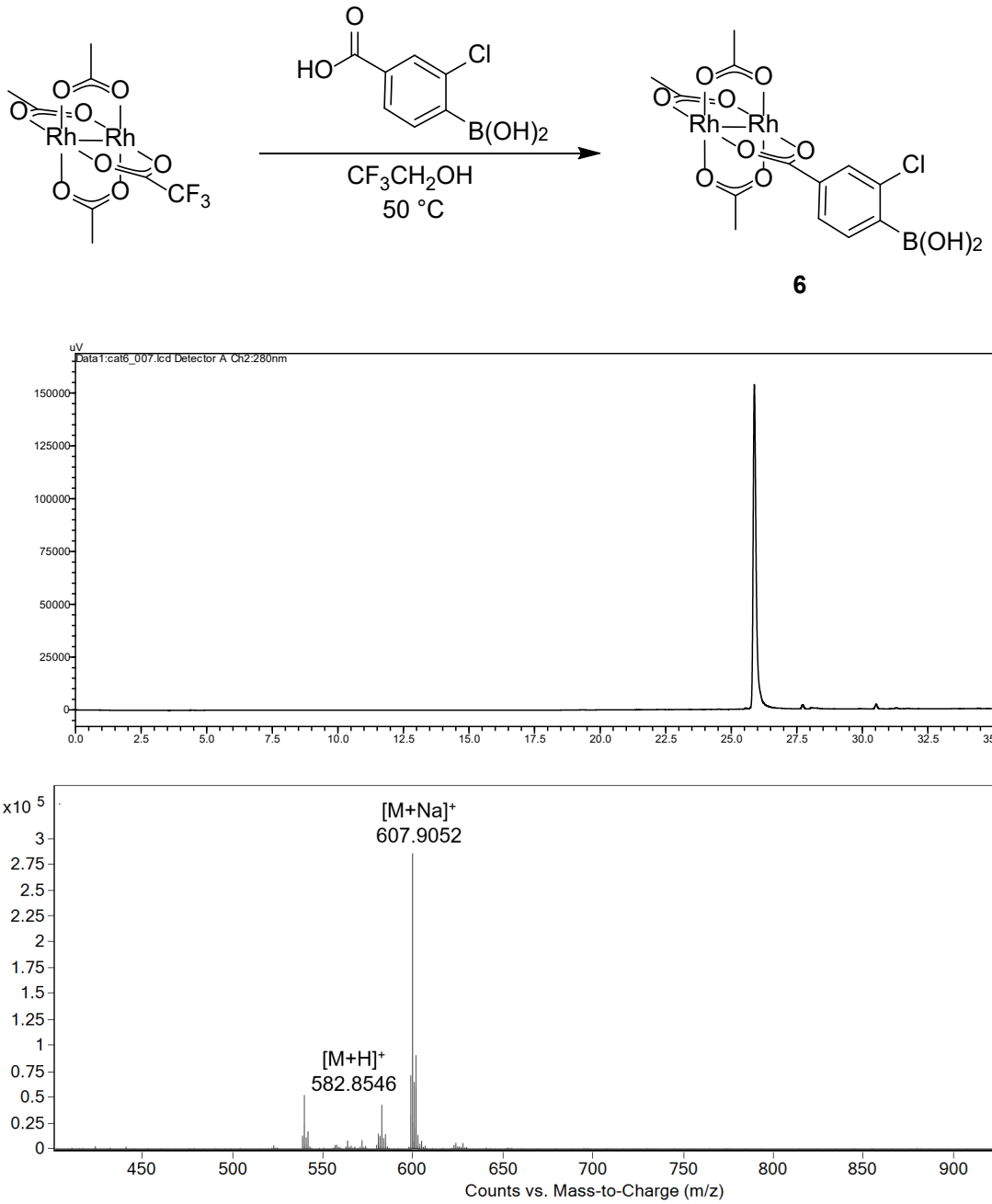

Figure S68. RP-HPLC trace at 280 nm (5-70% MeCN over 40 min) and ESI-MS spectrum of purified boronic acid-Rh(II) conjugate catalyst **6**. m/z 582.8546 and 607.9052 correspond to $[M+H]^+$ and $[M+Na]^+$ respectively.

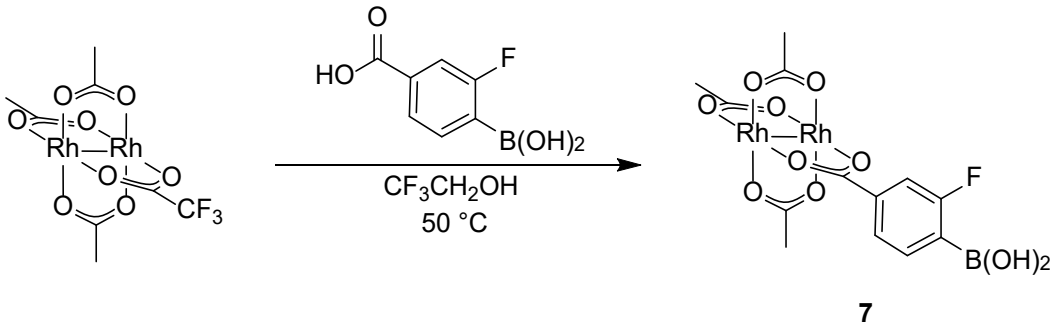

7

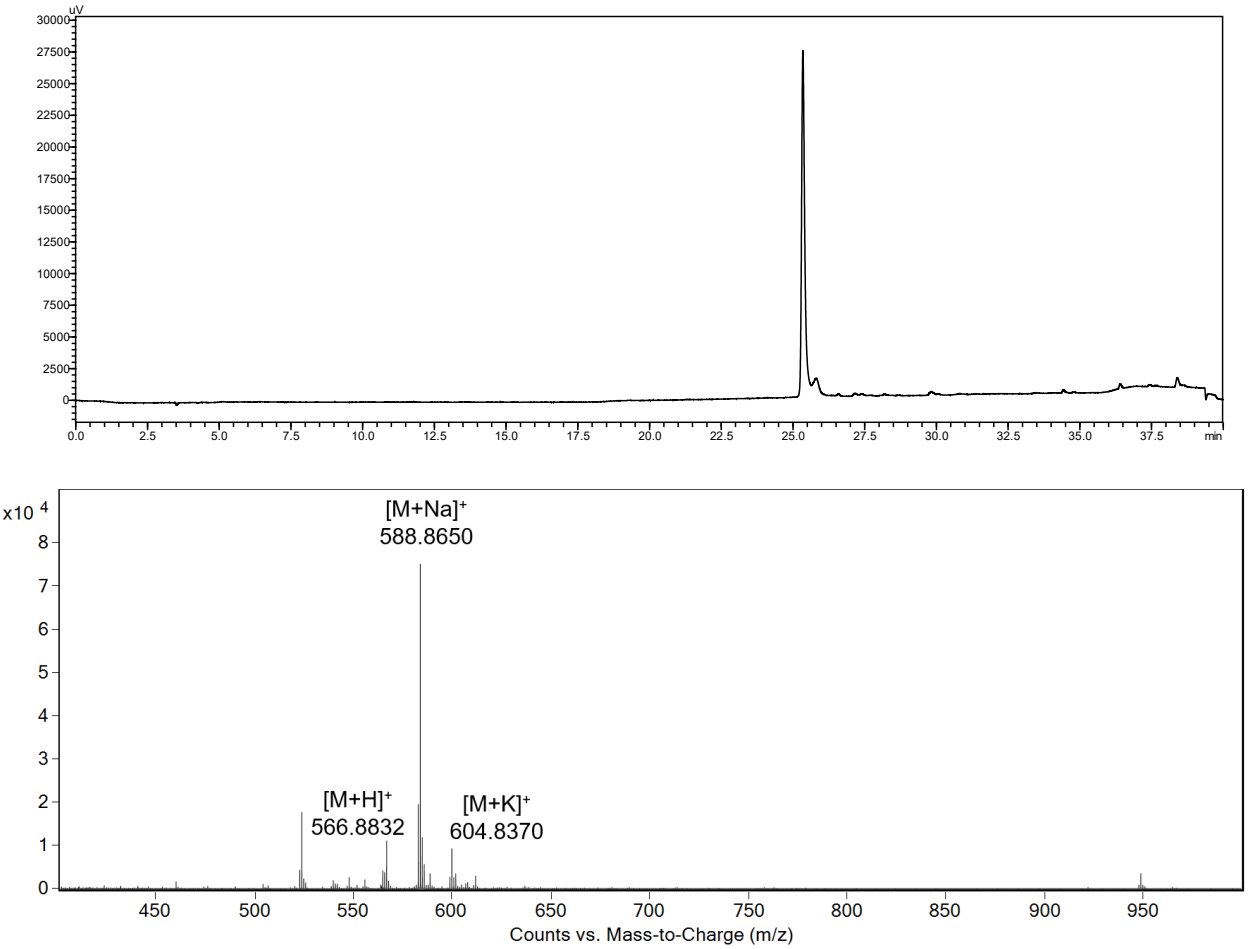

Figure S69. RP-HPLC trace at 280 nm (5-70% MeCN over 40 min) and ESI-MS spectrum of purified boronic acid-Rh(II) conjugate catalyst **7**. m/z 566.8832, 588.8650 and 604.8370 correspond to $[M+H]^+$, $[M+Na]^+$and $[M+K]^+$ respectively.

HPLC and ESI-MS of synthesized glycopeptide starting materials from tables 1, 2 and figures 3 and 4

Ac-D(D-glucamine)GGWQA-NH_2 (gpep1)

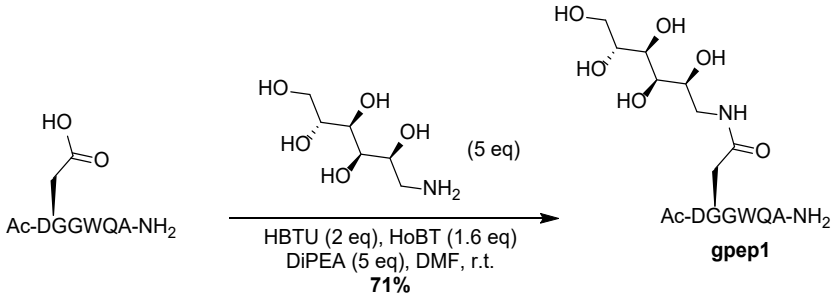

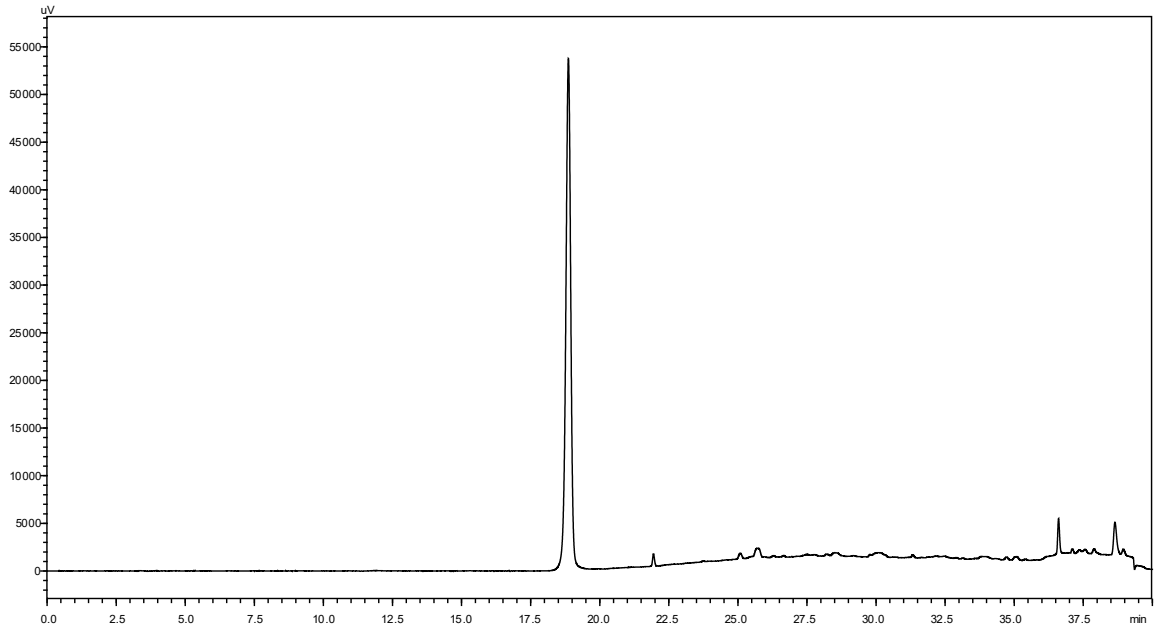

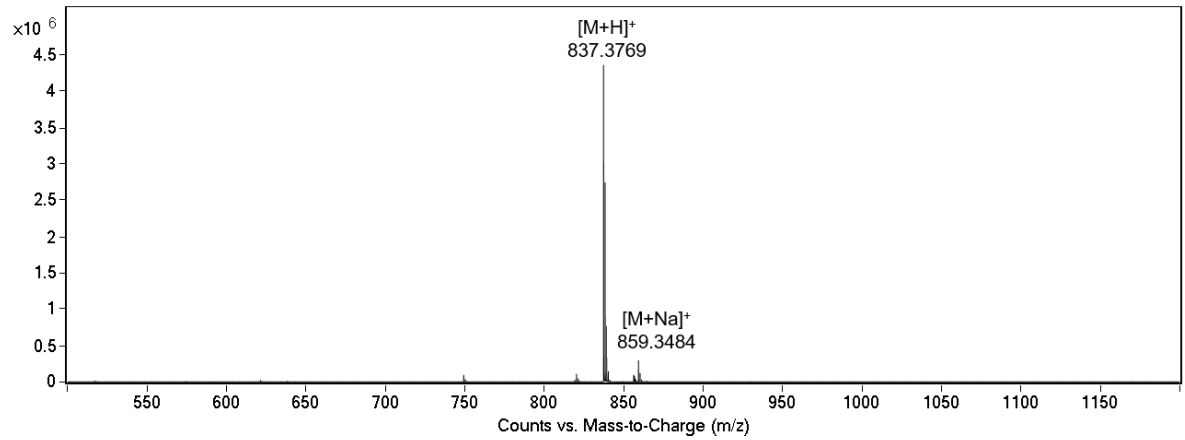

Figure S70. RP-HPLC trace at 280 nm (5-70% MeCN over 40 min) and ESI-MS spectrum of purified glycopeptide starting material **gpep1**. m/z 837.3769 and 859.3548 correspond to $[M+H]^+$ and $[M+Na]^+$ respectively.

Ac-D(D-glucamine)GWQA-NH$_2$ (gpep2)

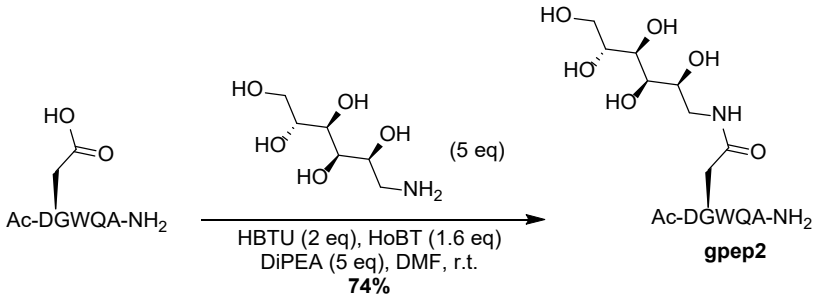

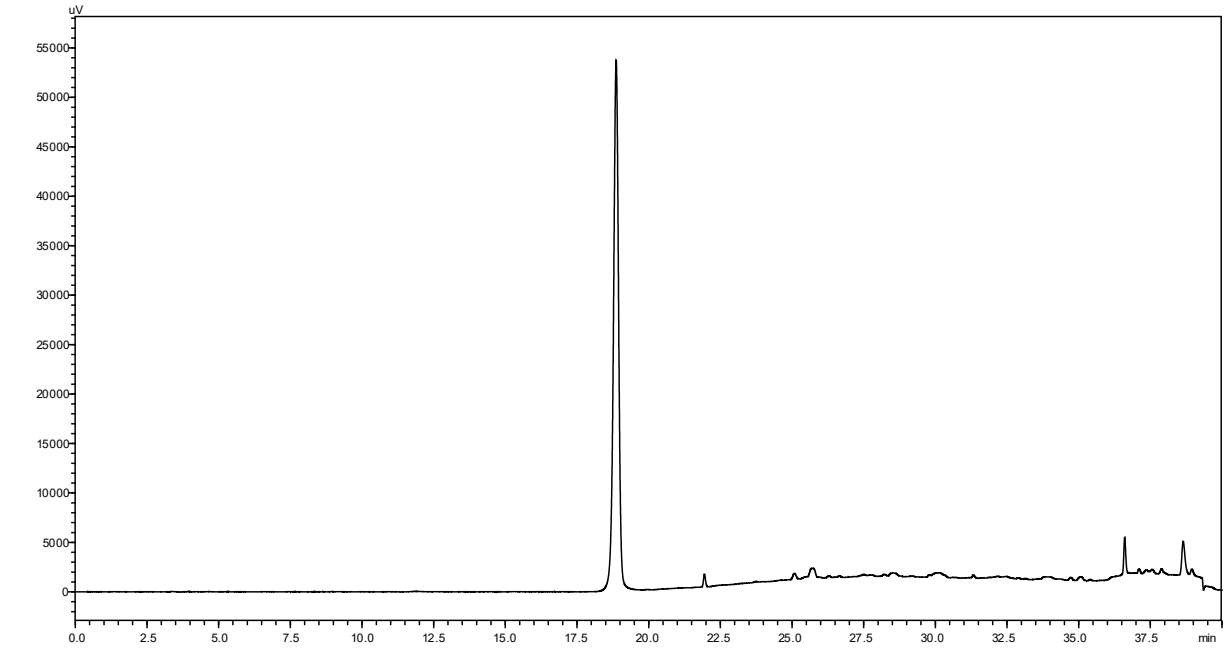

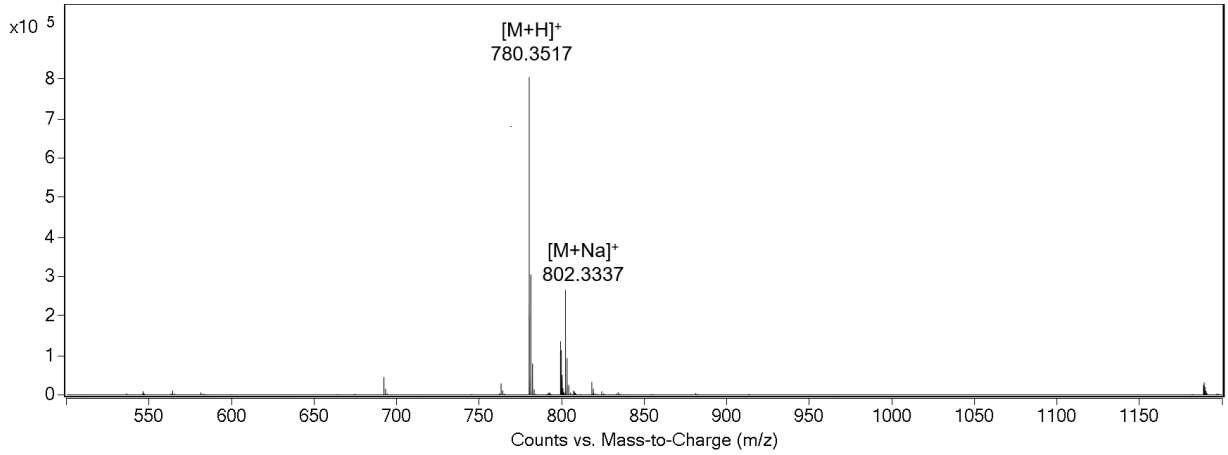

Figure S71. RP-HPLC trace at 280 nm (5-70% MeCN over 40 min) and ESI-MS spectrum of purified glycopeptide starting material **gpep2**. m/z 780.3517, 820.3337 and 818.2989 correspond to $[M+H]^+$, $[M+Na]^+$ and $[M+K]^+$respectively.

Ac-D(D-glucamine)AAAWQA-NH$_2$ (gpep3)

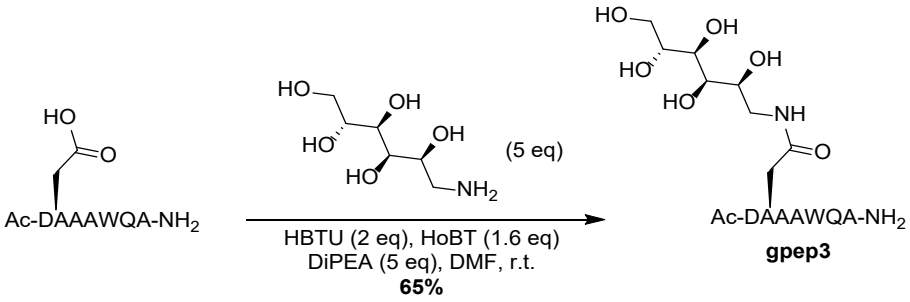

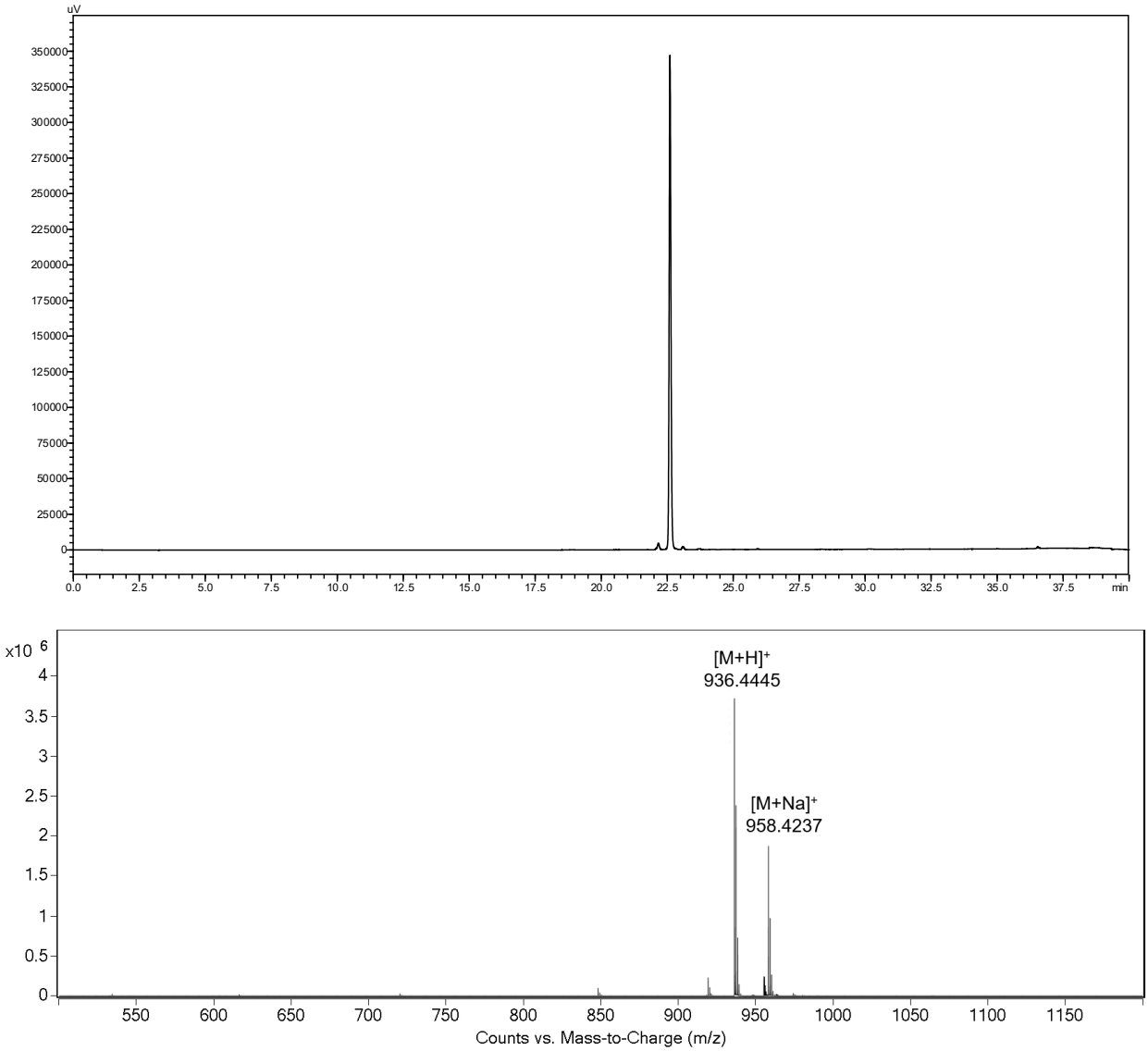

Figure S72. RP-HPLC trace at 280 nm (5-70% MeCN over 40 min) and ESI-MS spectrum of purified glycopeptide starting material **gpep3**. m/z 936.4445 and 958.4237 correspond to $[M+H]^+$ and $[M+Na]^+$ respectively.

Ac-D(D-glucamine)AAWQA-NH$_2$ (gpep4)

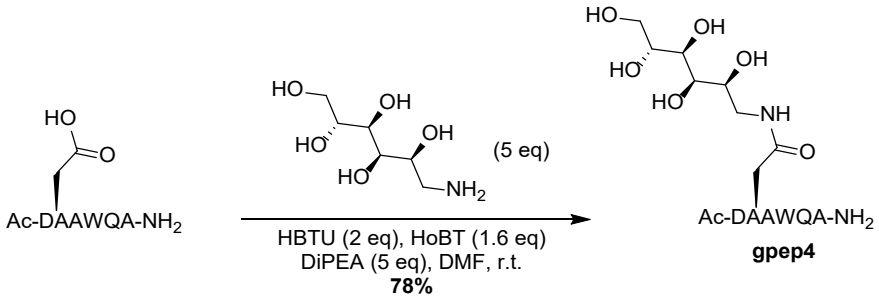

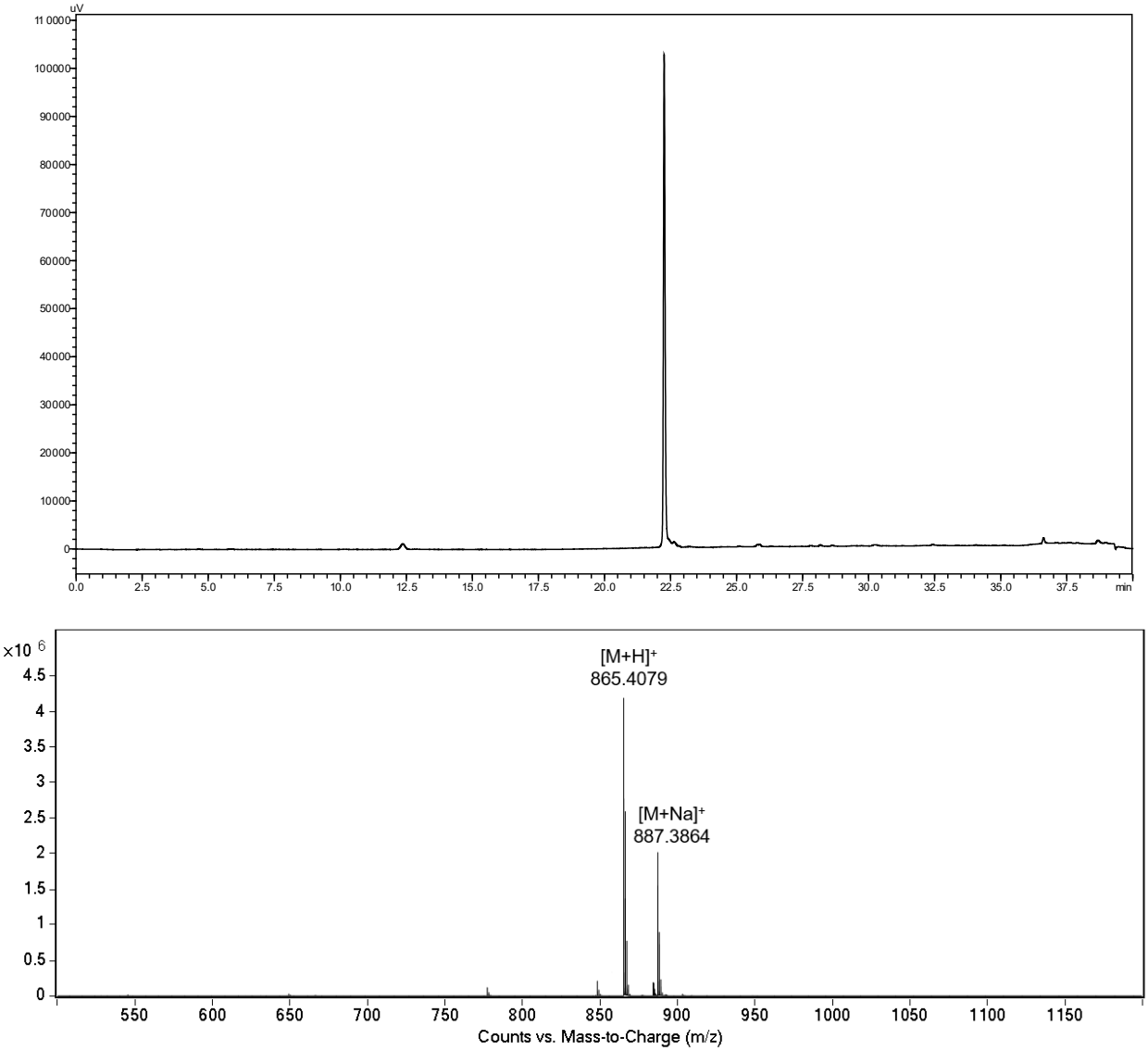

Figure S73. RP-HPLC trace at 280 nm (5-70% MeCN over 40 min) and ESI-MS spectrum of purified glycopeptide starting material **gpep4**. m/z 865.4079 and 887.3864 correspond to $[M+H]^+$ and $[M+Na]^+$ respectively.

Ac-D(D-glucamine)PPPWQA-NH_2 (gpep5)

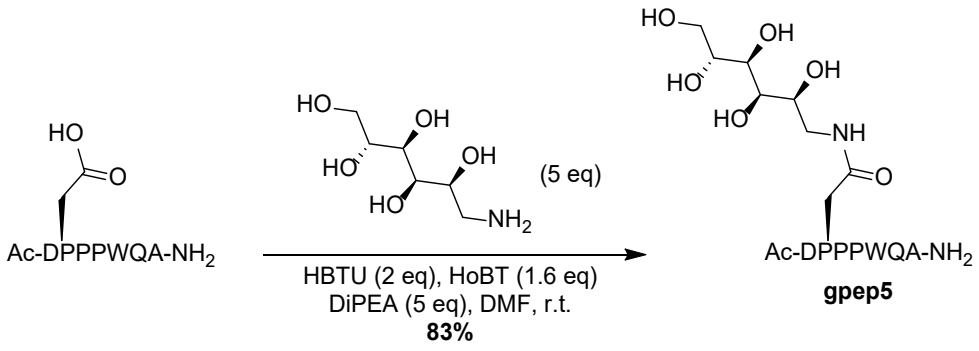

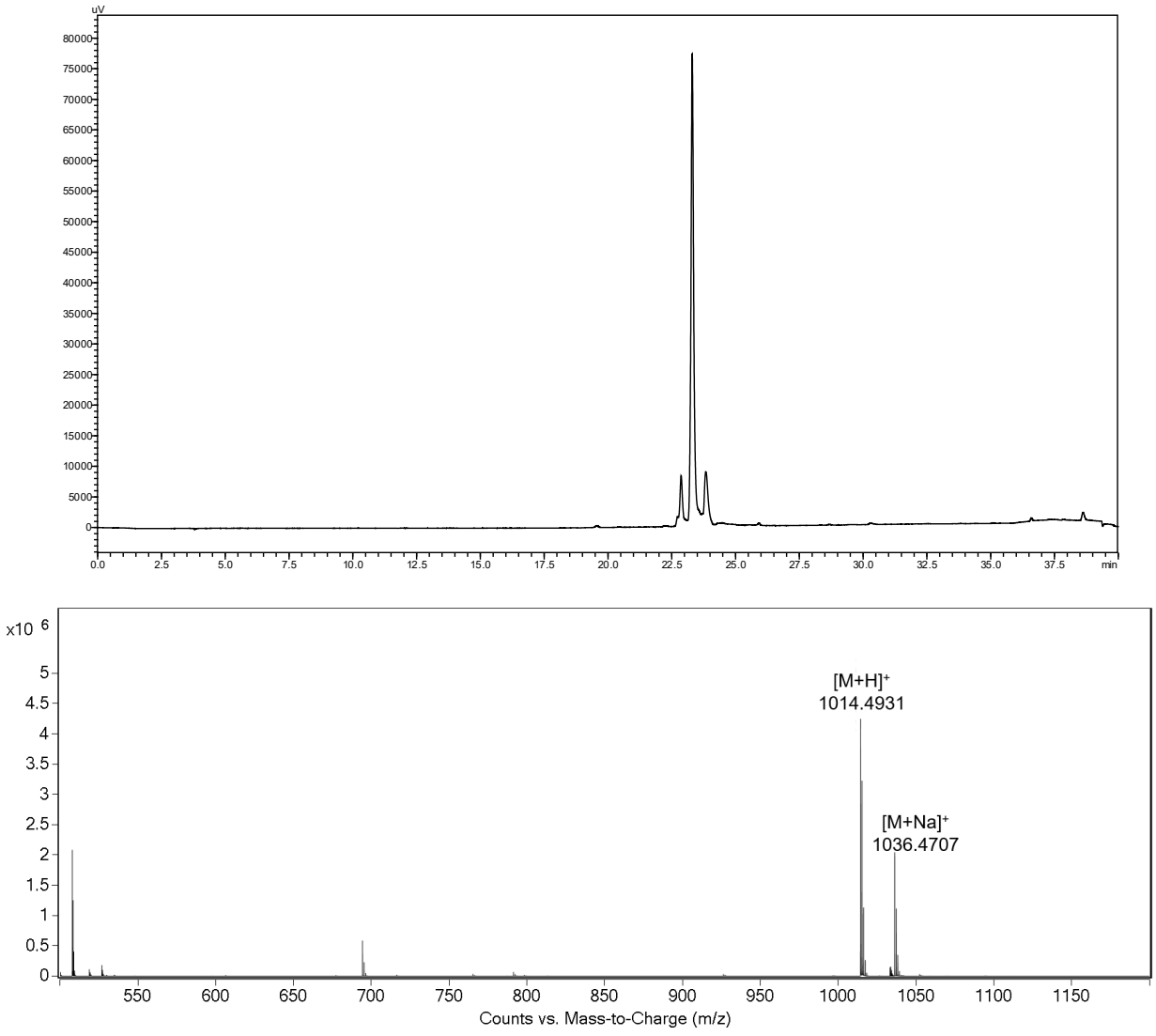

Figure S74. RP-HPLC trace at 280 nm (5-70% MeCN over 40 min) and ESI-MS spectrum of purified glycopeptide starting material **gpep5**. m/z 1014.4931 and 1036.4707 correspond to $[M+H]^+$ and $[M+Na]^+$ respectively. The tree peaks were analyzed by MS and correspond to **gpep5**, the different retention times are expected to be cis-trans isomers of the prolines residues in the structure[4].

Ac-D(D-glucamine)PPWQA-NH$_2$ (gpep6)

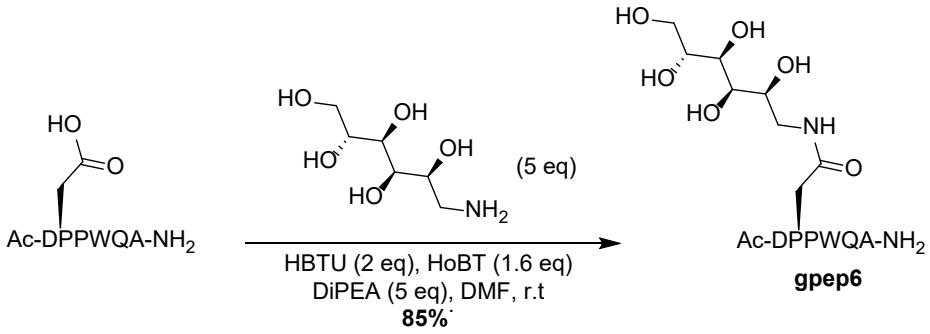

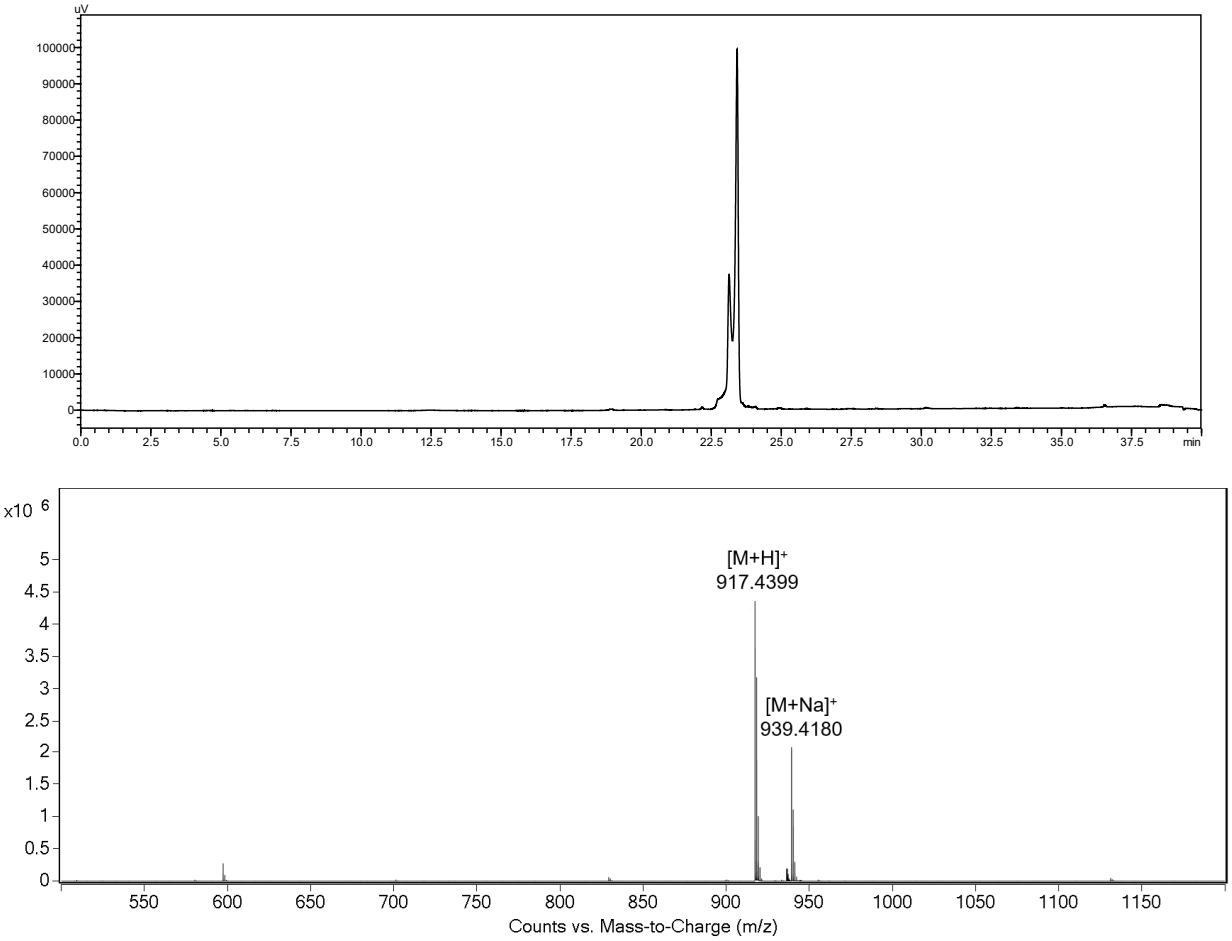

Figure S75. RP-HPLC trace at 280 nm (5-70% MeCN over 40 min) and ESI-MS spectrum of purified glycopeptide starting material **gpep6**. m/z 917.4399 and 939.4180 correspond to $[M+H]^+$ and $[M+Na]^+$ respectively. The two peaks were analyzed by MS and correspond to **gpep**, the different retention times are expected to be cis-trans isomers of the prolines residues in the structure[4].

Ac-TLD(D-glucamine)AAWSV-NH$_2$ (gpep7)

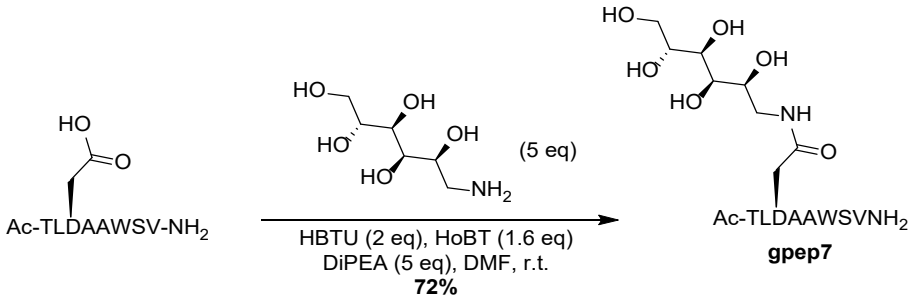

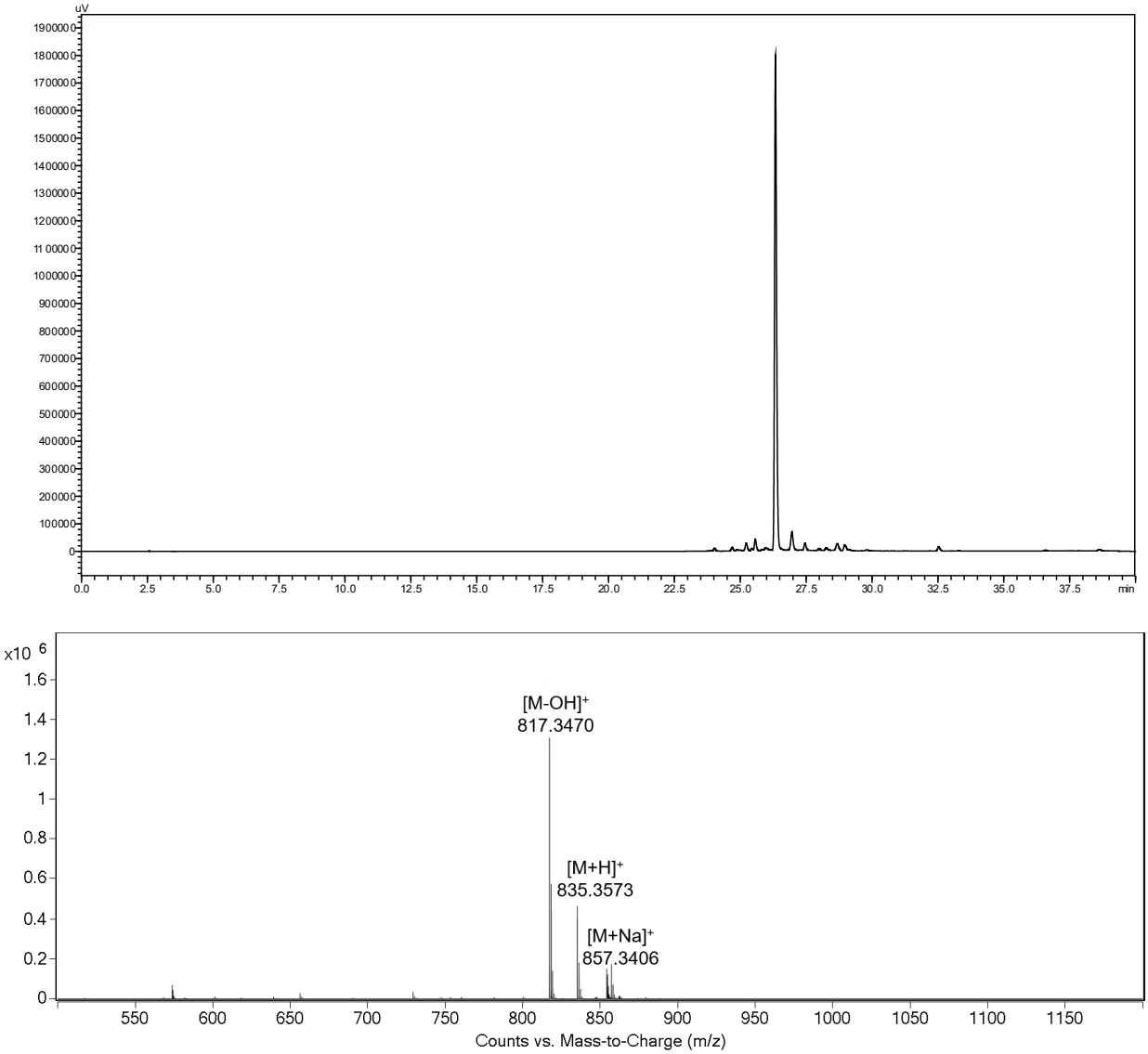

Figure S76. RP-HPLC trace at 280 nm (5-70% MeCN over 40 min) and ESI-MS spectrum of purified glycopeptide starting material **gpep7**. m/z 1049.5154, 1065.5414 and 1088.5237 correspond to $[M\text{-}OH]^+$, $[M+H]^+$ and $[M+Na]^+$ respectively.

Ac-D(D-glucosamine)GGWQA-NH_2 (gpep8)

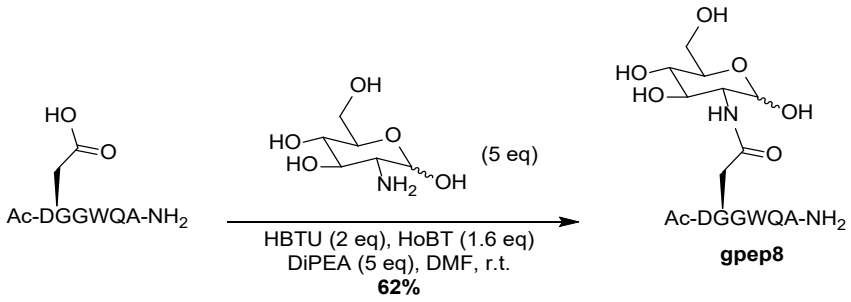

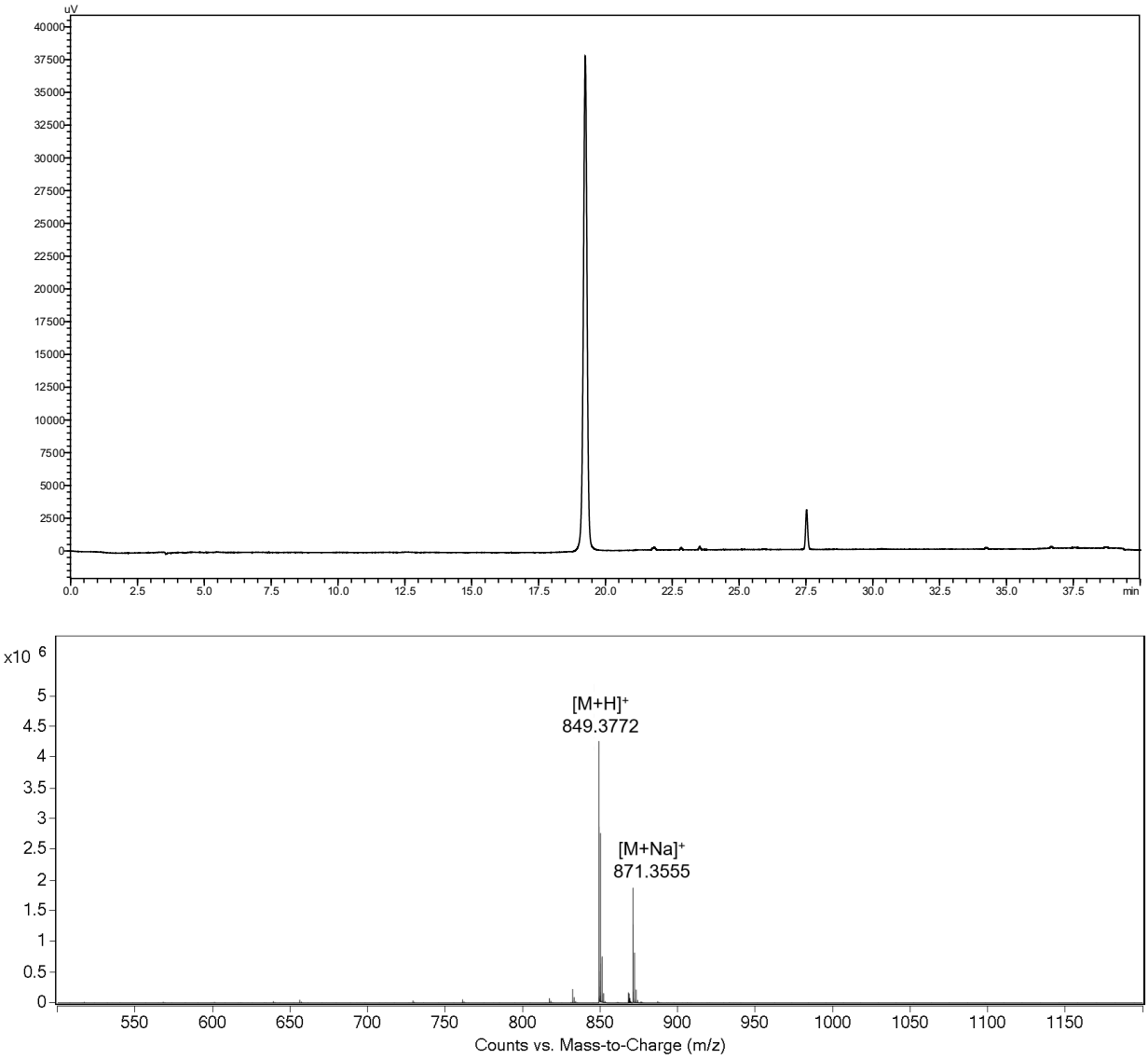

Figure S77. RP-HPLC trace at 280 nm (5-70% MeCN over 40 min) and ESI-MS spectrum of purified glycopeptide starting material **gpep8**. m/z 817.3470, 835.3573 and 857.3406 correspond to $[M\text{-}OH]^+$, $[M+H]^+$ and $[M+Na]^+$ respectively.

Ac-D(methyl 2-amino-2-deoxy-D-glucopyranoside)GGWQA-NH_2 (gpep9)

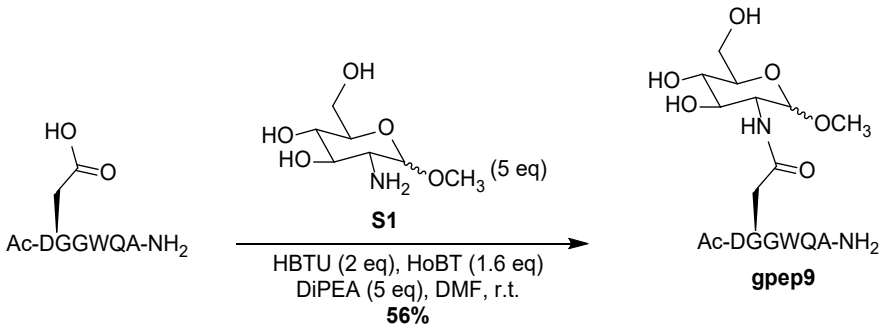

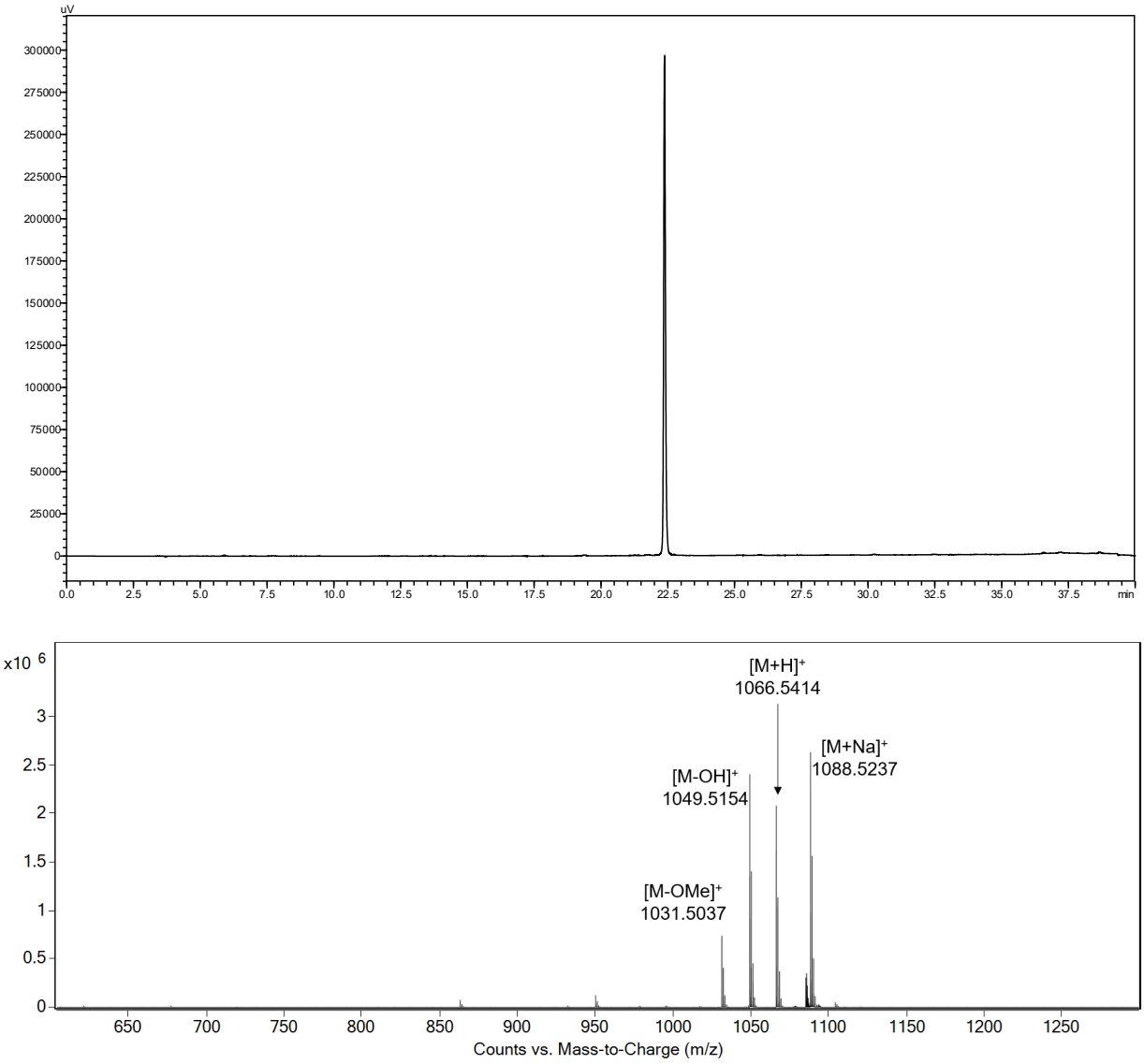

Figure S78. RP-HPLC trace at 280 nm (5-70% MeCN over 40 min) and ESI-MS spectrum of purified glycopeptide starting material **gpep9**. m/z 849.3772 and 871.3555 correspond to $[M+H]^+$ and $[M+Na]^+$ respectively.

Ac-D(D-glucamine)AAFQA-NH_2 (gpep10)

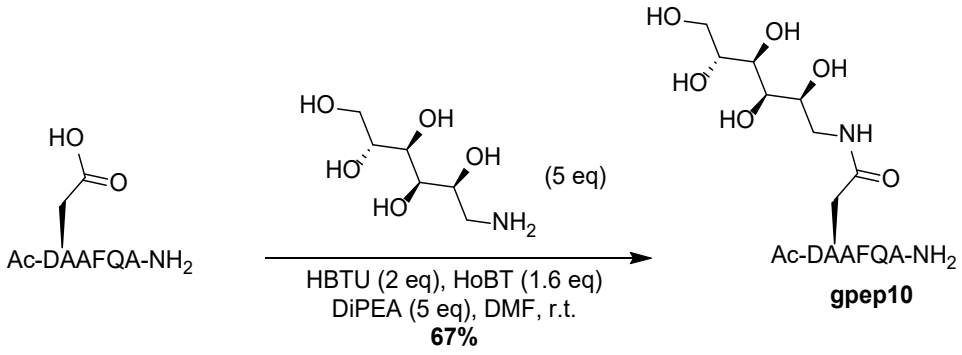

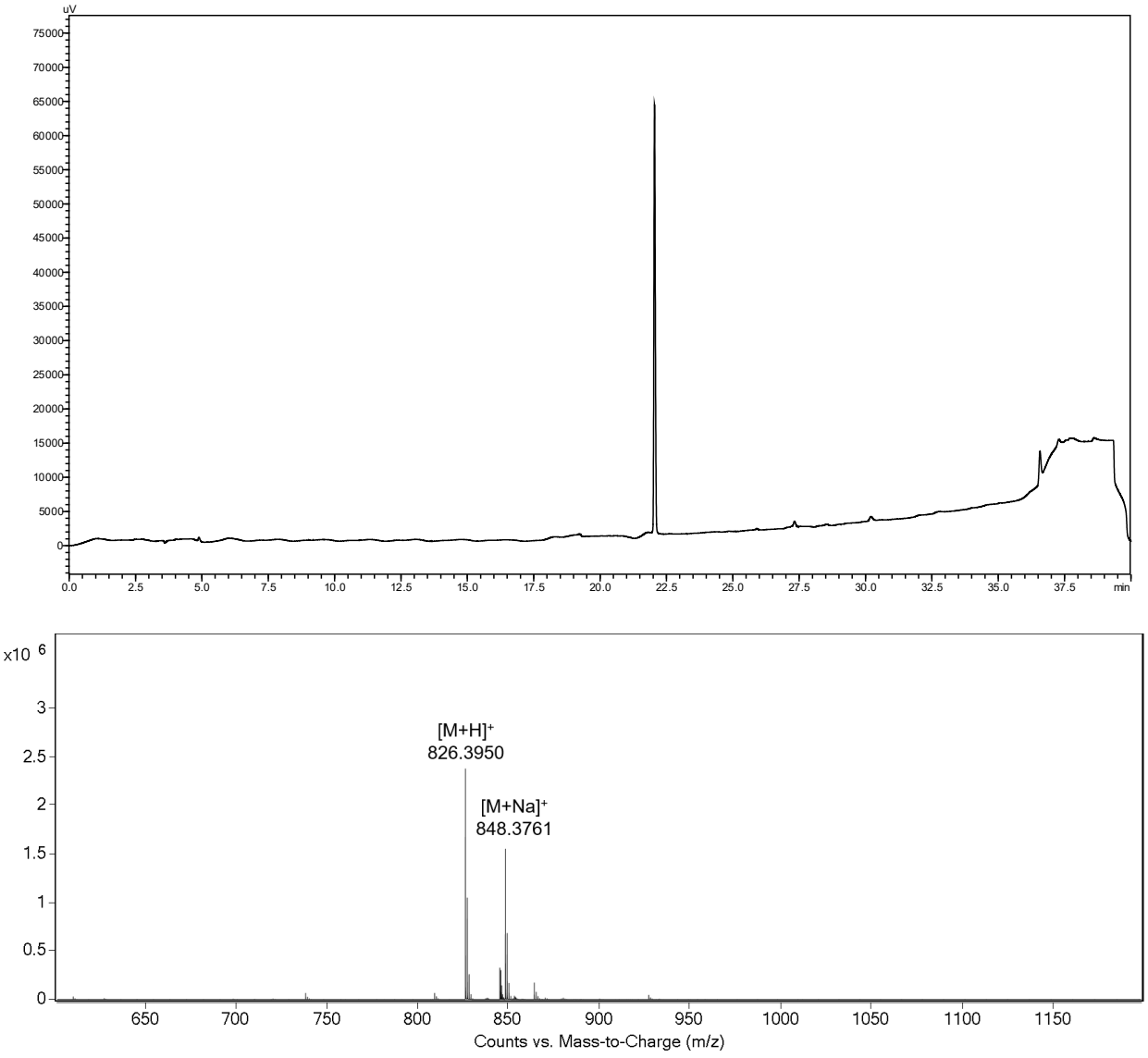

Figure S79. RP-HPLC trace at 254 nm (5-70% MeCN over 40 min) and ESI-MS spectrum of purified glycopeptide starting material **gpep10**. m/z 826.3950 and 848.3761 correspond to $[M+H]^+$ and $[M+Na]^+$ respectively.

Ac-D(D-glucamine)AAYQA-NH$_2$ (gpep11)

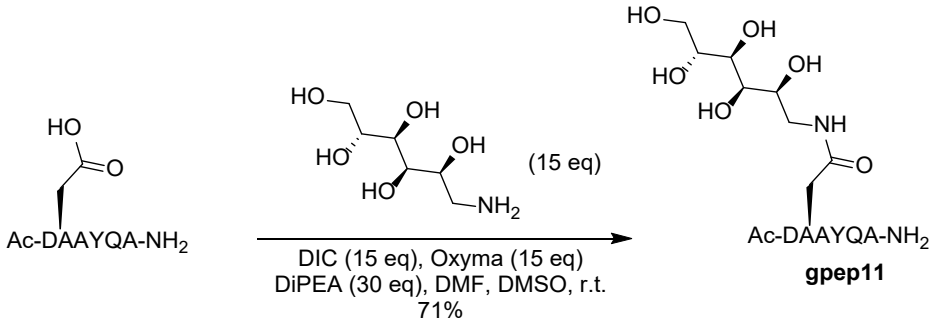

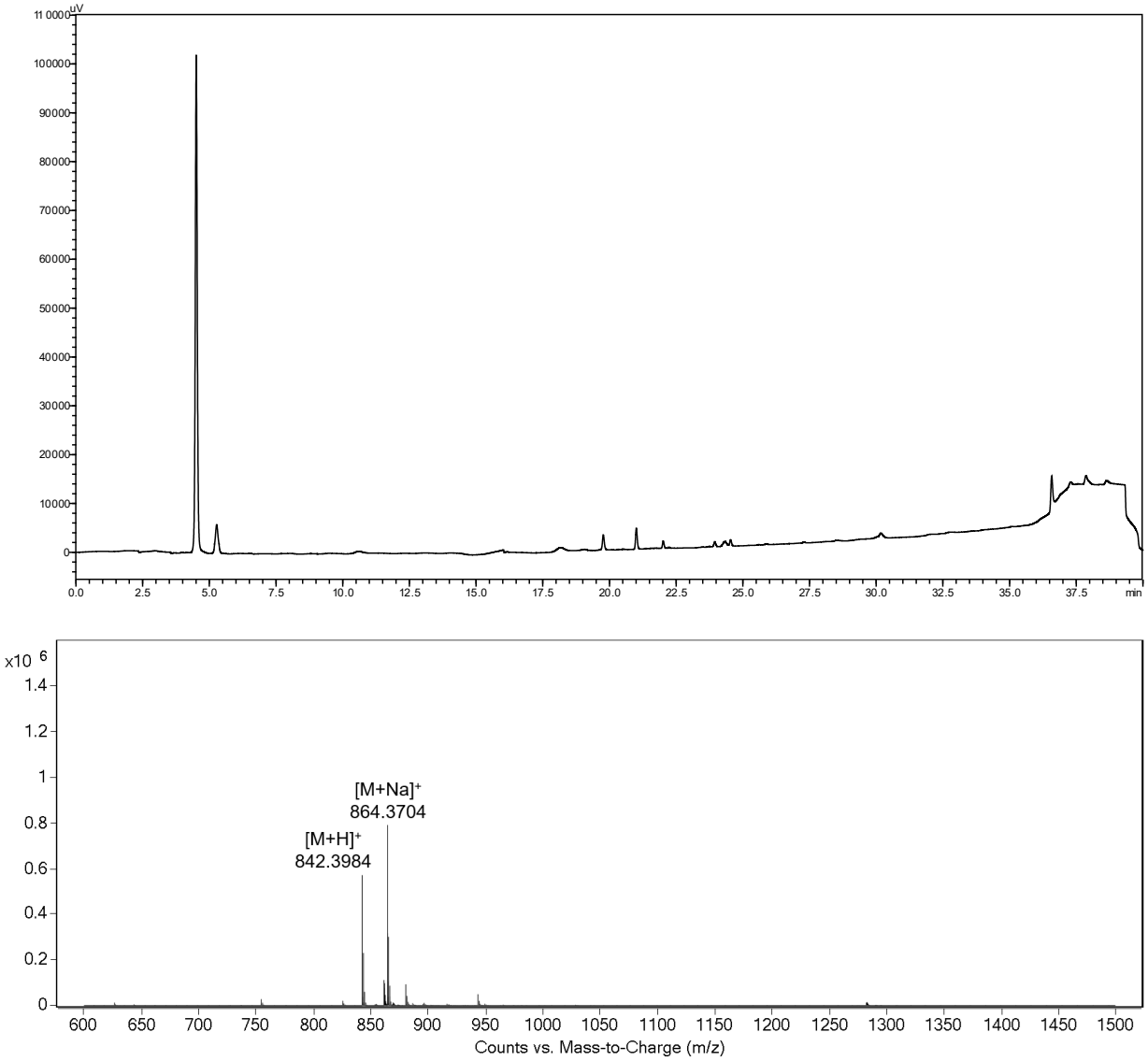

Figure S80. RP-HPLC trace at 254 nm (5-70% MeCN over 40 min) and ESI-MS spectrum of purified glycopeptide starting material **gpep11**. m/z 8492.3984 and 864.3704 correspond to $[M+H]^+$ and $[M+Na]^+$ respectively.

References

(1) Emmerson, D. P. G.; Villard, R.; Mugnaini, C.; Batsanov, A.; Howard, J. A. K.; Hems, W. P.; Tooze, R. P.; Davis, B. G. Precise Structure Activity Relationships in Asymmetric Catalysis Using Carbohydrate Scaffolds to Allow Ready Fine Tuning: Dialkylzinc–Aldehyde Additions. *Org Biomol Chem* **2003**, *1* (21), 3826–3838. https://doi.org/10.1039/B309715N.

(2) Hu, X.; Zhang, W.; Carmichael, I.; Serianni, A. S. Amide Cis−Trans Isomerization in Aqueous Solutions of Methyl N -Formyl- d -Glucosaminides and Methyl N -Acetyl- d -Glucosaminides: Chemical Equilibria and Exchange Kinetics. *J. Am. Chem. Soc.* **2010**, *132* (13), 4641–4652. https://doi.org/10.1021/ja9086787.

(3) Doscher, M. S. [48] Solid-Phase Peptide Synthesis; 1977; pp 578–617. https://doi.org/10.1016/0076-6879(77)47050-2.

(4) Jacobson, J.; Melander, W.; Vaisnys, G.; Horvath, C. Kinetic Study on Cis-Trans Proline Isomerization by High-Performance Liquid Chromatography. *J. Phys. Chem.* **1984**, *88* (20), 4536–4542. https://doi.org/10.1021/j150664a018.